Optimization and Control of Petroleum Reservoirs

AGUS HASAN

DOCTORAL THESIS

SUBMITTED FOR THE PARTIAL FULFILLMENT OF THE REQUIREMENTS FOR THE DEGREE OF

DOCTOR OF PHILOSOPHY

Department of Engineering Cybernetics
Faculty of Information Technology, Mathematics and Electrical Engineering
Norwegian University of Science and Technology

March 4, 2013

NTNU
Norges Teknisk Naturvitenskapelige Universitet
Norwegian University of Science and Technology

Thesis for the Degree of Doctor of Philosophy

Faculty of Information Technology, Mathematics, and Electrical Engineering
Department of Engineering Cybernetics

ISBN 978-82-471-4282-0 (printed version)
ISBN 978-82-471-4284-4 (electronic version)
ISSN 1503-8181
ITK Report 2013-4-W
Thesis at NTNU, 2013:91
Printed in Norway by NTNU-trykk, Trondheim

TO WYNDA AND AISYAH

Summary

Closed-loop reservoir management consists of two main tasks; state and parameter estimation & control and optimization. This thesis focuses on control and optimization. First, two cases are considered. The first case is optimization of oil production under gas coning conditions. In this case, the problem is formulated as a boundary control problem. We develop a novel control and optimization approach to design optimal well rate controllers using Lyapunov and backstepping methods. The results are presented in Chapter 2. The second case is optimization of oil production under water-flooding conditions. In this case, we propose a switching time approach based on gradient calculation for bang-bang control. Bang-bang control has a major practical advantage because it can be implemented with simple on-off valves. The results are presented in Chapter 3.

Second, we observed that the optimal solution depends on the length of the time horizon. Therefore, the optimization may be divided into a short-term and a long-term horizon. In Chapter 4, we propose a method which combines long-term and short-term optimization using an approach that is based on a priori articulation of preferences, i.e., the decision maker is allowed to specify preferences in terms of the relative importance between long-term and short-term objectives.

Finally, we extended the boundary control problem in Chapter 2 to a theoretical study of more general fluid flow systems which in this case means surface wave models. These results are presented in Chapter 5. A summary of each chapter is presented below.

Summary of Chapter 2: Gas coning control

Quite often, a well is produced with a constant oil rate and a constant gas-oil ratio (GOR) during the subcritical phase, i.e., before gas breakthrough. The presence of gas coning in production wells may reduce the oil production since free gas, which occurs after gas breakthrough, will occupy significant volumes in the well and pipeline system. From an economical and operational point of view, this condition will be undesirable for several reasons; the gas price is much lower than the oil price, the afflicted well may be abandoned early, and the gas handling capacity often is a constraint. Therefore, there is an incentive to produce such wells in their subcritical phase for an extended period of time. In this chapter, the gas coning process in a gas-oil reservoir completed with a single horizontal well is analytically modeled, simulated, and analyzed applying a nonlinear control approach. The horizontal well model which describes the interaction between the well and the reservoir may be cast into a boundary control problem of the porous media equation with two boundary conditions; a homogeneous Neumann boundary condition describing a no-flow at the outer boundary of the reservoir, and a nonlinear boundary condition describing the well production rate. A well rate controller for the boundary control problem is designed using the Lyapunov and back-

stepping methods for linear and nonlinear cases. Using the backstepping method, one can construct an observer for the particular system if measurements inside the domain, i.e., not on the boundary, are required in a similar way to the backstepping control design itself. To this end, we consider a case where influx occurs at the outer boundary of the reservoir. In this case, the controller requires the use of an observer. A convergent observer was presented for this purpose. The controllers hold some formal performance guarantees and require information on the gas-oil contact (GOC) at the well heel only. Furthermore, the controller has a tuning parameter which can be used to maximize a suitable performance measure, e.g., the net present value (NPV). The controller is evaluated using a detailed Eclipse simulator of a gas coning reservoir. Simulation results show significant improvement of production profit of the proposed method compared to a conventional method which usually uses a constant rate until gas breakthrough.

Summary of Chapter 3: Water-flooding control

Production optimization involving water injection has successfully improved oil production by increasing recovery. This technique is now combined with information obtained from gradient-based methods for calculating optimal flow rates or bottom hole pressures (BHPs) for long-term optimization. It has been shown that if the objective function is linear in the control inputs and the only constraints are the upper and lower bounds on the control input, then because of its particular structure, the problem may has bang-bang (on-off) optimal solutions. This chapter discusses an optimal control approach to life cycle optimization which computes optimal switching times for the bang-bang controls. Bang-bang control has a major practical advantage because it can be implemented with simple on-off valves. The optimal switching times are obtained from the adjoint method combined with the halving interval method. Two numerical examples which use realistic reservoir settings are included to illustrate the application of the proposed method.

Summary of Chapter 4: Long-term and short-term optimization

Optimization of oil production may be performed on different time horizons. Long-term optimization (typically years) is usually conducted by reservoir engineers while short-term optimization (typically days or weeks) is done by production engineers. Long-term objectives focus on finding the best strategy to drain as much oil as possible from reservoirs. However, in reality it is often short-term goals like maximizing daily oil rates that dictate the operational strategy. Unfortunately, these goals may be in conflict with each other. Therefore, incorporating long-term goals into short-term objectives makes sense. In this chapter, we present a novel approach to systematically combine long-term and short-term production optimization. The approach is based on a priori articulation of preferences, i.e., the decision maker is allowed to specify preferences which may be articulated in terms of goals or the relative importance between long-term and short-term objectives. To this end, the long-term strategy is computed using an adjoint-based method while the short-term strategy is computed using

the reactive control method. The approach is applied to a simplified model of the south wing of the Voador field in the Campos basin, Brazil. The results are presented as Pareto-like plots which can be used for decision support to balance long-term and short-term goals.

Summary of Chapter 5: Boundary stabilization of the wave equations

The boundary stabilization problem for the generalized Korteweg-de Vries-Burgers (KdV-Burgers) and Benjamin-Bona-Mahony-Burgers (BBM-Burgers) equations are considered. For the KdV-Burgers equation, the control laws achieve global exponential stability in the L^2-sense. Adaptive control laws are also constructed when the dissipation coefficient is unknown. Finally, an observer for the control laws where measurements inside the domain is needed is derived. Again closed-loop exponential stability is shown. For the BBM-Burgers equation, the proposed control laws are used to achieve global exponential stability for the linear system and semi-global exponential stability for the nonlinear system in the H^1-sense. An H^2 bound of the solution for the nonlinear system is also derived. A numerical example is included to illustrate the application of the proposed control laws.

Preface

This thesis is submitted to the Norwegian University of Science and Technology (NTNU) for partial fulfillment of the requirements for the degree of philosophy doctor. The doctoral work has been performed at the Engineering Cybernetics department under the supervision of Professor Bjarne Foss. The research was sponsored by the Center for Integrated Operations in the Petroleum Industry (IO Center).

During my study at NTNU, I am really grateful to be given the opportunity and experiences from wonderful people who offered their advices and inspirations. Nevertheless, without downplaying the role of others, on this occasion I will mention a few people who have contributed greatly to my work.

At the top of my list, I would like to thank to my supervisor, Professor Bjarne Foss, for the patient guidance, encouragement, and all the good discussions we have had through these years. I have been fortunate to have him as my supervisor who cared so much about my work and who responded to all my queries so promptly.

I would like to thank to Professor Svein Ivar Sagatun at Statoil who introduced me to gas coning problem and gave me an opportunity to work with Statoil reservoir engineers in Bergen. I also would like to thank to Dr. Stein Krogstad at SINTEF for helping me with MRST and Professor Ole Morten Aamo of NTNU for teaching me how to use boundary control properly.

Special thanks go to Mr. Alex Teixeira and Dr. Vidar Gunnerud who assisted me during my visit to Petrobras research center (CENPES) in Rio de Janeiro, Brazil.

I also would like to thank to Professor Arnold Heemink, Dr. Marta Duenas Diez, and Professor Jan Tommy Gravdahl for their willingness to be on the thesis defense committee.

Finally, I would like to thank my wife Wynda and my daughter Aisyah for their support and unconditional ♡.

Table of Contents

List of Tables

List of Figures

Chapter 1

Introduction

It is a fact that fossil fuel is a key energy source today. After more than one hundred years in use, petroleum products play an important role in our daily lives. For some countries, oil has become the backbone of their economies. The discovery of gas and oil fields in the North Sea in the late of 60s has helped Norway to become a prosperous country with the highest living standard in the World (Larsen, 2005). The discoveries of giant oil fields in the Middle East countries have placed them onto the map and they are currently the top oil exporters (Matsumoto et al., 2012). Advanced industrial countries like the USA and EU countries are among the largest importers (Chu and Chang, 2012). The rise of China and India with a total population of over two and half billions combined will require much more energy in the years to come (Li and Du, 2004).

On a different note, the discoveries of (giant) oil fields have been decreasing and most of the remaining oil is from unconventional resources like in Canada (Isaacs, 2008). Even though in recent years Brazil has announced the discovery of giant fields in the Santos basin (Huang et al., 2009), the overall world oil reserve has been decreasing significantly during the last decades. Today, many oil reservoirs are in their mature stage as can be observed from high water cut and gas oil ratio (GOR).

On a high level, a petroleum production system can be divided into two categories; surface and sub-surface production systems. Surface production systems consist of all facilities to separate and treat produced oil and gas, e.g., pipes and separator tanks. Sub-surface production systems consist of reservoirs and wells. It may be noted that surface production systems according to this division may include sub-sea equipment. This thesis focusses on optimization and control of the sub-surface production system. To this end, we introduce some control theory techniques such as optimal control method, switching time method, and backstepping method to solve the gas coning and water-flooding problems.

This chapter starts by providing a brief background on oil petroleum production systems and closed-loop reservoir management. Subsequently, the choice of research topics is motivated before some background theory on control and optimization is included. Finally, the thesis contributions and publications are listed.

1.1 Sub-surface Production Systems

In this section, we present a brief introduction to sub-surface petroleum production systems which consist of reservoirs and injection/production wells.

1.1.1 Petroleum Reservoirs

A petroleum reservoir is a subsurface pool of hydrocarbons (oil and gas) contained in porous or fractured rock formations and trapped by overlying rock formations with zero permeability. Since the reservoirs are located hundreds or thousands of meters beneath the ground, it is a challenge to obtain a description of such reservoir. The common way to visualize the reservoir is to model it based on the first principles, i.e., a model of a physical process from the continuity equations and the Darcy law (Aziz and Settari, 1979). The model can be written as a system of partial differential equations (PDEs). The number of differential equations varies depending on how we consider the fluids. If we consider the fluids as gas, oil, and water, (known as the black-oil formulation) then we will have three differential equations with three unknown; oil pressure, water saturation, and gas saturation. On the other hand, if we consider the fluids as individual chemical components (known as the compositional formulation) then the number of the differential equations will be equal to the number of the chemical components. Thus, theoretically the former is easier to solve.

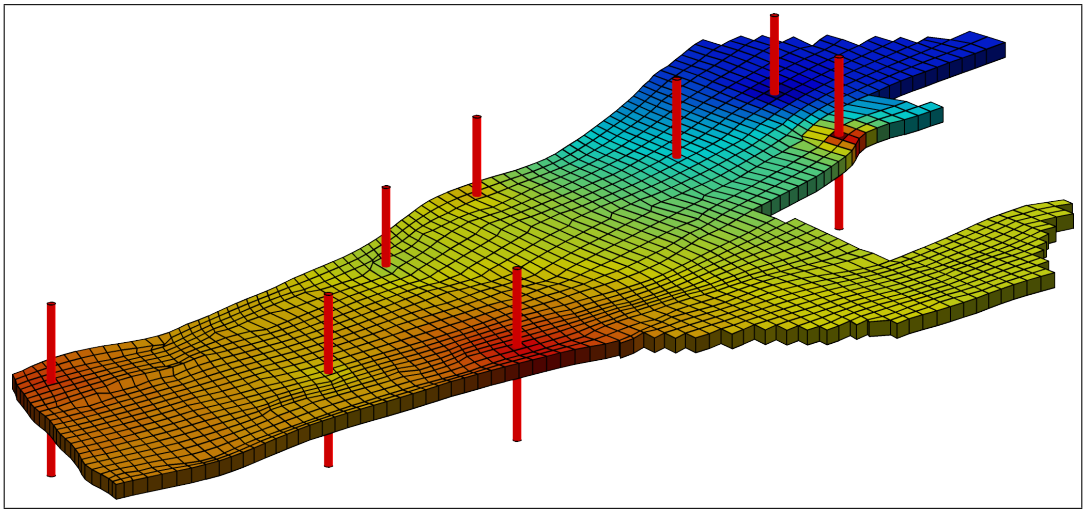

Figure 1.1: An example of a reservoir model: The Norne field.

In general the reservoirs are heterogeneous with respect to permeability and porosity. Therefore, solving the PDEs analytically is almost impossible and hence numerical schemes are needed (Ertekin et al., 2001). An important consideration when discretizing the PDEs is that the reservoir may have a large dimension and an irregular shape (**Fig. 1.1**). Thus, selecting appropriate grid cells can be crucial. In practice, the number of grid cells can enter

the millions. This poses a challenge in the numerical computation. To this end, methods to reduce model order plays an important role.

1.1.2 Petroleum Wells

To produce the oil, a number of production wells are drilled through the reservoir formations. The difference between the reservoir pressure and the surface pressure usually becomes the driving force for lifting the oil and other fluids from the reservoir toward the surface facilities. If the reservoir pressure is too low, injection wells may be drilled to inject water and/or gas. When water is used, the process is called water-flooding. Water-flooding is the most common secondary recovery technique used today. Besides to maintain the pressure, water-flooding could also be used to sweep the oil in the reservoirs towards the production wells; hence, it may increase the recovery. There exists numerous other technologies for increased oil recovery. At a given well, production may increase through artificial lift techniques like gas-lift or electrical submersible pumps (ESPs), and on a field level there exist injection strategies which mobilizes immobilized oil through tertiary recovery techniques. For more on this we refer to Jayawardena et al. (2007); Rooks et al. (2012); Trujillo et al. (2010).

The wells can be placed vertically, horizontally, or at an angle somewhere in-between. The horizontal wells increase the pay zone considerably compared to vertical wells in many cases such as thin oil zones and in shale gas reservoirs. Hence, this technology has been an enabler for the development of many assets. However, the average horizontal well is more expensive and technically difficult to drill than vertical wells. A development of particular interest for this study is the increased use of intelligent wells or intelligent completions. This includes more downhole sensors, and valves which may me operated as control valves. This is definitely an important enabler for closed-loop control of reservoirs (Jansen et al., 2009; Foss, 2012; Foss and Jensen, 2011).

The well connects the reservoir to the surface facilities; thus, control and optimization of oil and gas production must be done via injection and production wells. In practice, the amount of fluid rates can be set by changing bottom hole pressure (BHP). Hence, the main idea of this thesis is to design optimal fluid rates or BHP values of the injection and production wells such that the oil revenue can be maximized.

1.2 Closed-loop Reservoir Management

Field development of life cycle oil production optimization can be represented by a closed-loop reservoir management (Jansen et al., 2009). It has two main blocks; (i) state and parameter estimation (or observer design) and (ii) optimization and control (**Fig. 1.2**). This thesis focusses on the second block.

Uncertainties are always part of reservoir simulation models. Therefore, having a model that can be trusted is critical. The idea of the first block is to estimate the reservoir states (pressure and saturation) and the reservoir parameters (permeability and porosity) to obtain

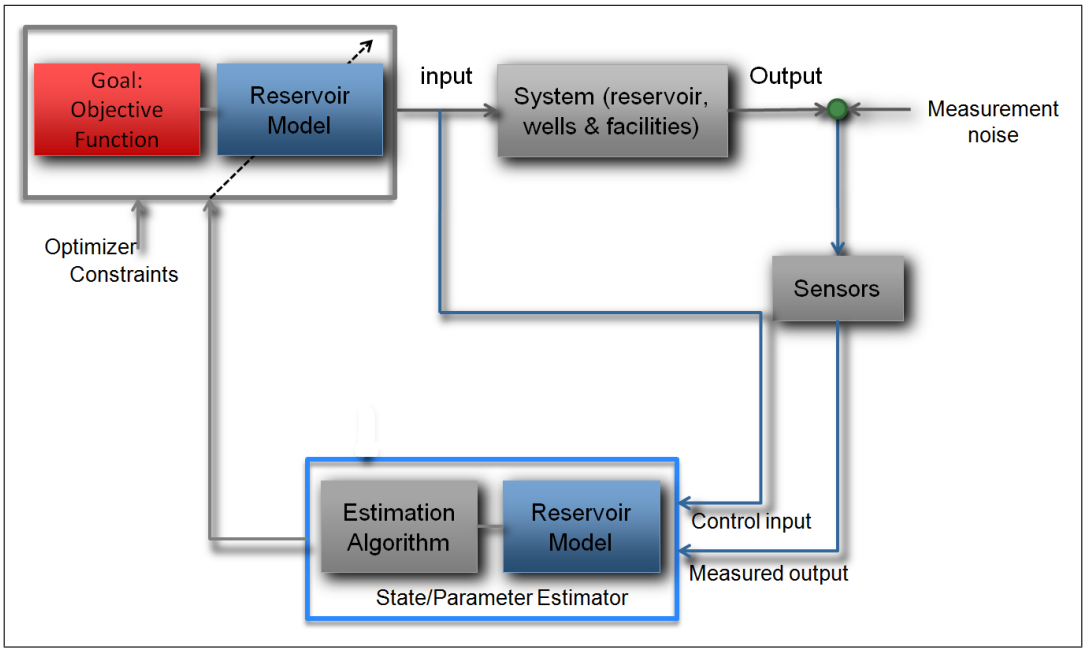

Figure 1.2: A simple illustration of closed-loop reservoir management (Suwartadi, 2012).

confidence in the model. There are several (analytic, stochastic, or heuristic) techniques that can be used. One method commonly used is (automatic) history matching. The accuracy of the history matching depends on the quality of the reservoir model and the quality and quantity of pressure and production data as well as other data. In recent years, more advanced techniques have been developed, e.g., see the ensemble based methods discussed in Aanonsen et al. (2009); Oliver et al. (2008).

In the second block, the idea is to find optimal production settings (usually the BHPs of the production and injection wells) such that the oil revenue can be maximized. Since a reservoir simulation can take up to hours, an efficient optimization technique is required. A common technique is to use gradient based optimization where the gradients can be efficiently calculated using the adjoint method (Brouwer and Jansen, 2004; Sarma and Chen, 2008; Suwartadi, 2012).

1.3 Motivation

In this section, we motivate our choice of research topics. In some senses, it shows relation between chapters.

Gas coning control

Horizontal well technology is becoming increasingly popular albeit the cost of such wells. The reason is increased sweep. They are particularly efficient for thin oil layers which are

sandwiched between a water aquifer below and a large gas cap above. An example of this is the Statoil Troll B and C oil asset on the Norwegian Continental Shelf. After drilling the well and starting production, the oil and gas will move to the well perforation. The difference in mobility between the oil phase and the gas phase will drives the gas layer downwards and it enters the well. This causes the gas to dominate the flow inside the production well; thus, reducing the oil production. Since the oil price is much higher than the gas price, this situation is undesirable. Further, the afflicted well may be abandoned early, and the gas handling capacity is often a constraint. Therefore, there is an incentive to prolong the subcritical production phase, i.e., before free gas enters the well.

In this research, we proposed a novel approach to optimize oil production under gas coning conditions in a closed-loop reservoir management framework. The problem can be considered as a boundary control problem and is solved using an advanced control theory called the backstepping method. The rate controller requires measurements at the well only; thus, it is an advantage from practical point of view. Further, we also consider a case where the controller requires measurements inside the domain. To this end, an observer is designed.

Water-flooding control

Control of flow rates and BHPs is important for the efficiency of water-flooding schemes. Hence, control laws for this purpose is of interest. We observed that under certain conditions, the solution of the optimization problem is equivalent to bang-bang control. Bang-bang control has a major practical advantage because it can be implemented with simple on-off valves. Therefore, we develop a method to compute the switching time control of flow rates or BHPs for bang-bang control. Two examples of realistic reservoirs show that the proposed method can be used to increase oil revenue significantly.

Long-term and short-term production optimization

Several authors have observed that there is a conflict between long term optimization focusing on recovery and short term aggressive production schemes such as reactive control, e.g., see van Essen and Van den Hof (2011). In reality, it is often the short-term goal which dictates the course of the operational strategy. Therefore, incorporating long-term goals into short-term objectives is crucial. To this end, we develop a method to systematically combine long-term and short-term goals. Further, the method is evaluated on a realistic field case.

Boundary stabilization of the wave equations

A possible generalization of reservoir flow models are general wave equations (Vazquez, 2007). Hence, extending results from the gas coning case, in particular the use of Lyapunov theory, to such models was pursued. The unidirectional wave propagation models described by the generalized Korteweg-de Vries-Burgers (KdV-Burgers) and the Benjamin-Bona-Mahony-Burgers (BBM-Burgers) equations were studied.

To this end, we design boundary controllers for both PDEs using the Lyapunov method. The controllers only require measurement at the boundary of the systems which is an advantage from a practical point of view. A numerical example is presented to visualize results. This topic is presented in chapter 5 and it is not directly linked to any petroleum engineering problems.

1.4 Control Theory

In this section, we present a brief introduction to some methods adopted from control theory which are used in this thesis.

1.4.1 Boundary control

Based on the location of the actuators and the sensors, control of PDEs can be divided into two settings; in-domain control where the actuation and sensing are distributed inside the domain, and boundary control where the actuation and sensing are applied only through boundary conditions. Physically, boundary control is considered to be more realistic since the actuation and the sensing are non-intrusive (Krstic and Smyshlyaev, 2008). For example, when we consider a sub-surface petroleum system which consists of a reservoir and wells, each well can be considered as the boundary of the system. In this case, the sensor and actuator are collocated at the well.

The aim of boundary control is to stabilize the solution of the dynamical system into its equilibrium point via its boundary conditions. Stability of the system in the context of oil production means that the system state, e.g., the height of an oil column, approaches its equilibrium point in an exponentially or asymptotically decreasing rate. One may rightly argue that a reservoir always will exhibit stable behavior. The guarantee of exponential stability implies that the drainage of oil from the reservoir is exponential, which may be advantageous from a business point of view. Two methods are presented below.

The Lyapunov method

Whether stable or not, a dynamical system can be analyzed through its explicit solutions. However, for more complex problems the explicit solution usually cannot be found, and even physical considerations may not be conclusive. Thus, it is important to develop a tool for analyzing the stability of such PDEs without actually solving them. For example, consider the following boundary value problem of the heat equation

$$w_t(x,t) = w_{xx}(x,t),\ 0<x<1,\ t>0 \tag{1.1}$$
$$w(0,t) = 0,\ t\geq 0 \tag{1.2}$$
$$w(1,t) = 0,\ t\geq 0 \tag{1.3}$$

From a physical point of view, this system is clearly stable since there is no heat generation in the system. Moreover, using separation of variables one can obtain an explicit solution which is stable, i.e., the solution goes to its equilibrium point as time approach infinity. Using the Lyapunov method, it is possible to analyze the type of stability of the above equation without solving it. To this end, consider the following energy function

$$V(t) = \frac{1}{2}\int_0^1 w^2(x,t)\,\mathrm{d}x \tag{1.4}$$

Computing its time derivative and using integration by parts, yield

$$\begin{aligned}
\dot{V}(t) &= \int_0^1 w(x,t)w_t(x,t)\,\mathrm{d}x \\
&= \int_0^1 w(x,t)w_{xx}(x,t)\,\mathrm{d}x \\
&= w(x,t)w_x(x,t)|_0^1 - \int_0^1 w_x^2(x,t)\,\mathrm{d}x \\
&= -\int_0^1 w_x^2(x,t)\,\mathrm{d}x
\end{aligned} \tag{1.5}$$

From Poincare inequality, we have

$$-\int_0^1 w_x^2(x,t)\,\mathrm{d}x \leq -\frac{1}{4}\int_0^1 w^2(x,t)\,\mathrm{d}x \tag{1.6}$$

Hence

$$\dot{V}(t) \leq -\frac{1}{4}\int_0^1 w^2(x,t)\,\mathrm{d}x = -\frac{1}{2}V(t) \tag{1.7}$$

This implies that the energy decay rate is bounded by

$$V(t) \leq V(0)e^{-\frac{t}{2}} \tag{1.8}$$

or by

$$\|w(t)\| \leq \|w(0)\|e^{-\frac{t}{4}} \tag{1.9}$$

Since the energy function is in the L^2 form, the system (1.1)-(1.3) is exponentially stable in the L^2-sense.

The backstepping method

The idea of backstepping is to use coordinate transformation

$$w(x,t) = u(x,t) - \int_0^x \kappa(x,y)u(y,t)\,\mathrm{d}y \tag{1.10}$$

to transform the original system into a target system (Krstic and Smyshlyaev, 2008). The target system is chosen such that the performance including stability properties of the target system candidate is known and fit the given problem. In our context, the target system replicates a preferred outcome of a reservoir drainage strategy. The transformation (1.10) is called the Volterra integral transformation where $\kappa(x,y)$ denotes the transformation kernel to be determined. An important property of the Volterra integral transformation is that it is invertible, so that stability of the target system translates into stability of the closed-loop system consisted the plant plus boundary controller. The inverse of (1.10) can be written in the following form

$$u(x,t) = w(x,t) + \int_0^x \gamma(x,y)w(y,t)\,\mathrm{d}y \tag{1.11}$$

where $\gamma(x,y)$ is the kernel of the inverse transformation. The problem now is to find the kernel transformation $\kappa(x,y)$ which makes the original system behave as the target system.

As an example, consider the following unstable reaction-diffusion equation (Krstic and Smyshlyaev, 2008)

$$\begin{aligned} u_t(x,t) &= u_{xx}(x,t) + \lambda u(x,y),\ 0 < x < 1,\ t > 0 && (1.12)\\ u(0,t) &= 0,\ t \geq 0 && (1.13)\\ u(1,t) &= U(t),\ t \geq 0 && (1.14) \end{aligned}$$

Under the homogeneous Dirichlet boundary conditions, the term λu is the source of unstability for $\lambda > \frac{\pi}{4}$. Using the coordinate transformation (1.10), the unstable system is transformed into the stable system (1.1)-(1.3). The kernel transformation can be found by substituting (1.10) into (1.1)-(1.3) and use the plan equations (1.12)-(1.14). This will result in the following three conditions which have to be satisfied

$$\begin{aligned} \kappa_{xx}(x,y) - \kappa_{yy}(x,y) &= \lambda\kappa(x,y) && (1.15)\\ \kappa(x,0) &= 0 && (1.16)\\ \kappa(x,x) &= -\frac{\lambda}{2}x && (1.17) \end{aligned}$$

Solving the above system using the method of successive approximations yields

$$\kappa(x,y) = -\lambda y \frac{I\left(\sqrt{\lambda(x^2-y^2)}\right)}{\left(\sqrt{\lambda(x^2-y^2)}\right)} \tag{1.18}$$

where I is the first order modified Bessel function of the first kind as follows

$$I(x) = \sum_{n=0}^{\infty} \frac{\left(\frac{x}{2}\right)^{2n+1}}{n!(n+1)!} \tag{1.19}$$

Finally, from (1.3), (1.10), and (1.14), the boundary controller can be written as

$$U(t) = -\int_0^1 \lambda y \frac{I\left(\sqrt{\lambda(x^2-y^2)}\right)}{\left(\sqrt{\lambda(x^2-y^2)}\right)} u(y,t)\,\mathrm{d}y \tag{1.20}$$

The measurements in distributed parameter systems are rarely available across the domain. It is more common for the sensors to be placed only at the boundaries. This is particularly true in problems involving fluid flows. Using backstepping method, it is possible to reconstruct the state in the domain given a measurement at the boundary only.

1.4.2 Optimal control

When formulating an optimal control problem, the variables are divided into two classes, namely the state variables and the control variables. The change in the control variables dictates the state variables via a set of differential equations. In a sub-surface petroleum system, the state variables are the fluid pressure and the saturation, while the control variables are the flow rates or BHPs of the well. An optimal control problem can be stated in a canonical form as follows

$$\begin{aligned}
\min_{\mathbf{u}} \; J(\mathbf{u}) &= \psi(\mathbf{x}(T)) + \int_0^T \mathcal{L}(\mathbf{x}(t),\mathbf{u}(t))\,\mathrm{d}t && (1.21)\\
\text{subject to } \dot{\mathbf{x}}(t) &= \mathbf{f}(\mathbf{x}(t),\mathbf{u}(t)) && (1.22)\\
\mathbf{x}(0) &= \bar{\mathbf{x}}_0 && (1.23)\\
\mathbf{u}(t) &\in \mathcal{U},\ \forall t \in [0,T] && (1.24)\\
\mathcal{U} &= \{\mathbf{q} \in \mathbb{R}^m : \mathbf{u}_{\min} \le \mathbf{q} \le \mathbf{u}_{\max}\} && (1.25)
\end{aligned}$$

where $\mathbf{x}$ denotes the state variable. Here, the objective function J in a Bolza form is to be minimized by changing the control variable $\mathbf{u}$ subject to the dynamical system (1.22)-(1.23) and control constraints (1.24)-(1.25) in a fixed time interval $[0,T]$. To solve the optimal control problem (1.21)-(1.25), the gradient can be computed using the adjoint method by employing the variation principle (Teo et al., 1991). The constraint can be appended into the cost function by introducing the Lagrange multiplier $\boldsymbol{\lambda}$ such that

$$\bar{J}(\mathbf{u}) = \psi(\mathbf{x}(T)) + \int_0^T \mathcal{L}(\mathbf{x}(t),\mathbf{u}(t)) + \boldsymbol{\lambda}^\intercal(t)[\mathbf{f}(\mathbf{x}(t),\mathbf{u}(t)) - \dot{\mathbf{x}}(t)]\,\mathrm{d}t \tag{1.26}$$

where $^\intercal$ is used as a symbol for the transpose. For simplicity, define the so-called Hamiltonian as

$$H(\mathbf{x}(t), \mathbf{u}(t), \boldsymbol{\lambda}(t)) = \mathcal{L}(\mathbf{x}(t), \mathbf{u}(t)) + \boldsymbol{\lambda}^\intercal(t)\left(\mathbf{f}(\mathbf{x}(t), \mathbf{u}(t))\right) \tag{1.27}$$

Substituting (1.27) into (1.26) and applying integration by parts, yield

$$\begin{aligned} \bar{J}(\mathbf{u}) &= \psi(\mathbf{x}(T)) - \boldsymbol{\lambda}^\intercal(T)\mathbf{x}(T) + \boldsymbol{\lambda}^\intercal(0)\mathbf{x}(0) \\ &\quad + \int_0^T \{H(\mathbf{x}(t), \mathbf{u}(t), \boldsymbol{\lambda}(t)) + \dot{\boldsymbol{\lambda}}^\intercal(t)\mathbf{x}(t)\}\,\mathrm{d}t \end{aligned} \tag{1.28}$$

For a small variation $\delta\mathbf{u}$ in $\mathbf{u}$, the corresponding first order variations $\delta\bar{J}(\mathbf{u})$ can be computed as follows

$$\begin{aligned} \delta\bar{J}(\mathbf{u}) &= \left[\frac{\partial\psi(\mathbf{x}(T))}{\partial\mathbf{x}} - \boldsymbol{\lambda}^\intercal(T)\right]\delta\mathbf{x}(T) + \boldsymbol{\lambda}^\intercal(0)\delta\mathbf{x}(0) \\ &\quad + \int_0^T \left\{\left[\frac{\partial H(\mathbf{x}(t), \mathbf{u}(t), \boldsymbol{\lambda}(t))}{\partial\mathbf{x}} + \dot{\boldsymbol{\lambda}}^\intercal(t)\right]\delta\mathbf{x}(t) + \frac{\partial H(\mathbf{x}(t), \mathbf{u}(t), \boldsymbol{\lambda}(t))}{\partial\mathbf{u}}\delta\mathbf{u}\right\}\mathrm{d}t \end{aligned} \tag{1.29}$$

Because the initial condition $\mathbf{x}(0)$ is fixed, $\delta\mathbf{x}(0)$ vanishes. Furthermore, because $\boldsymbol{\lambda}$ is arbitrary, we can set it such that

$$\dot{\boldsymbol{\lambda}}^\intercal(t) = -\frac{\partial H(\mathbf{x}(t), \mathbf{u}(t), \boldsymbol{\lambda}(t))}{\partial\mathbf{x}} \tag{1.30}$$

$$\boldsymbol{\lambda}^\intercal(T) = \frac{\partial\psi(\mathbf{x}(T))}{\partial\mathbf{x}} \tag{1.31}$$

These equations are the so-called costate equations. Because of the first order optimality condition, if the control $\mathbf{u}$ is unconstrained, then

$$\frac{\partial H(\mathbf{x}(t), \mathbf{u}(t), \boldsymbol{\lambda}(t))}{\partial\mathbf{u}} = 0 \tag{1.32}$$

If the control is constrained, then the optimal control strategy optimizes H. Hence, for a minimization problem

$$H(\mathbf{x}(t), \mathbf{u}_{\text{opt}}(t), \boldsymbol{\lambda}(t)) \leq H(\mathbf{x}(t), \mathbf{u}(t), \boldsymbol{\lambda}(t)) \tag{1.33}$$

which is called the Pontryagin Maximum Principle (Luenberger, 1979). To calculate the optimal switching times, first the dynamical system (reservoir) is simulated on the horizon $[0, T]$ to obtain the state vector $\mathbf{x}$ (pressure and saturation). Afterwards, the costate equation (1.30)-(1.31) is solved backwards to obtain the Lagrange multiplier $\boldsymbol{\lambda}$. The state and the multiplier are used to calculate the gradient of the objective function J. The gradient can be combined with a line search algorithm to find the optimal control settings.

1.4.3 Switching time method

One of the most common types of input function in control systems is the piecewise constant function, where a sequence of constant inputs is used to control a given system, with appropriate switching. As an example, let u be the control variable in $\mathbf{u}$ written in the following form

$$u = \sum_{k=0}^{M} \gamma_k \chi_{[t_k, t_{k+1})}(t) \tag{1.34}$$

where the basis of the piecewise constant function is given as

$$\chi_I(t) = \begin{cases} 1, & t \in I \\ 0, & \text{otherwise} \end{cases} \tag{1.35}$$

In the form of (1.34), the common control problem is to find the value of γ_k where the switching times t_k are fixed over the time horizon $t \in [0, T]$. However, there are some cases where γ_k is given or it only can take a few values. For example a well may only have on-off valves. This means that γ_k is a binary variable, or known as the bang-bang control.

Using optimal control theory (Teo et al., 1991), the gradient of the switching times with respect to the objective function J can be computed as follow

$$\frac{\partial J}{\partial t_k} = H(\mathbf{x}(t^-), u, \boldsymbol{\lambda}(t^-)) - H(\mathbf{x}(t^+), u, \boldsymbol{\lambda}(t^+)) \tag{1.36}$$

where H is defined as (1.27). The gradient is simply the difference between the left and the right limit of the Hamiltonian with respect to the switching times.

1.5 Contributions of this Thesis

Gas coning control

We proposed a boundary control technique for PDEs, called the backstepping method, for designing a well rate controller for the gas coning problem. The advantage of using the backstepping method is that we can construct an observer, in case measurements inside the domain are needed, in a similar way to the backstepping control design itself. To this end, a case where flow influx occurs at the outer boundary of the reservoir is considered. In this case, the controller depends on measurements inside the domain. Thus, an observer is designed using the backstepping method. Further, the rate controller is tested on a complex reservoir simulator.

Switching time method

We proposed a switching time method under bang-bang control for oil production optimization in an oil-water reservoir. The gradient is computed using the adjoint method. Further, we proposed a heuristic interval halving method to find the optimal well settings. We tested the method in realistic reservoir settings.

Long-term and short-term optimization

We proposed a method to combine long-term and short-term production optimization. The method is adopted from a multi-objective optimization method called the weighted-sum method, and is a Pareto-like approach. The proposed method is based on a priori articulation of preferences and can be used in a parallel computation framework. The method is tested on a simplified reservoir simulator of the south wing of the Voador field in the Campos basin, Brazil.

Boundary control of PDEs

We proposed two sets of boundary controllers for unidirectional waves governed by PDEs. The controllers are designed using the Lyapunov method and require measurements only at the boundary of the systems. A numerical example shows that the proposed scheme is indeed able to stabilize the solution exponentially.

1.6 Thesis Outline

This thesis is divided into 6 chapters. Chapter 1 and chapter 6 are introduction and discussion chapters. The rest of the chapters are prepared as follow:

- Chapter 2: **Optimization of oil production under gas coning conditions**.
  We formulate a proxy model of gas coning in a gas-oil reservoir as a boundary control problem. The model is written as a partial differential equation with two boundary conditions; a Neumann boundary condition representing the condition of the outer boundary of the reservoir (no external influx), and a nonlinear boundary condition representing the condition of the well. Some well rate controllers are designed for linear and non-linear cases using Lyapunov and backstepping methods. Each well rate controller is completed with a parameter that can be used to maximize a performance measure. A numerical example using a commercial simulator illustrates the merits of the method.
- Chapter 3: **Optimal time control of oil production under water-flooding conditions**.
  We optimize well operation in an oil-water reservoir. The reservoir model uses a state space representation and the control variables (flow rates or BHPs) are parameterized as piecewise constant functions over a fix time horizon assuming bang-bang control. The gradient with respect to the switching time is computed using the adjoint method.

Further, the gradient is combined with the halving interval method to find the optimal switching time. A numerical example shows the switching time method can increase recovery significantly compared to conventional reactive control.

- Chapter 4: **Decision analysis for long-term and short-term optimization**.
  There is much evidence that there exists a trade-off between long-term and short-term production goals. Here, we propose a method that combines the two goals. The novel approach is based on a priori articulation of preferences, i.e., the decision maker is allowed to specify preferences which may be articulated in terms of goals or the relative importance between long-term and short-term objectives. The method is applied to a simplified model of a real field.

- Chapter 5: **Boundary stabilization of the wave equations**.
  Unidirectional propagation of long waves in certain nonlinear dispersive systems can be modelled by the generalized Korteweg-de Vries-Burgers (KdV-Burgers) and Benjamin-Bona-Mahony-Burgers (BBM-Burgers) equations. For high order nonlinearities, both equations may have unstable solutions. In this chapter, we propose boundary controllers which stabilize both equations using the Lyapunov method. A numerical example is included to illustrate the theory.

1.7 List of Publications

Journal papers

- Hasan, A., Foss, B., Sagatun, S., Tjostheim, B., Svandal, A., Hatland, C., 2011. Modeling, Simulation, and Optimal Control of Oil Production under Gas Coning Conditions. SPE Journal of Petroleum Technology, Volume 63, Number 7, pp. 79-80.

- Hasan, A., Foss, B., Sagatun, S., 2012. Flow Control of Fluids Through Porous Media. Applied Mathematics and Computation, Volume 219, Number 7, pp. 3323-3335.

- Hasan, A., Aamo, O. M., Foss, B., 2013. Boundary Control for a Class of Pseudoparabolic Differential Equations. Systems and Control Letters, Volume 62, Number 1, pp. 63-69.

- Hasan, A., Foss, B., Sagatun, S., 2013. Optimization of Oil Production under Gas Coning Conditions. Accepted for Journal of Petroleum Science and Engineering (2013).

Conference papers

- Hasan, A., Foss, B., Sagatun, S., 2010. Boundary Control of Fluid Flow Through Porous Media. Proceedings of the 8th International Conference on Numerical Analysis and Applied Mathematics (ICNAAM), American Institute of Physics (AIP), ISBN 978-0-7354-0834-0, p. 171-174. Rhodos, Greece.

- Hasan, A., Sagatun, S., Foss, B., 2010. Well Rate Control Design for Gas Coning Problems. IEEE 49th CDC Conference Proceeding, ISBN 978-1-4244-7744-9, p. 5845-5850. Atlanta, USA.

- Hasan, A., Foss, B., Sagatun, S., Tjostheim, B., Svandal, A., Hatland, C., 2011. Modeling, Simulation, and Optimal Control of Oil Production under Gas Coning Conditions. 73rd EAGE/SPE Conference Proceeding, ISBN 978-90-73834-12-5. Vienna, Austria.

- Hasan, A., Foss, B., 2011. Global Stabilization of the Generalized Burgers-Korteweg-de Vries Equation by Boundary Control. Proceedings of the 18th IFAC World Congress, ISBN 978-3-902661-93-7, pp. 6771-6776. Milan, Italy.

- Hasan, A., Foss, B., Aamo, O. M., 2011. Boundary Control of Long Waves in Nonlinear Dispersive Systems. Proceedings of the 1st Australian Control Conference, ISBN 978-1-4244-9245-9, pp. 230-235. Melbourne, Australia.

- Hasan, A., Aamo, O. M., Foss, B., 2013. Global Boundary Feedback Stabilization for a Class of Pseudo-Parabolic PDEs. Accepted for American Control Conference. Washington DC, USA.

- Hasan, A., Foss, B., 2013. Optimal Wells Scheduling of a Petroleum Reservoir. Accepted for European Control Conference. Zurich, Swiss.

- Hasan, A., Foss, B., Krogstad, S., Gunnerud, V., Teixeira, A., 2013. Decision Analysis for Long-term and Short-term Production Optimization Applied to the South Wing of the Voador Field. Submitted to SPE Reservoir Characterisation and Simulation Conference and Exhibition.

Talks

- Hasan, A., Ciaurri, D. E., Foss, B., 2010. Optimal Well Scheduling and Control of A Petroleum Reservoir. 5th Smart Field Annual Meeting. Stanford University, USA.

- Hasan, A., Sagatun, S., Foss, B., 2010. Boundary Control of PDE's: An Application to the Gas Coning Reservoirs. ISAPP Symposium, Shell International E&P Premises. Rijswijk, The Netherland.

- Hasan, A., Foss, B., 2012. Optimal Time Control for Reservoir Optimization. 7th Smart Field Annual Meeting. Stanford University, USA.

Chapter 2

Optimization of Oil Production under Gas coning Conditions

This chapter is based on Hasan et al. (2012) which has been published in Applied Mathematics and Computation, vol 219:7, 2012 and Hasan et al. (2013b) which has been accepted in Journal of Petroleum Science and Engineering, 2013. A brief paper was also selected to appear in SPE Journal of Petroleum Technology, vol 63:7, 2011 (Hasan et al., 2011b).

2.1 Introduction

We present a brief introduction to reservoir management and gas coning control. Further, we discuss some literature reviews related to this topic.

2.1.1 Reservoir Management

The use of recovery techniques such as water-flooding and surfactant injection has been proven successful to increase recovery significantly. These techniques are now being supported by the growing interest in smart well technologies. A smart well is usually equipped with several downhole valves that can be regulated over the time (**Fig. 2.1**). Questions regarding how to operate these valves can be partially answered using optimal control theory, in particular when it is combined with the adjoint method (Brouwer and Jansen, 2004; Liu et al., 1993; Sarma and Chen, 2008). Adjoint-based optimization can also be used to determine optimal well placement (Zandvliet et al., 2008) and for history matching (Oliver et al., 2008; Oliver and Chen, 2011). Optimal control theory combined with data assimilation form the basis of closed-loop reservoir management. A comprehensive summary of this concept may be found in (Jansen et al., 2009).

The adjoint method is highly efficient for gradient calculation in large reservoir models. Hence, it provides a basis for efficient optimization algorithms. The adjoint method is how-

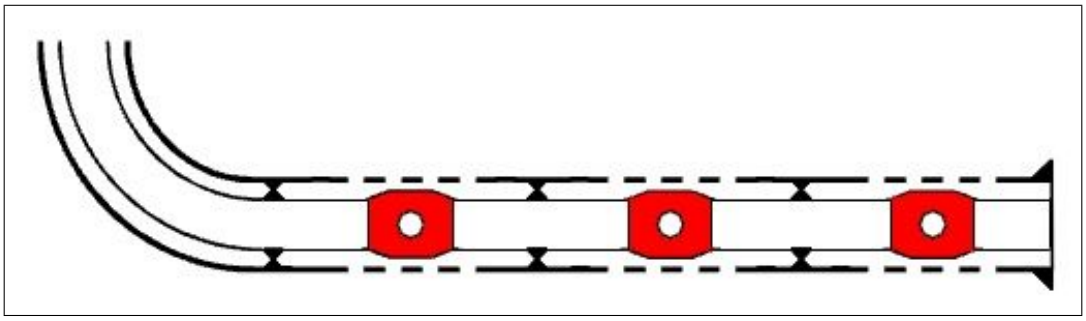

Figure 2.1: Smart horizontal well consisting of three segments, each having a down-hole control valve (Brouwer and Jansen, 2004).

ever difficult to implement, in particular for high-fidelity reservoir models. This is because one needs access to reservoir simulator code in order to implement the algorithm.

An alternative to detailed models are simpler proxy models. Just like high-fidelity models, a proxy model may be derived from physics applying mass conservation and empirical correlations like Darcy's law, however with further simplifying assumptions, or it may be derived using simulator data. An example of the latter would be proper orthogonal decomposition (POD) (Willcox and Peraire, 2002). Since the proxy model by construction is simpler than its high-fidelity counterpart, working with a proxy model is certainly much easier than working with its detailed model counterpart.

2.1.2 Automatic Control of Gas Coning

Fig. 2.2 shows a reservoir containing gas, oil, and water trapped by an overlying rock formation with zero permeability. The water layer will be assumed to be zero permeability; thus, water coning is neglected. The reservoir is completed with a single horizontal well located in the middle of the reservoir at the oil-water contact (OWC). In order for the oil to flow inside the horizontal well from the well toe to the well heel, the pressure at the well heel should be lower than the pressure at the well toe. Therefore, the difference between the average reservoir pressure and the well heel pressure will be larger than the difference between the average reservoir pressure and the well toe pressure. Since the pressure difference control fluids movements inside the reservoir, it will determine the velocity and the volume of fluid phases through the well perforation. The difference in mobility between the oil phase and the gas phase will drive the gas layer downwards. This depletion will create an inverse cone contour of the gas-oil contact (GOC) towards the well perforation. This phenomenon is called gas coning.

Typically, a well is produced with a constant oil rate with constant gas-oil ratio (GOR) during the subcritical phase, i.e., before gas breakthrough. The presence of gas coning in the production wells may reduce the oil production. The decline in the oil rate will be followed by an increase in the well head pressure. As oil price is higher than the gas price, this condition is not desirable. Moreover, the gas handling capacity often is a constraint. Therefore, there is

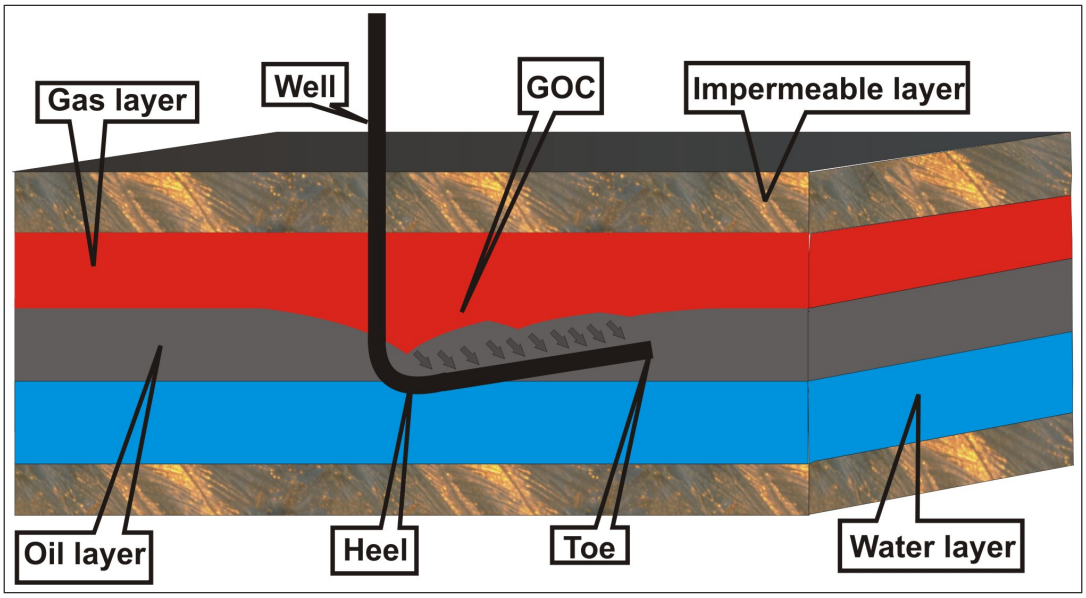

Figure 2.2: Gas coning process in a reservoir with a horizontal well.

an incentive to produce such wells in their subcritical phase, i.e., before the GOC reaches the horizontal well perforation for an extended period of time.

2.1.3 Literature Review

The first gas coning model was proposed by Muskat (1937). The model was derived from the thermodynamic relations under isothermal expansion. Using a different approach, Konieczek (1990) arrives at the same equation. In addition, in his article he introduced the boundary conditions at the outer boundary of the well and at the well heel. Mjaavatten et al. (2008), based on Konieczek's work, developed a mathematical model that could predict gas coning behaviour. Despite a simple model structure and short computation time, the accuracy of the predictions has been reported to be good. Furthermore, the model forms the basis of the gas-oil ratio model (GORM) computer program which has been used for production planning and optimization at the Troll B and C since 2003.

The use of control theory for the gas coning problem using a linear proxy model was first proposed by Sagatun (2010). In his article, he formulates an optimal oil production problem as a boundary control problem. This work was the basis for further studies where some non-linear control designs like Lyapunov and backstepping methods are introduced (Hasan et al., 2012, 2011c, 2010b,a). Other approaches on gas coning control for smart wells using a dynamic coupled well-reservoir simulator may be found in (Nennie et al., 2009) and (Leemhuis et al., 2008).

2.2 Reservoir Model

The following assumptions are used in the forthcoming reservoir model (Mjaavatten et al., 2008).

1. Only one transversal section of the reservoir will be studied; this is the section where the gas breakthrough will occur first.

2. The flow in the longitudinal direction, i.e., parallel with the well, in the reservoir is neglected. This can be justified for long reservoirs where transversal width is much less than the longitudinal distance.

3. There will be hydrostatic equilibrium in the vertical direction.

4. The vertical flow component is neglected. This may be justified because the reservoir thickness is much smaller than the reservoir width. The flow close to the wellbore is neglected.

5. It is assumed that the reservoir section is rectangular, isotropic, and homogeneous with respect to porosity and permeability. Later, we assume that the well is located in the middle of the reservoir at the OWC; thus, only half of the reservoir needs to be considered.

6. The reservoir has a free gas cap with constant pressure in time and space covering the entire reservoir top.

7. The reservoir bottom is assumed to be no-flow boundary; thus, water coning is neglected.

8. The reservoir outer boundary is a no-flow boundary.

9. The capillary forces are neglected, and a segregated flow is assumed; thus, there is a well-defined GOC. A consequence of this is that we neglect the effect of connate-water saturation and residual oil.

10. The oil and gas pressure-volume-temperature (PVT) properties are assumed constant in the reservoir. Thus, the oil is treated as incompressible. Investigation of the PVT properties reveals that this assumption is valid for many homogeneous horizontal reservoir. The model used can be updated for slowly varying PVT properties if required.

11. Horizontal reservoir pressure gradients are neglected.

12. Only Darcy's flow from the gravity based pressure gradient is considered.

Assumptions 4 and 11 are the so-called Dupuit assumption (Bear, 1972).

The model may now be derived. The equation of continuity may be written as

$$-\nabla q + s = (h\phi)_t \tag{2.1}$$

where q is the volumetric flux per unit well length, s represent the source per unit well area, ϕ is the effective porosity, i.e., the volume fraction occupied by movable oil, and h is the height of the oil column. Assumptions 7 and 8 ensure that $s = 0$.

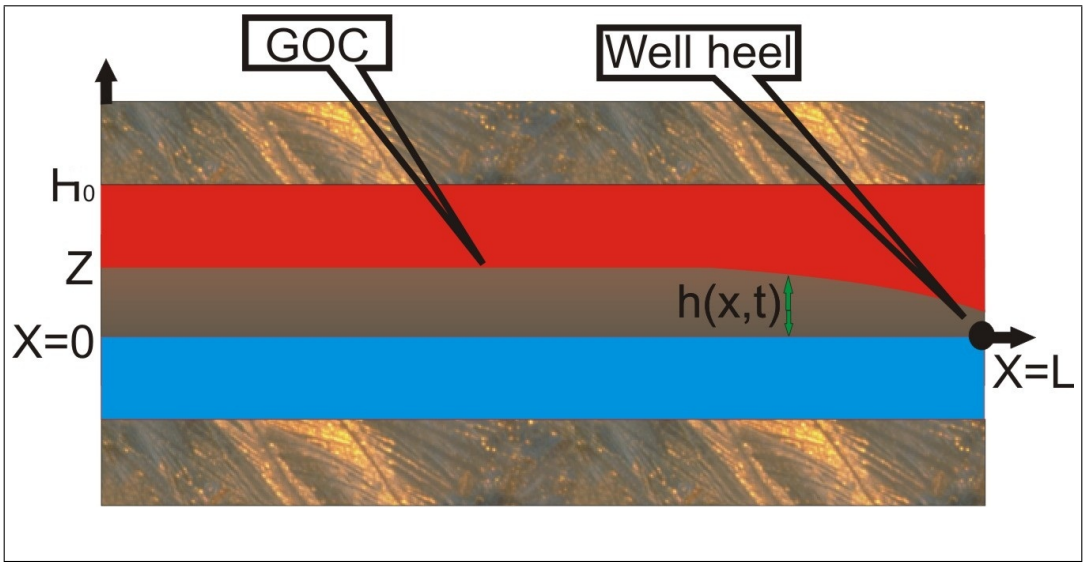

Figure 2.3: Cross section of GOC at the well heel (half domain).

Since the pressure difference between the average reservoir pressure and the horizontal well pressure is higher at the well heel than at the well toe, gas coning will occur first at the well heel. Considering the subcritical phase only, i.e., before the free gas reaches the well perforation, the model can be reduced into a one dimensional problem at the well heel (**Fig. 2.3**). Here, h_0 denotes the thickness of the gas and oil layers. Denote the pressure in the reservoir at level $z = h_0$ by p_0. By assumptions 1 and 3, the pressure in the oil column in the range $z \in [0, h(x,t)]$ at any point $x \in \mathbb{R}[0, L]$ and any given time $t \in \mathbb{R} > 0$ is given by

$$p(x,z,t) = p_0 + \rho_g g[h_0 - h(x,t)] + \rho_o g[h(x,t) - z] \tag{2.2}$$

where ρ_o and ρ_g denote the oil and gas densities, respectively, and g is the gravity constant. Thus, the pressure gradient in the oil column along the x-direction is given by

$$p_x = \Delta\rho g h_x \tag{2.3}$$

where $\Delta\rho = (\rho_o - \rho_g)$. The oil velocity in the reservoir is described by Darcy's law as

$$v = \frac{\mathbb{K}}{\mu_o} p_x = \frac{\mathbb{K}}{\mu_o} \Delta\rho g h_x \tag{2.4}$$

where $\mathbb{K}$ is the permeability tensor while μ_o is the oil viscosity. By assumption 5, the permeability tensor is reduced to $\mathbb{K} = k_h$. The volumetric flow rate q per unit well length is given by

$$q = -\int_0^{h(x,t)} \nu \, \mathrm{d}z = -\frac{k_h}{\mu_o} \Delta\rho g h h_x \tag{2.5}$$

Substituting (2.5) into (2.1), the height of the oil column in **Fig. 2.3** can be described by a nonlinear diffusion equation (Muskat, 1937; Konieczek, 1990)

$$h_t(x,t) = \alpha(h(x,t)h_x(x,t))_x \tag{2.6}$$

where $\alpha = \frac{k_h g \Delta\rho}{\mu_o \phi}$. For a thin oil reservoir ($L >> h$), the outer boundary of the well drainage area is modeled as a no-flow boundary (assumption 8)

$$h_x(0,t) = 0 \tag{2.7}$$

Accounting for the half well symmetry, the well production rate is given by (Konieczek, 1990)

$$u(t) = -2\alpha\phi h(L,t)h_x(L,t) \tag{2.8}$$

Further, (5.9)-(5.12) are made dimensionless by the following transformation

$$\bar{h} = \frac{h}{L}, \quad \bar{x} = \frac{x}{L}, \quad \bar{t} = t\frac{k_h g \Delta\rho}{\mu_o \phi L}, \quad \bar{u} = u\frac{\mu}{k_h g \Delta\rho L} \tag{2.9}$$

This yields the following partial differential equation (PDE)

$$\bar{h}_{\bar{t}}(\bar{x},\bar{t}) = (\bar{h}(\bar{x},\bar{t})\bar{h}_{\bar{x}}(\bar{x},\bar{t}))_{\bar{x}}, \; 0 < \bar{x} < 1, \; t > 0 \tag{2.10}$$

$$\bar{h}_{\bar{x}}(0,\bar{t}) = 0, \; \bar{t} \geq 0 \tag{2.11}$$

$$\bar{h}(1,\bar{t})\bar{h}_{\bar{x}}(1,\bar{t}) = -\frac{1}{2}\bar{u}(\bar{t}), \; \bar{t} \geq 0 \tag{2.12}$$

where $\bar{x} \in \mathbb{R}[0,1]$ and $\bar{t} \in \mathbb{R} > 0$. The initial condition for this system is given by

$$\bar{h}(\bar{x},0) = h_0(\bar{x}), \; 0 < \bar{x} < 1 \tag{2.13}$$

where h_0 is constant over $\bar{x} \in \mathbb{R}[0,1]$. For brevity, in the following section the bars denoting dimensionless parameters will be omitted.

Remark that system (2.10)-(2.12) is a boundary control problem of a nonlinear diffusion equation with nonlinear boundary conditions. Equation (2.10) is called the Boussinesq equation (in some literature referred to as the porous media equation). According to Kochina (1962), (2.10) can be simplified to any of the following equations

$$h_t(x,t) = h_c h_{xx}(x,t), \; 0 < x < 1, \; t > 0 \tag{2.14}$$

$$h_t(x,t) = h_x^2(x,t), \; 0 < x < 1, \; t > 0 \tag{2.15}$$

$$h_t(x,t) = h_c h_{xx}(x,t) + h_x^2(x,t), \; 0 < x < 1, \; t > 0 \tag{2.16}$$

where the subscript c denotes a constant and h_c represents the height where the GOC is assumed to be when depleting the reservoir subcritically. Without loss of generality choose $h_c = 1$. Equation (2.14) is known as the heat equation, an important PDE that describes the distribution of heat. This approximation is valid when $h(x,t) \approx 0$ which occurs when the oil layer thickness (h_0) is much less than reservoir width (L). Equation (2.15) is known as the Eikonal equation, a first-order equation of the Hamilton-Jacobi type that propagates along characteristics. This approximation is valid when $h(x,t) \approx 1$ which occurs when the reservoir width is close to the reservoir thickness. The equation(2.16) combines (2.14) and (2.15) and is called the inhomogeneous heat equation. In the following section, the boundary control of the linear and nonlinear equations above will be discussed in more detail.

2.3 Well Rate Lyapunov Based Design

In this section, the well production rate $u(t)$ will be constructed using the Lyapunov method for different cases. The aim is to design simple control laws. The first subsection starts with the quadratic control law for the heat equation in Sagatun (2010), inspects the models and uses stability criteria to arrive at the proposed controllers.

Recall that there is an incentive to produce as much oil as possible before the gas reaches the well perforation (subcritical phase). Thus, the question on how to control the gas through the reservoir is translated into a question on how to construct the control input $u(t)$ such that the oil thickness $h(x,t) \to 0$ asymptotically or exponentially. In other words, the task is to design a well rate controller $u(t)$ such that the system (2.10)-(2.12) is exponentially (or at least asymptotically) stable. Exponential stability means that the system state, i.e., the height of oil column h, approaches its equilibrium point ($h \equiv 0$) in a way which is bounded above by an exponentially decreasing function. One may rightly argue that a reservoir always will exhibit stable behavior. The guarantee of exponential stability in this context implies that the drainage of oil from the reservoir is exponential, thus advantageous from a business point of view. Furthermore, the exponential stability property is useful when the well rate controller $u(t)$ is combined with more advanced production strategies involving injection. Furthermore, the controller will include a parameter that can be tuned to maximize a suitable measure such as net present value before gas breakthrough.

Investigation during the subcritical phase also means that the height of the oil column will be above the well diameter h_w. Thus, $h(x,t)$ is bounded by

$$\inf_{x\in[0,1]} \|h(x,t)\| = h_w \leq h(x,t) \leq h_0 = \sup_{x\in[0,1]} \|h(x,t)\| \tag{2.17}$$

The Lyapunov method will be applied to construct the controllers for the systems. This method is a common tool to analyze the stability of the dynamical system (Khalil, 2001).

Definition 1. *A Lyapunov function is a scalar function $V(x)$ defined on a region D that is continuous, positive definite ($V(x) > 0, \forall x \neq 0$), and has continuous first-order derivatives at every point of D.*

The existence of a Lyapunov function for which $\dot{V}(x)$ is negative definite on some region D containing the origin guarantees asymptotic stability of the zero solution of the system. Exponential stability is a stricter form of asymptotic stability bacause it requires exponential decay towards the origin.

2.3.1 Linear Heat Equation

Consider the boundary value problem of the linear heat equation as follows

$$\begin{aligned} h_t(x,t) &= h_{xx}(x,t),\ 0<x<1,\ t>0 && (2.18)\\ h_x(0,t) &= 0,\ t\geq 0 && (2.19)\\ h(1,t)h_x(1,t) &= -\frac{1}{2}u(t),\ t\geq 0 && (2.20) \end{aligned}$$

Define the Lyapunov function as

$$V(t)=\int_0^1 h^2(x,t)\,\mathrm{d}x \tag{2.21}$$

Computing its time derivative and using integration by parts, yields

$$\dot{V}(t)=-u(t)-2\int_0^1 h_x^2(x,t)\,\mathrm{d}x \tag{2.22}$$

Let

$$u(t)=\alpha h^2(1,t) \tag{2.23}$$

hence

$$\dot{V}(t)=-\alpha h^2(1,t)-2\int_0^1 h_x^2(x,t)\,\mathrm{d}x \tag{2.24}$$

Using Poincare's inequality

$$\int_0^1 h^2(x,t)\,\mathrm{d}x\leq 2h^2(1,t)+4\int_0^1 h_x^2(x,t)\,\mathrm{d}x \tag{2.25}$$

yields

$$\dot{V}(t)\leq -\frac{1}{2}\min(1,\alpha)\int_0^1 h^2(x,t)\,\mathrm{d}x=-\frac{1}{2}\min(1,\alpha)V(t) \tag{2.26}$$

which implies that the Lyapunov function is bounded by

$$V(t)\leq V(0)e^{-\min\left(\frac{1}{2},\frac{\alpha}{2}\right)t} \tag{2.27}$$

or by

$$\|h(t)\| \leq \|h_0\| e^{-\min\left(\frac{1}{4}, \frac{\alpha}{4}\right)t} \tag{2.28}$$

where $h_0 = h(x, 0)$ is the initial condition and $\|\cdot\|$ denotes the L^2-norm of a function of x, namely

$$\|h(t)\| = \left(\int_0^1 h^2(x,t)\,\mathrm{d}x \right)^{\frac{1}{2}} \tag{2.29}$$

Furthermore, this equation implies that the equilibrium $h(x, t) \equiv 0$ is globally exponentially stable in $L^2[0, 1]$. Hence, the control law (2.23) where $\alpha > 0$, exponentially stabilizes the zero solution $h(x, t) \equiv 0$ of the system (2.18)-(2.20) in the L^2-norm. Remark that the control law (2.23) is equal to the control law proposed in Sagatun (2010).

2.3.2 Eikonal Equation

For the second case, consider the following boundary value problem

$$h_t(x,t) = h_x^2(x,t),\ 0 < x < 1,\ t > 0 \tag{2.30}$$

$$h_x(0,t) = 0,\ t \geq 0 \tag{2.31}$$

$$h(1,t)h_x(1,t) = -\frac{1}{2}u(t),\ t \geq 0 \tag{2.32}$$

Differentiating (2.30) with respect to x yields

$$h_{tx}(x,t) = 2h_x(x,t)h_{xx}(x,t) \tag{2.33}$$

Let

$$w(x,t) = h_x(x,t) \tag{2.34}$$

then

$$h(x,t) = \int_0^x w(\xi,t)\,\mathrm{d}\xi \tag{2.35}$$

Substituting (2.34) into (2.33) yields

$$w_t(x,t) = 2w(x,t)w_x(x,t) \tag{2.36}$$

Further, let

$$u(t) = -2h(1,t)q(t) \tag{2.37}$$

Then, the nonlinear boundary condition (2.32) becomes a Neumann boundary condition

$$h_x(1,t) = q(t) \tag{2.38}$$

and system (2.30)-(2.32) is equivalent to the following system

$$\begin{aligned} w_t(x,t) &= 2w(x,t)w_x(x,t) && (2.39)\\ w(0,t) &= 0 && (2.40)\\ w(1,t) &= q(t) && (2.41) \end{aligned}$$

Next, define the Lyapunov function

$$V(t) = \int_0^1 w^2(x,t)\,\mathrm{d}x \tag{2.42}$$

and compute its time derivative using the transformed system above, which yields

$$\dot{V}(t) = \frac{4}{3}q^3(t) \tag{2.43}$$

Choose

$$q(t) = -\sqrt[3]{\frac{3}{4}\beta \int_0^1 |w_x(x,t)|^3\,\mathrm{d}x} \tag{2.44}$$

where $\beta > 0$, which yields

$$\dot{V}(t) = -\beta \int_0^1 |w_x(x,t)|^3\,\mathrm{d}x \tag{2.45}$$

From Poincare's and Holder's inequalities

$$\begin{aligned} \int_0^1 w^2\,\mathrm{d}x &\leq 2\int_0^1 w_x^2(x,t)\,\mathrm{d}x && (2.46)\\ &\leq 2\left(\int_0^1 |w_x(x,t)|^3\,\mathrm{d}x\right)^{\frac{2}{3}}\left(\int_0^1 1^3\,\mathrm{d}x\right)^{\frac{1}{3}} && (2.47)\\ &\leq 2\left(\int_0^1 |w_x(x,t)|^3\,\mathrm{d}x\right)^{\frac{2}{3}} && (2.48) \end{aligned}$$

This yields

$$\dot{V}(t) \leq -\frac{\beta}{2^{\frac{3}{2}}}V^{\frac{3}{2}}(t) \tag{2.49}$$

It then follows that

$$\int_0^1 w(x,t)^2\,\mathrm{d}x \leq \frac{\int_0^1 w(x,0)^2\,\mathrm{d}x}{\left(1+t\frac{\beta}{8}\sqrt{\int_0^1 w(x,0)^2\,\mathrm{d}x}\right)^2} \tag{2.50}$$

This implies that the equilibrium $w(x,t) \equiv 0$ is globally asymptotically stable in $L^2[0,1]$. Because $w(x,t) = \frac{\partial h}{\partial x}(x,t)$, the equilibrium $h(x,t) \equiv 0$ is globally asymptotically stable in $H^1[0,1]$. Thus, The control law

$$u(t) = 2h(1,t)\sqrt[3]{\frac{3}{4}\beta\int_0^1 |h_{xx}(x,t)|^3\,\mathrm{d}x} \tag{2.51}$$

where $\beta > 0$, asymptotically stabilizes the zero solution $h(x,t) \equiv 0$ of the system (2.30)-(2.32) in $H^1[0,1]$. Remark that the control law (2.51) requires measurements from the interior of the domain. Thus, we have an in-domain controller. Because these measurements may be impossible to obtain, an observer who estimates $\frac{\partial^2 h}{\partial x^2}(x,t)$ should be constructed. This observer could be obtained using a backstepping method (Hasan et al., 2010b).

2.3.3 Inhomogeneous Heat Equation

For the third case, consider the following boundary value problem

$$h_t(x,t) = h_{xx}(x,t) + h_x^2(x,t),\ 0 < x < 1,\ t > 0 \tag{2.52}$$
$$h_x(0,t) = 0,\ t \geq 0 \tag{2.53}$$
$$h(1,t)h_x(1,t) = -\frac{1}{2}u(t),\ t \geq 0 \tag{2.54}$$

Define the Lyapunov function

$$V(t) = \int_0^1 h^2(x,t)\,\mathrm{d}x \tag{2.55}$$

and compute its time derivative, which yields

$$\dot{V}(t) = 2\int_0^1 h(x,t)\Big(h_{xx}(x,t) + h_x^2(x,t)\Big)\,\mathrm{d}x \tag{2.56}$$

Using integration by parts, (2.56) yields

$$\dot{V}(t) = 2h(x,t)h_x(x,t)|_0^1 - 2\int_0^1 h_x^2(x,t)\,\mathrm{d}x + 2\int_0^1 h(x,t)h_x^2(x,t)\,\mathrm{d}x \tag{2.57}$$

Substituting (2.53) and (2.54) into (2.57) and using (2.17) yields

$$\dot{V}(t) \leq -u(t) - 2\int_0^1 h_x^2(x,t)\,\mathrm{d}x + 2\sup_{x\in[0,1]}\|h(x,t)\|\int_0^1 h_x^2(x,t)\,\mathrm{d}x \tag{2.58}$$

Choose

$$u(t) = \lambda h^2(1,t) \tag{2.59}$$

hence

$$\dot{V}(t) = -\lambda h^2(1,t) \leq 0 \tag{2.60}$$

This implies that the equilibrium $h(x,t) \equiv 0$ is globally asymptotically stable in $L^2[0,1]$. Thus, the control law (2.59) where $\lambda > 0$, asymptotically stabilizes the zero solution $h(x,t) \equiv 0$ of the system (2.52)-(2.54) in the L^2-norm.

2.3.4 Boussinesq Equation

Now, consider the following boundary value problem

$$\begin{aligned} h_t(x,t) &= h(x,t)h_{xx}(x,t) + h_x^2(x,t),\ 0 < x < 1,\ t > 0 && (2.61)\\ h_x(0,t) &= 0,\ t \geq 0 && (2.62)\\ h(1,t)h_x(1,t) &= -\frac{1}{2}u(t),\ t \geq 0 && (2.63) \end{aligned}$$

Define the Lyapunov function

$$V(t) = \int_0^1 h^2(x,t)\,\mathrm{d}x \tag{2.64}$$

and compute its time derivative

$$\dot{V}(t) = 2\int_0^1 h(x,t)\Big(h(x,t)h_{xx}(x,t) + h_x^2(x,t)\Big)\,\mathrm{d}x \tag{2.65}$$

Using integration by parts, (2.65) yields

$$\begin{aligned} \dot{V}(t) &= 2h^2(x,t)h_x(x,t)|_0^1 - 4\int_0^1 h(x,t)hx^2(x,t)\,\mathrm{d}x && (2.66)\\ &\quad +2\int_0^1 h(x,t)h_x^2(x,t)\,\mathrm{d}x && (2.67)\\ &= 2h^2(x,t)h_x(x,t)|_0^1 - 2\int_0^1 h(x,t)h_x^2(x,t)\,\mathrm{d}x && (2.68) \end{aligned}$$

Substituting (2.62) and (2.63) into (2.68), and using (2.17), yields

$$\dot{V}(t) \leq -u(t)h(1,t) - 2\inf_{x\in[0,1]}\|h(x,t)\|\int_0^1 h_x^2(x,t)\,\mathrm{d}x \tag{2.69}$$

$$= -u(t)h(1,t) - 2h_w\int_0^1 h_x^2(x,t)\,\mathrm{d}x \tag{2.70}$$

Choose

$$u(t) = \gamma h(1,t) \tag{2.71}$$

This equation yields

$$\dot{V}(t) \leq -\gamma h^2(1,t) - 2h_w\int_0^1 h_x^2(x,t)\,\mathrm{d}x \tag{2.72}$$

Using Poincare's inequality

$$\int_0^1 h^2(x,t)\,\mathrm{d}x \leq 2h^2(1,t) + 4\int_0^1 h_x^2(x,t)\,\mathrm{d}x \tag{2.73}$$

yields

$$\dot{V}(t) \leq -\frac{1}{2}\min(h_w,\gamma)\int_0^1 h^2(x,t)\,\mathrm{d}x = -\min\left(\frac{h_w}{2},\frac{\gamma}{2}\right)V(t) \tag{2.74}$$

This result implies that the equilibrium $h(x,t)\equiv 0$ is globally exponentially stable in $L^2[0,1]$. Thus, the control law (2.71) where $\gamma > 0$ exponentially stabilizes the zero solution $h(x,t)\equiv 0$ of the system (2.61)-(2.63) in $L^2[0,1]$.

2.3.5 Model Comparison

As mentioned in Section 2, the Boussinesq equation (2.10) can be approximated by the heat equation (2.14), the Eikonal equation (2.15) or the inhomogeneous heat equation (2.16). The heat equation and the inhomogeneous heat equation are valid when the reservoir thickness is much less than the reservoir width, i.e., $h(x,t)\approx 0$, while the Eikonal equation is valid when the reservoir thickness is close to the reservoir width, i.e., $h(x,t)\approx 1$. For these reasons, the comparison will be divided into two cases; $h(x,t)\approx 0$ and $h(x,t)\approx 1$.

Fig. 2.4 shows comparisons of GOC using (2.10), (2.14), and (2.16), respectively. These are cases where the reservoir thickness is much less than the reservoir width. It can be observed that the heat equation (linear model) and the inhomogeneous heat equation give a good approximation to the nonlinear Boussinesq equation. In practice, the linear model is often used for modeling a thin oil rim reservoir because it is easier to analyze a linear system

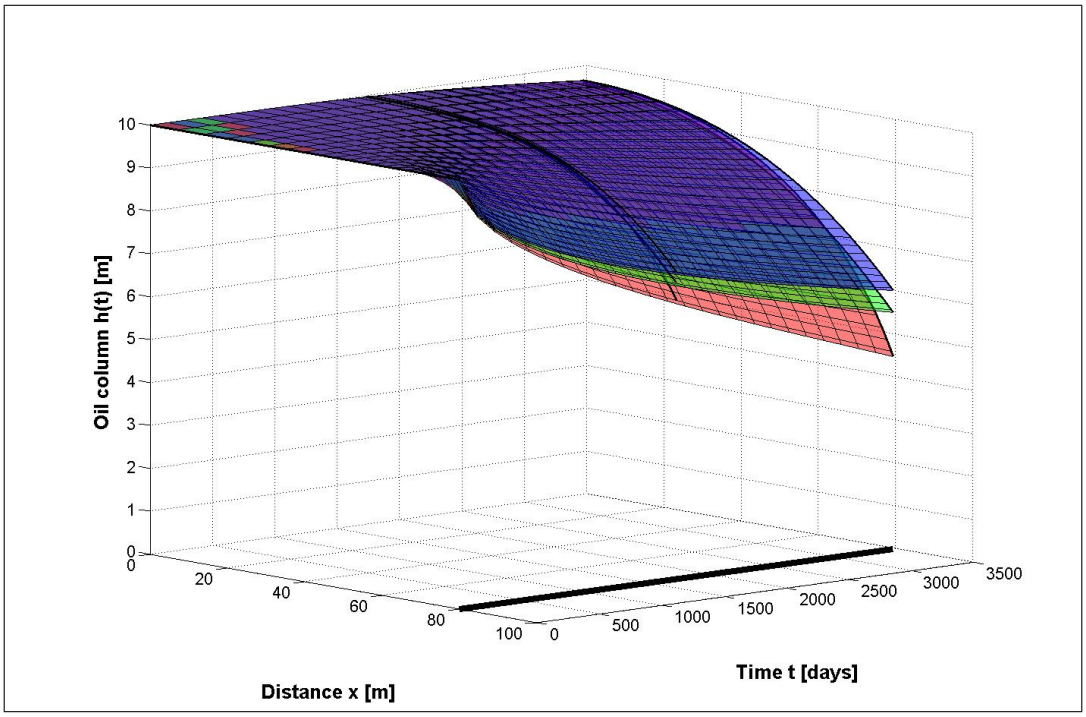

Figure 2.4: The nonlinear Boussinesq equation (red), the inhomogeneous heat equation (green), and the heat equation (blue) with the initial height of the oil column set at 10m. The surface shows the GOC as a function of time. The well heel is placed at $x = 80$m.

rather than a nonlinear system (Sagatun, 2010; Hasan et al., 2010b). Note that the figures show depletion at the well heel, which is only plotted along the time horizon t.

When the reservoir thickness is close to the reservoir width, the Eikonal equation (2.15) serves as a good approximation for the Boussinesq equation (2.10). This is confirmed by **Fig. 2.5** where the initial height of the oil column is increased to 80m. This approximation works because when $h(x,t) \approx 1$, the gradient term $\frac{\partial}{\partial x}h(x,t)$ will be the main factor for the fluid to flow through porous media.

The simulation is done using the *pdepe.m* function in MATLAB, which was written based on Skeel and Berzins (1990).

2.4 Well Rate Backstepping Based Design

In this section, the well production rate (2.12) is designed using the backstepping method. Backstepping and boundary control can be seen as a perfect match as explained by Krstic and Smyshlyaev (2008). Furthermore, using the backstepping method, one can construct an observer for the particular system if measurements inside the domain, i.e., not on the boundary, are required in a similar way to the backstepping control design itself. This feature is an advantage of the backstepping method over other methods, e.g., the Lyapunov method.

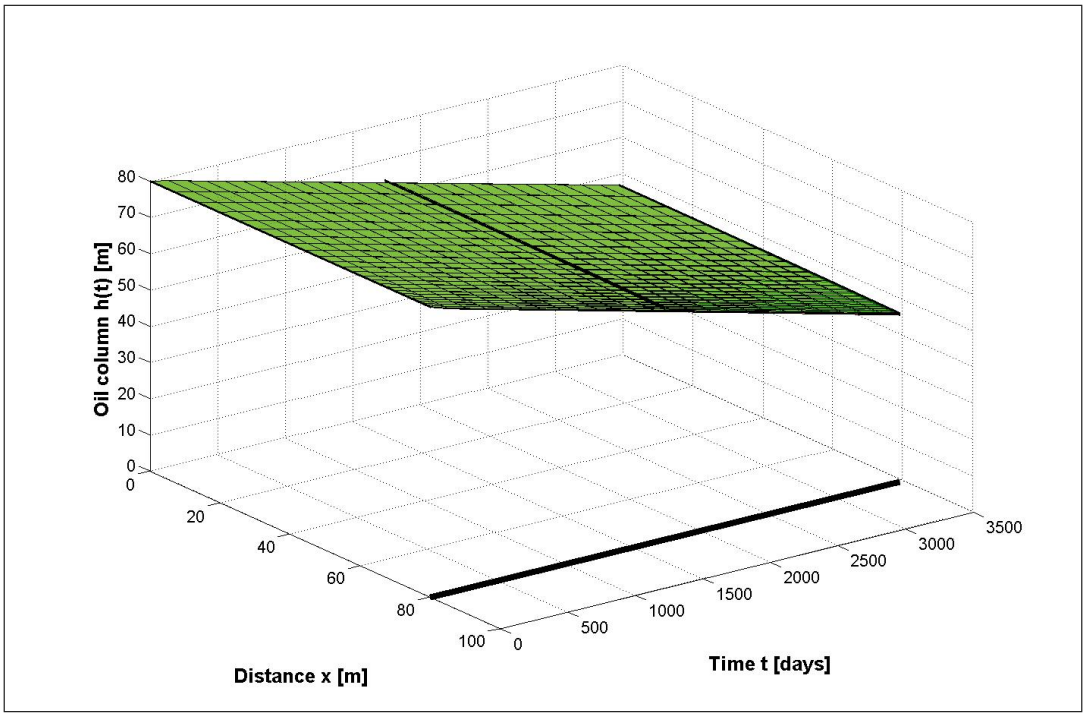

Figure 2.5: The nonlinear Boussinesq equation (red) and the Eikonal equation (green) are overlapping, with the initial height of oil the column set at 80m. The surface shows the GOC as a function of time. The well heel is placed at $x = 80$m.

The following dimensionless gas coning model is first considered.

$$h_t(x,t) = h_{xx}(x,t) \tag{2.75}$$
$$h_x(0,t) = 0 \tag{2.76}$$
$$h(1,t)h_x(1,t) = -\frac{1}{2}u(t) \tag{2.77}$$

The idea of backstepping is to use coordinate transformation

$$\omega(x,t) = h(x,t) - \int_0^x \kappa(x,y)h(y,t)\,\mathrm{d}y \tag{2.78}$$

to transform system (2.75)-(2.77) into a target system. The target system is chosen such that the performance including stability properties of the target system candidate is known and fit with the given problem. In this context, the target system replicated a preferred reservoir drainage strategy. The transformation (2.78) is called the Volterra integral transformation with $\kappa(x,y)$ denotes the transformation kernel to be determined. An important property of Volterra integral transformation is that it is invertible, so that stability of the target system translates into stability of the closed-loop system consisting the plant plus boundary con-

troller. The inverse of (2.78) can be written in the following form

$$h(x,t) = \omega(x,t) + \int_0^x \gamma(x,y)\omega(y,t)\,\mathrm{d}y \tag{2.79}$$

where $\gamma(x,y)$ is the kernel of the inverse transformation. The problem now is to find the kernel transformation $\kappa(x,y)$ that makes the system (2.75)-(2.77) behave as the target system.

The target system which is chosen for system (2.75)-(2.77) is the following heat equation with Robin and Neumann boundary conditions

$$\begin{aligned}
\omega_t(x,t) &= \omega_{xx}(x,t) && (2.80)\\
\omega_x(0,t) &= \frac{\lambda}{2}\omega(0,t) && (2.81)\\
\omega_x(1,t) &= 0 && (2.82)
\end{aligned}$$

where $\lambda > 0$, which is exponentially stable in the sense of an L^2-norm. Exponential stability in the L^2-norm means that the quantity of $\int_0^1 h^2(x,t)\,\mathrm{d}x$ decays to zero exponentially.

To construct the controller $u(t)$ using the backstepping method, first calculate the second derivative of the transformation (2.78) with respect to x. This yields

$$\begin{aligned}
\omega_{xx}(x,t) &= h_{xx}(x,t) - h(x,t)\frac{\mathrm{d}}{\mathrm{d}x}\kappa(x,x) - \kappa(x,x)h_x(x,t)\\
&\quad -\kappa_x(x,x)h(x,t) - \int_0^x \kappa_{xx}(x,y)h(y,t)\,\mathrm{d}y
\end{aligned} \tag{2.83}$$

Next, calculate the first derivative of the transformation (2.78) with respect to time t.

$$\begin{aligned}
\omega_t(x,t) &= h_{xx}(x,t) - \kappa(x,x)h_x(x,t) + \kappa(x,0)h_x(0,t) + \kappa_y(x,x)h(x,t)\\
&\quad -\kappa_y(x,0)h(0,t) - \int_0^x \kappa_{yy}(x,y)h(y,t)\,\mathrm{d}y
\end{aligned} \tag{2.84}$$

Subtracting the last two equations, leads to

$$\begin{aligned}
\omega_t(x,t) - \omega_{xx}(x,t) &= 2h(x,t)\frac{\mathrm{d}}{\mathrm{d}x}\kappa(x,x) - \kappa_y(x,0)h(0,t)\\
&\quad - \int_0^x (\kappa_{yy}(x,y) - \kappa_{xx}(x,t))h(y,t)\,\mathrm{d}y
\end{aligned} \tag{2.85}$$

In view of the target system (2.80)-(2.82), this leads to the three following conditions which should be satisfied

$$\begin{aligned}
\kappa_{yy}(x,y) &= \kappa_{xx}(x,y) && (2.86)\\
\kappa_y(x,0) &= 0 && (2.87)\\
\kappa(x,x) &= -\frac{\lambda}{2} && (2.88)
\end{aligned}$$

The solution of this system is given by

$$\kappa(x, y) = -\frac{\lambda}{2} \tag{2.89}$$

Note that

$$\omega_x(1, t) = h_x(1, t) + \frac{\lambda}{2} h(1, t) \tag{2.90}$$

Since $\omega_x(1, t) = 0$, then

$$h_x(1, t) = -\frac{\lambda}{2} h(1, t) \tag{2.91}$$

Hence, the rate controller is obtained by substituting (2.91) into (2.77), that is

$$u(t) = \lambda h^2(1, t) \tag{2.92}$$

The controller (2.92) is equal to the controller developed by Sagatun (2010). The control gain λ is a tuning parameter that can optimize a cost function, e.g., the accumulated oil production or the net present value (NPV) until gas breakthrough. The positive parameter λ can then be found using a simple search optimization method. This implies that one searches within a class of controllers which guarantees exponential behavior. Since the control rate (2.92) is developed for the subcritical phase, this method will be more suitable for a new well.

As an alternative, the optimal decay may be specified with multiple parameters, using e.g., polynomial basis functions of which the coefficients serve as the to be optimized parameters. However, based on criteria presented in this chapter, we perform a single-parameter optimization as given by (2.92).

2.5 Backstepping Based Design with Boundary Influx

In this section, consider the area around the well where the oil influx occurs; thus, the gradient of the oil column in the reservoir $\partial_x h(x, t) \neq 0$. Let $d \in \mathbb{R}[0, 1]$ be a distance from the well where the height of oil column starts to decrease significantly. This distance can be interpreted as an artificial boundary. Furthermore, assume that the gradient of the oil column is given by the following inflow condition $h_x(d, t) = -\epsilon h(d, t), \forall \epsilon > 0$. Without loss of generality let $d = 0$ and consider the following system

$$\begin{aligned} h_t(x, t) &= h_{xx}(x, t) && (2.93)\\ h_x(0, t) &= -\epsilon h(0, t) && (2.94)\\ h(1, t) h_x(1, t) &= -\frac{1}{2} u(t) && (2.95) \end{aligned}$$

The task is to design the well rate controller $u(t)$ such that the system (2.93)-(2.95) is exponentially stable. The target system chosen for this case is as follows

$$\begin{aligned} \omega_t(x,t) &= \omega_{xx}(x,t) && (2.96)\\ \omega_x(0,t) &= 0 && (2.97)\\ \omega_x(1,t) &= -\frac{\zeta}{2}\omega(1,t) && (2.98) \end{aligned}$$

where $\zeta > 0$, which also exponentially stable in the sense of the L^2 norm.

Substituting the Volterra integral transformation (2.78) into the target system (2.96)-(2.98), yields

$$\begin{aligned} \omega_t(x,t) - \omega_{xx}(x,t) &= 2h(x,t)\frac{\mathrm{d}}{\mathrm{d}x}\kappa(x,x) + \kappa(x,0)h_x(0,t) \\ &\quad -\kappa_y(x,0)h(0,t) \\ &\quad -\int_0^x (\kappa_{yy}(x,y) - \kappa_{xx}(x,y))h(y,t)\,\mathrm{d}y \end{aligned} \tag{2.99}$$

This leads to the three following conditions that should be satisfied

$$\begin{aligned} \kappa_{xx}(x,y) &= \kappa_{yy}(x,y) && (2.100)\\ \kappa_y(x,0) &= -\epsilon\kappa(x,0) && (2.101)\\ \kappa(x,x) &= -\epsilon && (2.102) \end{aligned}$$

This PDE is a type of hyperbolic equation which has a general solution $\kappa(x,y) = \varphi(x-y) + \psi(x+y)$. The fact that $\kappa(x,x) = -\epsilon$ makes it easy to show that $\psi = 0$. Thus, the particular solution for the system is given by

$$\kappa(x,y) = -\epsilon e^{\epsilon(x-y)} \tag{2.103}$$

Note that, since

$$\omega(1,t) = h(1,t) + \epsilon\int_0^1 e^{\epsilon(x-y)}h(y,t)\,\mathrm{d}y \tag{2.104}$$

and

$$\omega_x(1,t) = h_x(1,t) + \epsilon h(1,t) + \epsilon^2\int_0^1 e^{\epsilon(1-y)}h(y,t)\,\mathrm{d}y \tag{2.105}$$

Substituting (2.104) and (2.105) into (2.98), yields

$$h_x(1,t) = -\frac{1}{2}(2\epsilon+\zeta)h(1,t) - \frac{1}{2}(2\epsilon+\zeta)\epsilon\int_0^1 e^{\epsilon(1-y)}h(y,t)\,\mathrm{d}y \tag{2.106}$$

Hence, the controller is obtained by substituting (5.57) into (2.95), that is

$$u(t) = (\zeta + 2\epsilon)h^2(1,t) + (\zeta + 2\epsilon)\epsilon h(1,t)\int_0^1 e^{\epsilon(1-y)}h(y,t)\,\mathrm{d}y \tag{2.107}$$

When the influx parameter $\epsilon \to 0$, the solution of the closed-loop system (2.93)-(2.95) will converge to the solution of the closed-loop system (2.75)-(2.77). In particular, the controller (2.107) will converge to the controller (2.92). Since the kernel $\kappa(x,y)$ exists for the above problem, L^2 stability is guaranteed. The L^2 stability implies that there exists a positive constant $M \in \mathbb{R}$ such that

$$\int_0^1 |h(x,t)|^2\,\mathrm{d}x \le M < \infty \tag{2.108}$$

Remark that the controller (2.107) requires measurements inside the domain, as opposed to the controller in (2.92) which only need boundary information. Therefore, an observer needs to be constructed to implement such a controller. An observer is presented below.

2.5.1 Backstepping Observer Design

Consider system (2.93)-(2.95) with controller (2.107). The boundary condition (2.95) could be written in the form

$$h_x(1,t) = U(t) \tag{2.109}$$

with

$$U(t) = -\frac{1}{2}(\zeta + 2\epsilon)h(1,t) - \frac{1}{2}(\zeta + 2\epsilon)\epsilon\int_0^1 e^{\epsilon(1-y)}h(y,t)\,\mathrm{d}y \tag{2.110}$$

Thus, system (2.93)-(2.95) becomes

$$\begin{aligned} h_t(x,t) &= h_{xx}(x,t) && (2.111)\\ h_x(0,t) &= -\epsilon h(0,t) && (2.112)\\ h_x(1,t) &= U(t) && (2.113) \end{aligned}$$

We assume that $h(1,t)$ is measurable. Hence, the sensor and actuator are collocated. The observer for system (2.111)-(2.113) are designed as follows

$$\begin{aligned} \hat{h}_t(x,t) &= \hat{h}_{xx}(x,t) + \Pi(x)[h(1,t) - \hat{h}(1,t)] && (2.114)\\ \hat{h}_x(0,t) &= -\epsilon\hat{h}(0,t) && (2.115)\\ \hat{h}_x(1,t) &= U(t) + \pi[h(1,t) - \hat{h}(1,t)] && (2.116) \end{aligned}$$

The objective is to find a scalar function $\Pi(x)$ and a constant π such that $\hat{h}$ converges to h as time goes to infinity. Define the error

$$\tilde{h} = h - \hat{h} \tag{2.117}$$

such that (2.111)-(2.117) yields

$$\begin{aligned}
\tilde{h}_t(x,t) &= \tilde{h}_{xx}(x,t) - \Pi(x)\tilde{h}(1,t) && (2.118)\\
\tilde{h}_x(0,t) &= -\epsilon\tilde{h}(0,t) && (2.119)\\
\tilde{h}_x(1,t) &= -\pi\tilde{h}(1,t) && (2.120)
\end{aligned}$$

with the invertible transformation

$$\tilde{h}(x,t) = \tilde{u}(x,t) - \int_x^1 p(x,y)\tilde{u}(y,t)\,\mathrm{d}y \tag{2.121}$$

system (2.118)-(2.120) is mapped into the target system

$$\begin{aligned}
\tilde{u}_t(x,t) &= \tilde{u}_{xx}(x,t) && (2.122)\\
\tilde{u}_x(0,t) &= \epsilon\tilde{u}(0,t) && (2.123)\\
\tilde{u}_x(1,t) &= 0 && (2.124)
\end{aligned}$$

Substituting (2.122)-(2.124) into (2.118)-(2.120), yields the following PDE to be satisfied

$$\begin{aligned}
p_{xx}(x,y) &= p_{yy}(x,y) && (2.125)\\
p_x(0,y) &= -\epsilon p(0,y) && (2.126)\\
p(x,x) &= -2\epsilon && (2.127)
\end{aligned}$$

The solution of the PDE above is

$$p(x,y) = -2\epsilon e^{\epsilon(y-x)} \tag{2.128}$$

The observer gains are given by

$$\begin{aligned}
\Pi(x) &= -2\epsilon^2 e^{\epsilon(1-x)} && (2.129)\\
\pi &= 2\epsilon && (2.130)
\end{aligned}$$

Hence, the observer for system (2.93)-(2.95) becomes

$$\begin{aligned}
\hat{h}_t(x,t) &= \hat{h}_{xx}(x,t) - 2\epsilon^2 e^{\epsilon(1-x)}[h(1,t) - \hat{h}(1,t)] && (2.131)\\
\hat{h}_x(0,t) &= -\epsilon\hat{h}(0,t) && (2.132)\\
\hat{h}_x(1,t) &= U(t) + 2\epsilon[h(1,t) - \hat{h}(1,t)] && (2.133)
\end{aligned}$$

with $U(t)$ given by (2.110).

2.5.2 Controller Approximation

Its clear that the controller (2.107) is more complicated than (2.92) since it requires estimation of the height of oil column in the x-direction which necessitates the observer (2.131)-(2.133). However, controller (2.92) and (2.107) are closely linked as will be shown below. Using the Cauchy-Schwartz inequality in the second term of (2.107) and utilizing (2.108), yield

$$\begin{aligned} \left| \int_0^1 e^{\epsilon(1-y)} h(y,t)\,\mathrm{d}y \right| &\leq \left(\int_0^1 |e^{\epsilon(1-y)}|^2\,\mathrm{d}y \right)^{\frac{1}{2}} \left(\int_0^1 |h(y,t)|^2\,\mathrm{d}y \right)^{\frac{1}{2}} \\ &\leq \left(\frac{e^{2\epsilon}-1}{2\epsilon} \right)^{\frac{1}{2}} \sqrt{M} \end{aligned} \tag{2.134}$$

the Taylor series expansion gives

$$\frac{e^{2\epsilon}-1}{2\epsilon} = \sum_{n=1}^{\infty} \frac{(2\epsilon)^{n-1}}{n!} \leq \sum_{n=1}^{\infty} \frac{1}{n!} \leq e-1 \leq 2 \tag{2.135}$$

This yields

$$\left| \int_0^1 e^{\epsilon(1-y)} h(y,t)\,\mathrm{d}y \right| \leq \sqrt{2M} \tag{2.136}$$

Since $\left| \int_0^1 e^{\epsilon(1-y)} h(y,t)\,\mathrm{d}y \right|$ is bounded, it is important to note that for small flow influx ϵ, the controller (2.107) can be approximated as

$$u(t) \approx (\zeta + 2\epsilon) h^2(1,t) \tag{2.137}$$

Please note that the second term in (2.107) vanishes as $\epsilon \to 0$.

Clearly, controller (2.137) is much easier to implement compared to controller (2.107) since it only requires measurements at the well heel. The flow influx at the outer boundary of the reservoir was characterized by the coefficient ϵ in (2.137). If there is no-flow at the outer boundary of the reservoir, then the coefficient $\epsilon = 0$; hence, the controller (2.92) will be equal to (2.137) by taken $\lambda = \zeta$. This shows that the derivation of the controller using the backstepping method is consistent.

2.6 Numerical Example

To evaluate the theoretical results, consider a reservoir with a rectangular shape as shown in **Fig. 2.6**. A horizontal well is placed in the middle of the reservoir. The reservoir consists of gas, oil, and water with the oil layer located in the middle of the reservoir with a thickness of 25 m. The gas and water layers are set to be 100 m. The reservoir size is 2040 m x 1001 m x 225 m and is divided into 110 x 67 x 26 grid blocks. Porosity is 0.25 and assumed homogeneous in all parts of the reservoir. The permeability in the oil and the gas layers is 300 mD while in the water layer it is 0 mD. Permeability in the water layer is assumed to

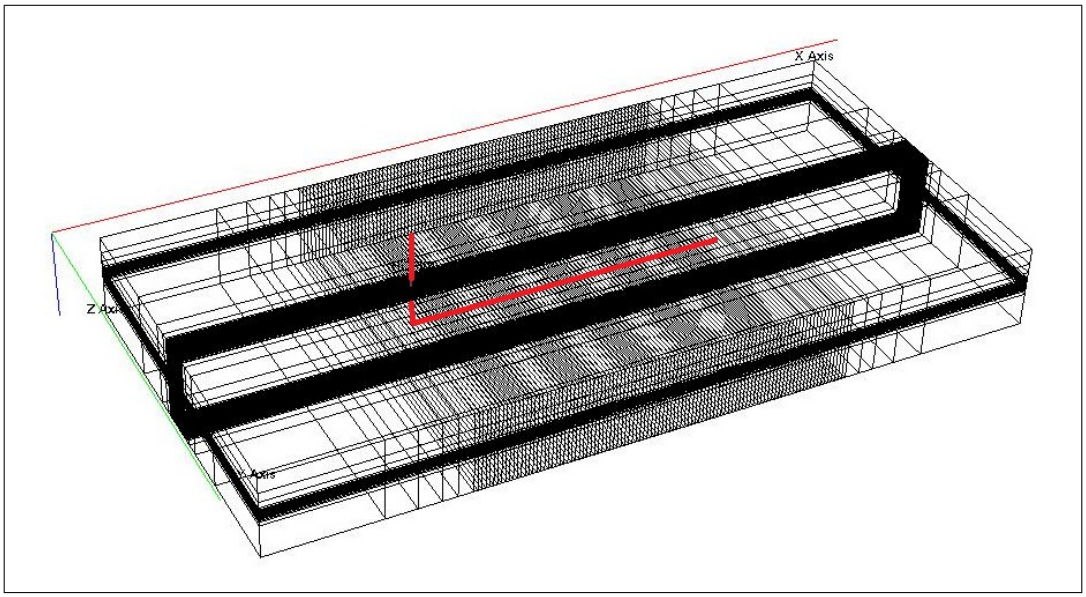

Figure 2.6: Reservoir model with a single horizontal well in the middle. The grid around the wells is refined using geometric progression rules

be zero to avoid the water coning effects which is not a topic of interest in this chapter. The initial pressure is set to be 140 Bara at the OWC. The capillary pressures at the GOC and the OWC are for simplicity assumed to be zero; hence, there is clear segregation between gas, oil, and water. In order to capture the dynamics of the gas coning, the grid around the wells is refined using geometric progression rules. The model is implemented in Eclipse. **Fig. 2.7** shows the variation of GOC from the beginning until the occurrence of gas breakthrough at the well heel using the control rate (2.92).

The NPV is used as a performance indicator for the rate controller. The NPV is written as follow

$$\text{NPV} = \int_0^{t_f} \underbrace{\lambda h^2(1,t)}_{u(t)} r_o (1+I)^{-ct} \, \mathrm{d}t \tag{2.138}$$

Here, t_f denotes the duration of the production time, c denotes the time constant, r_o denotes the oil price, and I is the discount factor. The oil price is set to be 80 US$/bbl or 504 US$/Sm^3 while the discount factor is set to be 10 %. The objective is to maximize the NPV over the production time t_f. The simulation will be done by using two different constraints. The first constraint is the production time, where production will be stopped when gas breakthrough occurs. The second constraint is related to the total gas produced, since the gas processing capacity may be a bottleneck.

Assuming no-flow at the outer boundary of the reservoir, the proposed control rate is calculated using (2.92). The control gain λ is found using a simple line search method since

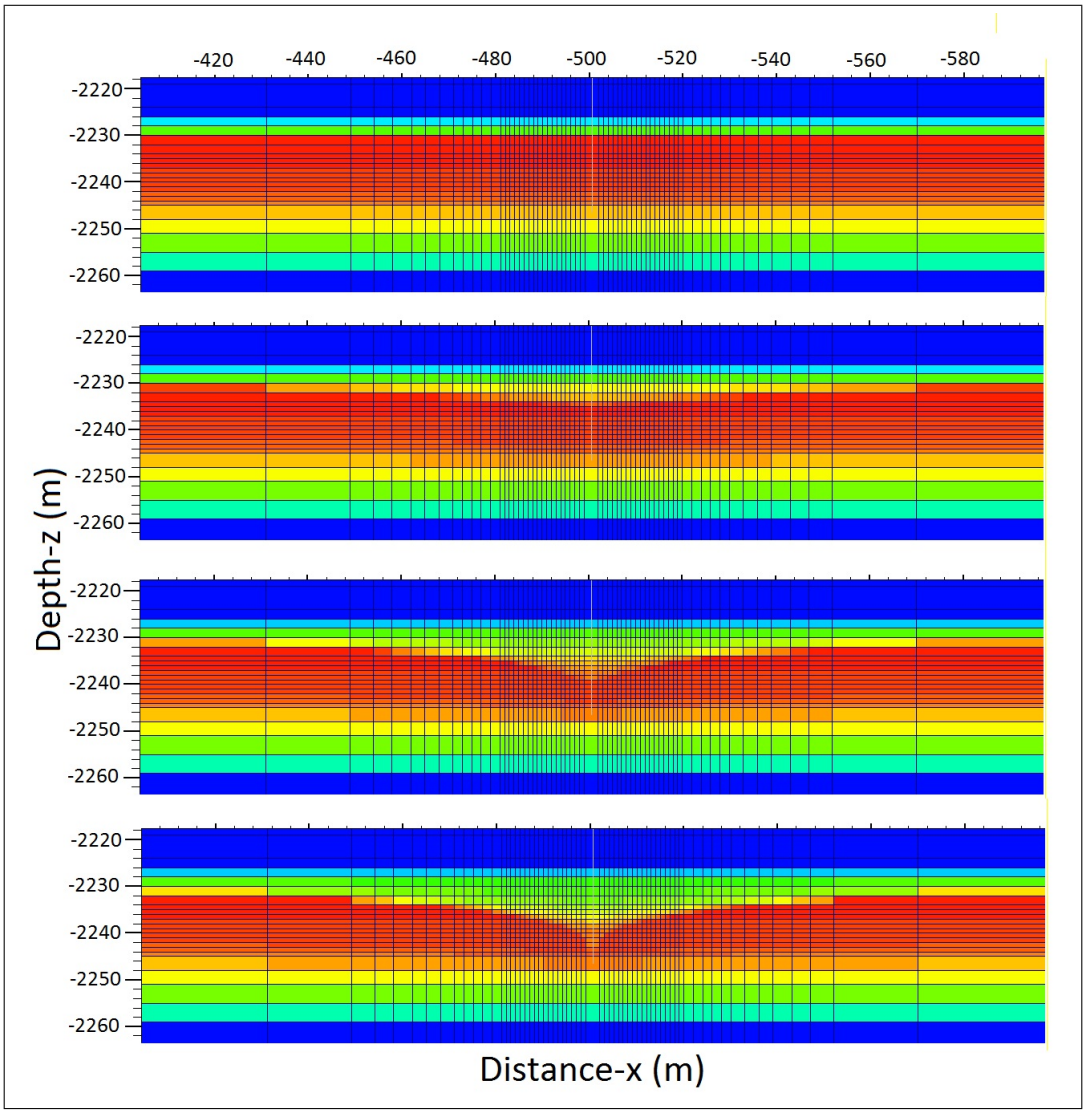

Figure 2.7: Simulation of gas coning in Eclipse using control rate (2.92). The colors represent the oil saturation with red as the highest. TOP: shows the initial GOC while BOTTOM: shows the GOC after 33 days. The snapshot was taken at the well heel.

there is only one parameter to be optimized. The gradient is computed using forward differencing. The optimal control rate will then be compared with five different constant control rates ranging from the minimum to the maximum rate which is the usual strategy in operation. The maximum and minimum rates are present due to operational limitation. For this simulation the minimum oil production limit is set to 400 Sm^3/day while the maximum is set to 1200 Sm^3/day.

Fig. 2.8 shows the NPV with gas breakthrough time as the production constraint. It can be observed that in a relatively short time the optimal production rate (2.92) gives higher

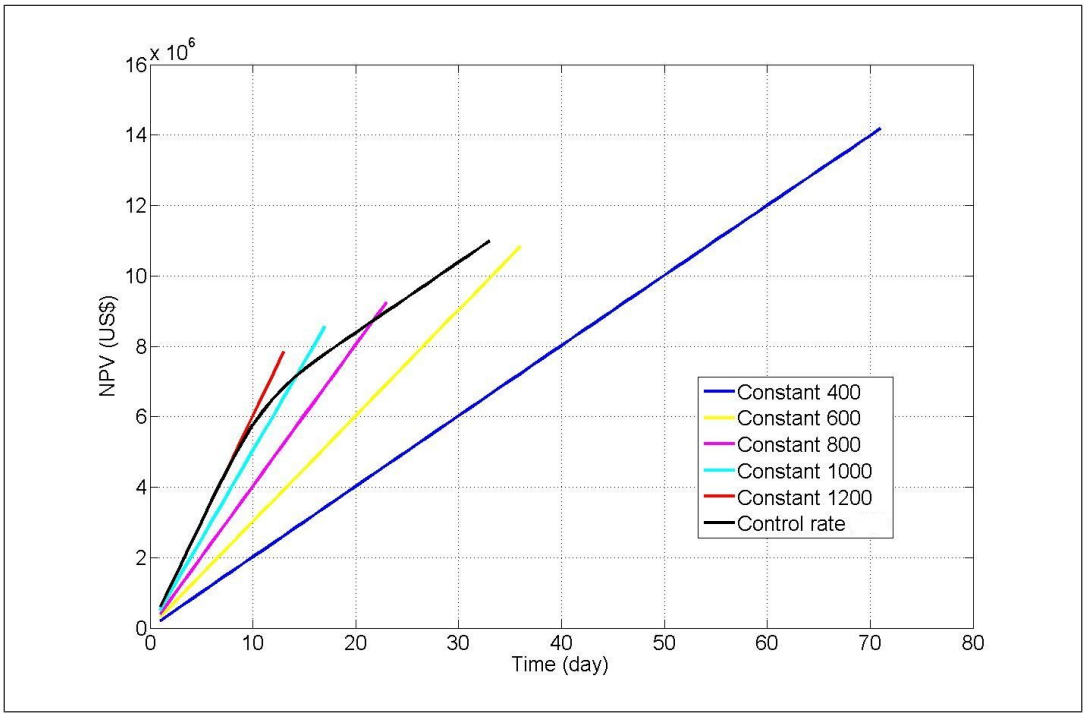

Figure 2.8: NPV in the subcritical phase for 5 different constant rates and the control rate (2.92).

Oil Rate (Sm^3/day)	**NPV** (MMUS$)	$\mathbf{t_f}$ (day)
Constant 400	14.2	71
Constant 600	10.8	36
Constant 800	9.2	23
Constant 1000	8.5	17
Constant 1200	7.8	13
Controller (2.92)	**10.9**	**33**

Table 2.1: NPV of 5 constant rates and the optimal rate from controller (2.92) with breakthrough time as the production constraint.

NPV compared to most of the constant control rates. The complete numerical comparison can be found in **Table 2.1**. In this case, the smallest constant rates give the highest NPV, but the production time is also much longer. A relatively fair comparison may be made between controller (2.92) and the constant control rate of 600 Sm^3/day where both rates achieve almost the same NPV. Arguably (2.92) is best since it achieves a slightly higher NPV in shorter time than the constant rate approach. The rates profile can be seen from **Fig. 2.9**.

Fig. 2.10 shows the GOR for different control strategies. The highest constant rate (1200 Sm^3/day) gives the fastest gas breakthrough while the lowest constant rate (400 Sm^3/day) gives the longest gas breakthrough time, as expected.

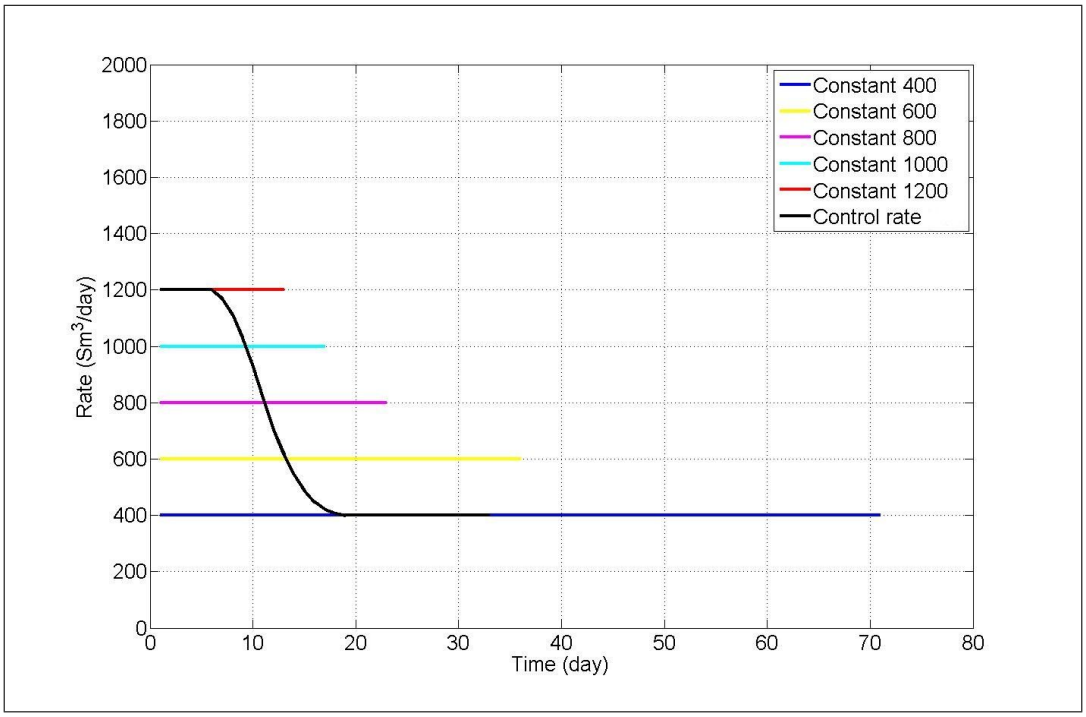

Figure 2.9: Oil production rates in the subcritical phase for 5 different constant rates and the control rate (2.92).

Oil Rate (Sm^3/day)	**NPV** (MMUS$)	$\mathbf{t_f}$ (day)
Constant 400	15.3	78
Constant 600	13.7	50
Constant 800	12.9	37
Constant 1000	12.3	29
Constant 1200	11.6	23
Controller (2.92)	**14.2**	**49**

Table 2.2: NPV of 5 constant rates and the optimal rate from controller (2.92) with total gas production of 1.5 $MMSm^3$ as the production constraint.

Fig. 2.11 shows the NPV with a total gas production of 1.5 $MMSm^3$ as the production constraint. It can be observed that the rate controller (2.92) gives higher NPV compared to some constant control rates. Again, the smallest constant rate gives the highest NPV but in a longer period. The complete numerical comparison can be found in **Table 2.2**.

Remark that a very small production rate (e.g., 10 Sm^3/day) will be able to drain the reservoir in a very long period without the well experiences gas breakthrough. However, this is definitely not a good choice from an operational standpoint. In practice, no one will ever use a small production rate in the beginning of production. In fact, they tend to produce as

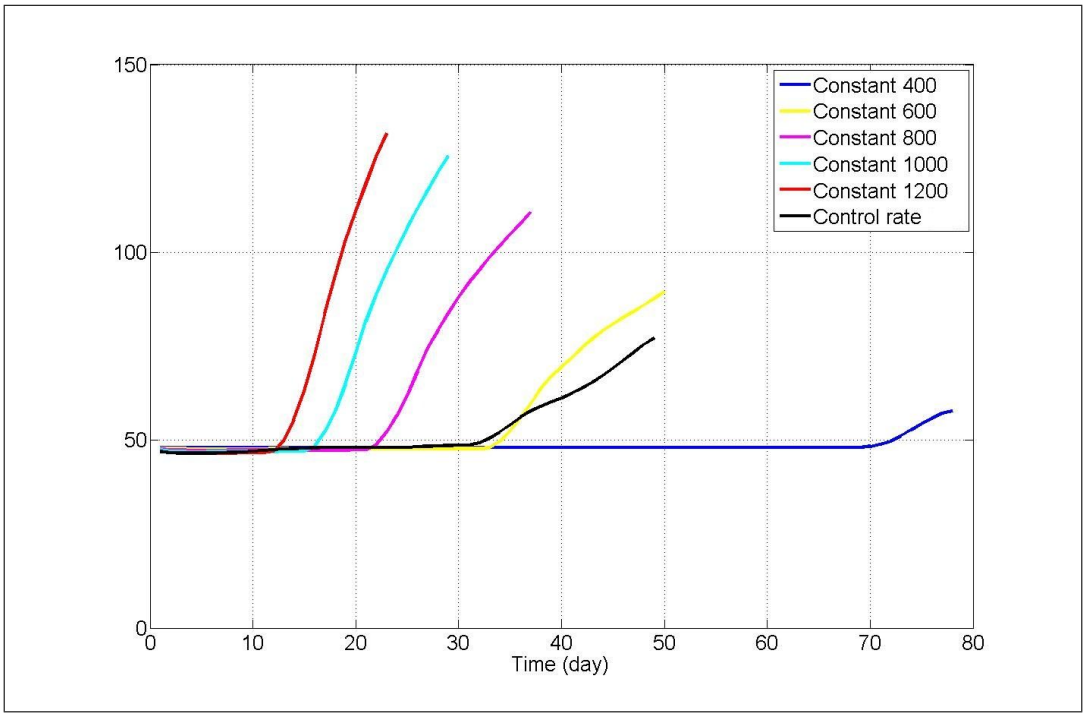

Figure 2.10: GOR with total gas constraint of 1.5 $MMSm^3$ for 5 different constant rates and the control rate (2.92).

much as possible in the first weeks in order to clean up the well from the brine set during completion and to get a good clean up of the near well reservoir. The control law presented here accommodates this. As can be seen in **Fig. 2.9** and **Fig. 2.12**, in the beginning the control law takes the maximum rate. After a while it declines step by step until it hits the minimum rate. Moreover, as discussed earlier lambda may be tuned to maximize any reasonable production measure. This provides flexibility to the control law since it can be adapted towards different objectives.

One may consider a model for smart wells as in **Fig. 2.1** where the downhole control valves enable the splitting up of the well into a number of segments which can be controlled individually. The proposed method may be applied to smart wells by including the control law for each segment. As a comment, there is a measurement challenge related to real-time measurements of the GOC at the well heel. This has not been studied in the present work.

2.7 Conclusions

A Lyapunov based design and a backstepping based design methods for the gas coning problem have been presented for linear and nonlinear cases. The rate controller is written explicitly and only requires measurement at the boundary of the reservoir. The controllers come with a control gain which can be used as a tuning parameter in an optimal control framework.

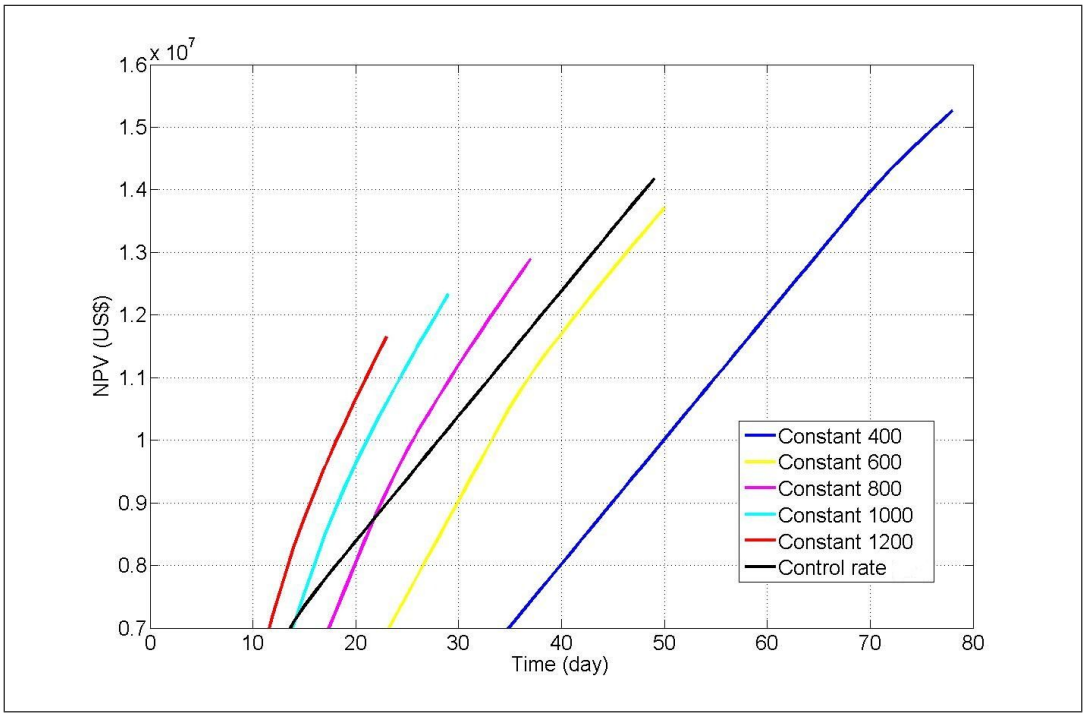

Figure 2.11: NPV with total gas constraint of 1.5 $MMSm^3$ for 5 different constant rates and the control rate (2.92).

For different production constraints, the simulation applying a fine-gridded Eclipse model shows that the proposed rate controller gives better results in term of usual economic measures compared with constant rate strategies. Furthermore, an alternative backstepping based controller was derived for a system with boundary influx. This controller requires the use of an observer. A convergent observer was presented for this purpose.

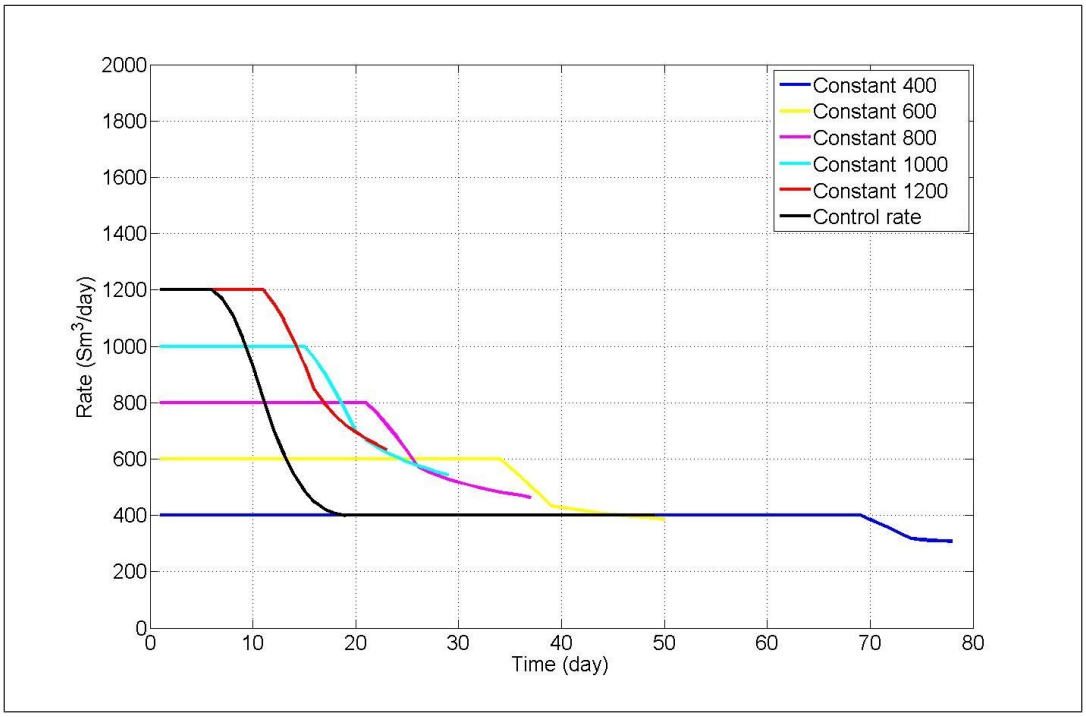

Figure 2.12: Oil production rate with total gas constraint of 1.5 MMSm^3 for 5 different constant rates and the control rate (2.92).

Nomenclature

Symbols

g = gravity constant (m/s^2)
h = height of oil column (m)
k = permeability (mD)
L = half length of the reservoir (m)
p = reservoir pressure (Pa)
q = volumetric flux per unit well length (m^3/s)
r = price (US$)
s = source per unit well area (m^3/s)
u = well rate (Sm^3/day)
I = discount factor (%)
μ_o = oil viscosity (Pa.s)
v = oil velocity (m/s)
ϕ = porosity (–)
ρ = density (kg/m^3)

Subscripts

g = gas
h = horizontal
o = oil

Chapter 3

Optimal Time Control of Oil Production under Water-flooding Conditions

This chapter is based on a paper which has been accepted for the European Control Conference 2013.

3.1 Introduction

Subsurface petroleum production comprises two main systems; reservoirs and wells. The reservoirs contain a large amount of hydrocarbon deposits. These deposits are located hundreds or thousands of meters beneath the ground and are trapped by overlaying rock formations that have zero permeability. To produce the hydrocarbons, especially oil, a number of production wells are drilled through the reservoir formations. Traditionally, the difference between the reservoir pressure and the surface pressure is the only driving force for lifting the oil from the reservoir toward the surface facilities. However, this method is most effective to producing oil that is close to the wells. As a result, a large amount of oil that is far from the production wells can still remain in the reservoir. Furthermore, as time goes by, the pressure will decline and the wells might be shut down. To sweep the remaining oil, injection wells are drilled and fluids (water, gas, polymer, or surfactant) are injected. When water is used, the process is called water-flooding.

3.1.1 Water-flooding

Water-flooding is the second most commonly used recovery technique today in the subsurface petroleum production system for several reasons; water is available almost everywhere and it has good sweep efficiency. To push the oil toward the production wells and to maintain the reservoir pressure, water is injected via injection wells which are usually drilled slightly above the oil-water contact (OWC). To track the water movement, a state-of-the-art reservoir simulator that is based on mass conservation and Darcy's law is usually employed, whereby

the inputs can be collected from geological data, e.g., seismic, core analysis, and well testing data (Aziz and Settari, 1979; Ertekin et al., 2001; Dake, 1983).

The water front will vary depending on the permeability and porosity distribution of the fields. Although the overall recovery could be increased by injecting water, the production might still be non-optimal. The typical way to operate the production well is to produce at a maximum rate at an early stage of production. Later, the wells will be completely closed if the water production is too high because larger water production is costly. The presence of high permeability channels between the injection and production wells will result in an early water breakthrough. Thus, water production will be dominant in the production wells, and the wells could be shut down early because they are not economical to maintain. On the other hand, low permeability regions will receive less water sweeping in spite of containing a large amount of oil. As a result, a large amount of recoverable oil still remains in the reservoir. Therefore, an optimal production setting is needed; the optimal production setting refers to how much water should be injected or oil should be produced in each injection or production well such that the production value is optimal. This problem can be partially answered by optimal control methods based on gradient calculations (Brouwer and Jansen, 2004).

In an optimal control framework, the variables are divided into two classes, namely the state variables and the control variables. The change in the control variables dictates the state variables via a set of differential equations. In this chapter, the state variables are the fluid pressure and the saturation, while the control variables are the flow rates or BHPs. Furthermore, an objective function is used as a performance measure. It has been shown that if the objective function is linear in the control and the only constraints are upper and lower bounds on the control, then because of their specific structure, the problem will sometimes have bang-bang optimal solutions (Zandvliet et al., 2007). Bang-bang control has a major practical advantage because it can be implemented with simple on-off valves.

3.1.2 Gradient-based optimization

The idea of gradient-based optimization is to calculate the gradient of the objective function with respect to the control variables. The objective function can be the net present value (NPV), the recovery factor, or grid saturations. The most common objective function in life cycle optimization is the NPV, which is used in this chapter. Furthermore, this function is linear in the control. The task is then to use gradient information to calculate the optimal control variables such that the NPV can be maximized. The gradient can be obtained in several ways; finite difference calculations, the forward sensitivity equation, and the adjoint method. However, for large-scale systems such as reservoirs for which the number of grids can be in the millions and the computational time can be up to hours, the first two methods become impractical. The adjoint method is, thus far, the most efficient way to calculate the gradient information for large-scale systems because it requires only two simulations; a forward simulation to calculate the reservoir state (pressure and saturation) and a backward simulation to calculate the Lagrange multiplier (Sarma and Chen, 2008; Zandvliet et al., 2008; Suwartadi, 2012).

The adjoint method has increasingly been used in the production optimization of petroleum reservoirs. The use of this method has been supported by the availability of the gradient calculation in commercial simulators. The adjoint method is combined with data assimilation to form the basis of closed-loop reservoir management. A comprehensive summary of this concept can be found in Jansen et al. (2009) and Foss and Jensen (2011).

The production optimization problem can be viewed as a scheduling problem. Intuitively, to sweep efficiently, the production wells in a high permeability region should be closed early on while the production wells in a low permeability region should be opened initially. In this chapter, a new approach to the optimization of oil production under water-flooding is presented by computing the optimal switching time control. The parameterized control variables use a special form of bang-bang (on-off) control settings. Hence, in this case, the switching time is defined as the time when a well changes from an on to an off mode, and vice versa. The gradient calculation of a single switching time requires the computation of the Hamiltonian on the left and the right limit with respect to the time control. It should be mentioned that the general switching time problem using optimal control theory has received much attention, see e.g., Teo et al. (1991); Bengea and DeCarlo (2005); Egerstedt et al. (2003); Lucas and Kaya (2001); Loxton et al. (2008, 2009); Sudaryanto and Yortsos (2000).

3.1.3 Optimal Control Theory

The optimal control problem can be stated in a canonical form as follows

$$\begin{aligned}
\min_{\mathbf{u}} \; J(\mathbf{u}) &= \psi(\mathbf{x}(T)) + \int_0^T \mathcal{L}(\mathbf{x}(t), \mathbf{u}(t))\,\mathrm{d}t && (3.1)\\
\text{subject to } \dot{\mathbf{x}}(t) &= \mathbf{f}(\mathbf{x}(t), \mathbf{u}(t)) && (3.2)\\
\mathbf{x}(0) &= \bar{\mathbf{x}}_0 && (3.3)\\
\mathbf{u}(t) &\in \mathcal{U},\ \forall t \in [0, T] && (3.4)\\
\mathcal{U} &= \{\mathbf{q} \in \mathbb{R}^m : \mathbf{u}_{\min} \leq \mathbf{q} \leq \mathbf{u}_{\max}\} && (3.5)
\end{aligned}$$

Here, the objective function J is to be minimized (or maximized) by changing the control variable $\mathbf{u}$ subject to the dynamical system (3.2)-(3.3) and control constraints (3.4)-(3.5) in a fixed time interval $[0, T]$. To solve the optimal control problem (3.1)-(3.5), the gradient is computed using the adjoint method by employing the variation principle. The constraint can be appended into the cost function by introducing the Lagrange multiplier $\boldsymbol{\lambda}$ such that

$$\bar{J}(\mathbf{u}) = \psi(\mathbf{x}(T)) + \int_0^T \mathcal{L}(\mathbf{x}(t), \mathbf{u}(t)) + \boldsymbol{\lambda}^\intercal(t)[\mathbf{f}(\mathbf{x}(t), \mathbf{u}(t)) - \dot{\mathbf{x}}(t)]\,\mathrm{d}t \tag{3.6}$$

where $^\intercal$ is used as a symbol for the transpose. For simplicity, define the so-called Hamiltonian as

$$H(\mathbf{x}(t), \mathbf{u}(t), \boldsymbol{\lambda}(t)) = \mathcal{L}(\mathbf{x}(t), \mathbf{u}(t)) + \boldsymbol{\lambda}^\intercal(t)\,(\mathbf{f}(\mathbf{x}(t), \mathbf{u}(t))) \tag{3.7}$$

Substituting (3.7) into (3.6) and applying integration by parts, yield

$$\begin{aligned}\bar{J}(\mathbf{u}) &= \psi(\mathbf{x}(T)) - \boldsymbol{\lambda}^{\intercal}(T)\mathbf{x}(T) + \boldsymbol{\lambda}^{\intercal}(0)\mathbf{x}(0) \\ &\quad + \int_0^T \{H(\mathbf{x}(t), \mathbf{u}(t), \boldsymbol{\lambda}(t)) + \dot{\boldsymbol{\lambda}}^{\intercal}(t)\mathbf{x}(t)\}\,\mathrm{d}t \end{aligned} \tag{3.8}$$

For a small variation $\delta\mathbf{u}$ in $\mathbf{u}$, the corresponding first order variations $\delta\bar{J}(\mathbf{u})$ can be computed as follows

$$\begin{aligned}\delta\bar{J}(\mathbf{u}) &= \left[\frac{\partial\psi(\mathbf{x}(T))}{\partial\mathbf{x}} - \boldsymbol{\lambda}^{\intercal}(T)\right]\delta\mathbf{x}(T) + \boldsymbol{\lambda}^{\intercal}(0)\delta\mathbf{x}(0) \\ &\quad + \int_0^T \left\{\left[\frac{\partial H(\mathbf{x}(t), \mathbf{u}(t), \boldsymbol{\lambda}(t))}{\partial\mathbf{x}} + \dot{\boldsymbol{\lambda}}^{\intercal}(t)\right]\delta\mathbf{x}(t) + \frac{\partial H(\mathbf{x}(t), \mathbf{u}(t), \boldsymbol{\lambda}(t))}{\partial\mathbf{u}}\delta\mathbf{u}\right\}\mathrm{d}t \end{aligned} \tag{3.9}$$

Because the initial condition $\mathbf{x}(0)$ is fixed, $\delta\mathbf{x}(0)$ vanishes. Furthermore, because $\boldsymbol{\lambda}$ is arbitrary, we can set it such that

$$\dot{\boldsymbol{\lambda}}^{\intercal}(t) = -\frac{\partial H(\mathbf{x}(t), \mathbf{u}(t), \boldsymbol{\lambda}(t))}{\partial\mathbf{x}} \tag{3.10}$$

$$\boldsymbol{\lambda}^{\intercal}(T) = \frac{\partial\psi(\mathbf{x}(T))}{\partial\mathbf{x}} \tag{3.11}$$

These equations are the so-called costate equations. Because of the first order optimality condition, if the control $\mathbf{u}$ is unconstrained, then

$$\frac{\partial H(\mathbf{x}(t), \mathbf{u}(t), \boldsymbol{\lambda}(t))}{\partial\mathbf{u}} = 0 \tag{3.12}$$

If the control is constrained, then the optimal control strategy optimizes H. Hence, for a minimization problem

$$H(\mathbf{x}(t), \mathbf{u}_{\mathrm{opt}}(t), \boldsymbol{\lambda}(t)) \leq H(\mathbf{x}(t), \mathbf{u}(t), \boldsymbol{\lambda}(t)) \tag{3.13}$$

which is called the Pontryagin Maximum Principle (Luenberger, 1979). To calculate the optimal switching time, first the dynamical system (reservoir) is simulated on the horizon $[0, T]$ to obtain the state vector $\mathbf{x}$ (pressure and saturation). Afterward, the costate equation (3.10)-(3.11) is solved backward to obtain the Lagrange multiplier $\boldsymbol{\lambda}$. The state and the multiplier are used to calculate the gradient of the objective function J (Brouwer and Jansen, 2004). The gradient can be combined with a line search algorithm to find the optimal switching time control.

3.1.4 Contributions of this chapter

In this chapter, a novel optimal control problem is formulated to maximize the NPV. The embedded gradient calculation for the bang-bang control comes with a formal proof. Examples of realistic reservoir settings are presented to show the potential application of the proposed method.

3.2 Reservoir Model

Ideally, to model the fluid flow in a reservoir, each component should be considered individually. However, this task is non-trivial because the number of components can be quite high, which leads to complex fluid flow models. As a consequence, the computation time could be extensive. To overcome this issue, a simpler model that considers only oil, water, and gas, and that is commonly used in the petroleum industry is presented. This type of model is known as the black-oil model.

3.2.1 Black-Oil Model

In this section, the water-flooding problem in an oil-water system using black-oil formulation will be considered. The mass conservation for an oil-water system can be written as

$$\frac{\partial}{\partial t}(\phi \rho_i s_i) = -\nabla \cdot (\rho_i \bar{u_i}) + q_i, \quad i \in \{o, w\} \tag{3.14}$$

where ϕ denotes the porosity, ρ is the density, and s is the saturation. The subscripts o and w refer to oil and water, respectively. The divergence operator is denoted by $\nabla\cdot$, while the source or the sink terms, i.e., the well flow rates, are denoted by q. The velocity of the fluid flow in the reservoir is calculated using the Darcy law as, as follows

$$\bar{u_i} = -\mathbb{K}\frac{k_{ri}}{\mu_i}\nabla p_i, \quad i \in \{o, w\} \tag{3.15}$$

where $\mathbb{K}$ denotes the permeability tensor, k_r is the relative permeability, μ is the viscosity, and p is the reservoir pressure. Assuming isotropic conditions, the permeability tensor can be simplified to $\mathbb{K} = k$. Furthermore, the relative permeability depends on the water saturation. Hence, it becomes a major source of nonlinearity.

Substituting (3.15) into (3.14) leads to two equations with four unknown variables; oil saturation (s_o), water saturation (s_w), oil pressure (p_o), and water pressure (p_w). For well-posed problem, two other equations are required. The first equation is obtained from the assumption that only oil and water are present in the reservoir, hence

$$s_o + s_w = 1 \tag{3.16}$$

Assuming zero capillary pressure, yields

$$p_o = p_w \tag{3.17}$$

For brevity, in the remainder of this chapter, $s = s_w$ and $p = p_o$. Hence, (3.14)-(3.17) can be reduced into the following system of equations

$$\frac{\partial}{\partial t}(\phi \rho_o [1 - s]) = \nabla \cdot \left(k \frac{k_{ro}}{\mu_o} \rho_o \nabla p \right) + q_o \tag{3.18}$$

$$\frac{\partial}{\partial t}(\phi \rho_w s) = \nabla \cdot \left(k \frac{k_{rw}}{\mu_w} \rho_w \nabla p \right) + q_w \tag{3.19}$$

where the unknown variables to be determined are the water saturation (s) and the oil pressure (p). The system of partial differential equations (3.18)-(3.19) is the standard model for the oil-water system in the black oil formulation (Aziz and Settari, 1979).

3.2.2 State-Space Representation

Because petroleum reservoirs are usually heterogeneous with respect to permeability and porosity, solving (3.18)-(3.19) analytically is nearly impossible. The most common procedure is to discretize the equations in the spatial variables into a finite number of grid blocks while assuming homogeneous geological properties in each block. In general, the larger the size of the grid blocks is, the lower the accuracy of the predicted solution. On the other hand, the larger the number of the grid blocks is, the longer the computational time. Hence, selecting an appropriate number of the grid blocks is an important issue in reservoir simulation. For the sake of simplicity, after discretization, (3.18)-(3.19) will be arranged into a canonical state space representation.

Let N denote the number of active grid blocks of the reservoir. Define the state vector $\mathbf{x}$ as a collection of pressure and saturation in each grid block as

$$\mathbf{x} = [\mathbf{p}^\top \mathbf{s}^\top]^\top \in \mathbb{R}^{2N} \tag{3.20}$$

where

$$\mathbf{p} = [p^1 \cdots p^N]^\top \in \mathbb{R}^N \tag{3.21}$$
$$\mathbf{s} = [s^1 \cdots s^N]^\top \in \mathbb{R}^N \tag{3.22}$$

Because the injection wells inject only water, the flow rates of each phase in a grid block j are computed by

$$q_o^j = 0 \tag{3.23}$$
$$q_w^j = \frac{\rho_w(p^j)}{v^j} q^j, \quad j \in \mathscr{N}_{inj} \tag{3.24}$$

where v^j is the volume of grid block j, q^j is the rate of the injected fluid, and $\mathscr{N}_{inj}$ is the set of grid block indices at which an injector is perforated. By defining the fractional flow rate of the water as

$$f_w^j = \frac{\frac{k_{rw}(s^j)}{\mu_w}}{\frac{k_{rw}(s^j)}{\mu_w} + \frac{k_{ro}(s^j)}{\mu_o}} \tag{3.25}$$

and because the production wells produce both oil and water, the flow rate of each phase in grid block j is computed by

$$q_o^j = \frac{\rho_o(p^j)}{v^j}\Big(1 - f_w^j(s^j)\Big) q^j \tag{3.26}$$
$$q_w^j = \frac{\rho_w(p^j)}{v^j} f_w^j(s^j) q^j, \quad j \in \mathscr{N}_{prod} \tag{3.27}$$

where q^j is the rate of produced fluid and $\mathcal{N}_{prod}$ is the set of grid block indices in which a producer is perforated. The fluid compressibility is defined as

$$c_i(p) = \frac{1}{\rho_i(p)} \frac{\mathrm{d}\rho_i(p)}{\mathrm{d}p}, \quad i \in \{o, w\} \tag{3.28}$$

The porosity will be assumed to be independent of the pressure and, upon applying the chain rule, we obtain the following

$$\frac{\partial}{\partial t}(\phi \rho_i s_i) = \phi \left(s_i \rho_i c_i \frac{\partial p_i}{\partial t} + \rho_i \frac{\partial s_i}{\partial t} \right), \quad i \in \{o, w\} \tag{3.29}$$

After the discretization of (3.18)-(3.19) and with the help of (3.29), the state space model can be written in the following form

$$\begin{aligned} \mathbf{E}(\mathbf{x}(t))\dot{\mathbf{x}}(t) &= \tilde{\mathbf{A}}(\mathbf{x}(t))\mathbf{x}(t) + \tilde{\mathbf{B}}(\mathbf{x}(t))\mathbf{u}(t) & (3.30) \\ \mathbf{x}(0) &= \bar{\mathbf{x}}_0 & (3.31) \end{aligned}$$

where $\mathbf{E}$, $\tilde{\mathbf{A}}$, and $\tilde{\mathbf{B}}$ are sparse matrices. $\mathbf{E}$ and $\tilde{\mathbf{A}}$ store information regarding rock and fluid properties while $\tilde{\mathbf{B}}$ stores information regarding the fractional flow of the wells. The manipulated control variables q^j will be stored in the vector column $\mathbf{u}$. By defining

$$\begin{aligned} \mathbf{A}(\mathbf{x}(t)) &= \mathbf{E}^{-1}(\mathbf{x}(t))\tilde{\mathbf{A}}(\mathbf{x}(t)) & (3.32) \\ \mathbf{B}(\mathbf{x}(t)) &= \mathbf{E}^{-1}(\mathbf{x}(t))\tilde{\mathbf{B}}(\mathbf{x}(t)) & (3.33) \end{aligned}$$

the system can be written in its canonical form as

$$\begin{aligned} \dot{\mathbf{x}}(t) &= \mathbf{A}(\mathbf{x}(t))\mathbf{x}(t) + \mathbf{B}(\mathbf{x}(t))\mathbf{u}(t) & (3.34) \\ \mathbf{x}(0) &= \bar{\mathbf{x}}_0 & (3.35) \end{aligned}$$

Let N_{inj} denote the number of injection wells, while N_{prod} denotes the number of production wells, and $N_w = N_{inj} + N_{prod}$ denotes the total number of wells. Then, the state matrix $\mathbf{A} \in \mathbb{R}^{2N \times 2N}$ and, the input matrix is $\mathbf{B} \in \mathbb{R}^{2N \times N_w}$, while the control input is $\mathbf{u} \in \mathbb{R}^{N_w}$. One can imagine that, for a reservoir with thousands of active grid blocks, $\mathbf{A}$ and $\mathbf{B}$ are very large matrices, which indicates an expensive computational time. One trick that can be used is to split the pressure and saturation equations using an operator splitting method and then to perform the computation using different time scales. Because the pressure change is relatively slow compared with the saturation, we can use a wider time step.

3.2.3 Well Model

The wells are modeled using the standard Peaceman well model as follows

$$q^j(t) = \alpha^j(t) w^j(s^j)(p_R^j - p_{bh}^j(t)), \quad j \in \{\mathcal{N}_{inj}, \mathcal{N}_{prod}\} \tag{3.36}$$

where the $\alpha^j(t)$ denote the valves opening, p_R is the reservoir pressure, and the productivity index w^j is computed by the following formula

$$w^j(s^j) = \frac{2\pi k^j \Delta z}{\ln\left(0.14\sqrt{\Delta x^2 + \Delta y^2}/r_w\right) + S} + \left(\frac{k_{ro}(s^j)}{\mu_o} + \frac{k_{rw}(s^j)}{\mu_w}\right) \tag{3.37}$$

If the valve setting $\alpha^j(t)$ is considered to be the control variable, then the term $q^j(t)$ in $\mathbf{u}$ is replaced by $\alpha^j(t)$ and the corresponding entries in $\tilde{\mathbf{B}}$ are modified to include the term $w^j(s^j)(p_R^j - p_{bh}^j(t))$. On the other hand, if p_{bh}^j is considered to be the control variable, then the term $q^j(t)$ in $\mathbf{u}$ is replaced by p_{bh}^j and the corresponding entries in $\tilde{\mathbf{B}}$ and $\tilde{\mathbf{A}}$ are modified to include the term $w^j(s^j)$.

3.3 Gradient Formulas

In this section, the gradient of the switching time control is calculated by using the steps presented in Teo et al. (1991). Suppose that the valve settings are considered to be the control variables. We start with the parameterizations of the control input $\mathbf{u}$ over the time horizon $[0, T]$.

The j^{th} component α^j for $j = 1, \cdots, N_w$ of the input control vector $\mathbf{u} \in \mathbb{R}^{N_w}$ is considered to be a piecewise constant function over the interval $[0, T]$ with switches at $t_1^j, \cdots, t_{M_j}^j$. Let $t_0^j = 0$, and $t_{M_{j+1}}^j = T$; the switching time $t_k^j, k = 1, \cdots, M_j$ can be distinguished such that

$$0 = t_0^j < t_1^j < \cdots < t_{M_j}^j < t_{M_{j+1}}^j = T \tag{3.38}$$

Mathematically, $\alpha^j(t)$ can be written in the following form

$$\alpha^j(t) = \sum_{k=0}^{M_j} \gamma_k^j \chi_{[t_k^j, t_{k+1}^j)}(t) \tag{3.39}$$

where the basis of the piecewise constant function is given as

$$\chi_I(t) = \begin{cases} 1, & t \in I \\ 0, & \text{otherwise} \end{cases} \tag{3.40}$$

and the multiplier coefficient γ_k^j is given by

$$\gamma_k^j = \begin{cases} 1, & k \geq 0 \text{ is an even number} \\ 0, & k \geq 0 \text{ is an odd number} \end{cases} \tag{3.41}$$

Let us define the vectors of the switching time as

$$\mathbf{v}^j = [t_1^j, \cdots, t_{M_j}^j]^\intercal \tag{3.42}$$

and the augmented vector of the switching time as

$$\mathbf{v} = [(\mathbf{v}^1)^\intercal, \cdots, (\mathbf{v}^{N_w})^\intercal]^\intercal \tag{3.43}$$

The symbol $\mathbf{u}(\cdot|\mathbf{v})$ will be used to describe a control input that is determined by the switching vector $\mathbf{v}$. The Hamiltonian based on (3.7) is defined as follows

$$H(\mathbf{x}(t), \mathbf{u}(t), \boldsymbol{\lambda}(t)) = \mathcal{L}(\mathbf{x}(t), \mathbf{u}(t)) + \boldsymbol{\lambda}^\intercal(t)\left(\mathbf{A}(\mathbf{x}(t))\mathbf{x}(t) + \mathbf{B}(\mathbf{x}(t))\mathbf{u}(t)\right) \tag{3.44}$$

Let $s_0^j = s_{M_{j+1}}^j = 0$ and $\mathbf{s}^j = [s_1^j, \cdots, s_{M_j}^j]^\intercal$ be an arbitrary but fixed dummy vector of times. Furthermore, let ϵ be a sufficiently small positive constant such that

$$0 \le t_1^j + \epsilon s_1^j \le \cdots \le t_{M_j}^j + \epsilon s_{M_j}^j \le T \tag{3.45}$$

Define a perturbation vector of well j as

$$\boldsymbol{\vartheta}^j(\epsilon) = [\cdots, (\mathbf{v}^{j-1})^\intercal, (\mathbf{v}^j + \epsilon s^j)^\intercal, (\mathbf{v}^{j+1})^\intercal, \cdots] \tag{3.46}$$

Let $t \in [t_l^j + \epsilon s_l^j, t_{l+1}^j + \epsilon s_{l+1}^j]$ for some $l \in \{0, \cdots, M_j\}$, then the explicit solution for (3.34) can be written as follows

$$\begin{aligned}
\mathbf{x}(t|\boldsymbol{\vartheta}^j(\epsilon)) \;=\; & \mathbf{x}(0) + \sum_{k=0}^{l-1} \int_{t_k^j + \epsilon s_k^j}^{t_{k+1}^j + \epsilon s_{k+1}^j} \\
& \left(\mathbf{A}(\mathbf{x}(\tau|\boldsymbol{\vartheta}^j(\epsilon)))\mathbf{x}(t|\boldsymbol{\vartheta}^j(\epsilon)) + \mathbf{B}(\mathbf{x}(t|\boldsymbol{\vartheta}^j(\epsilon)))\gamma_k^j\right) \mathrm{d}\tau \\
& + \int_{t_l^j + \epsilon s_l^j}^{t} \left(\mathbf{A}(\mathbf{x}(\tau|\boldsymbol{\vartheta}^j(\epsilon)))\mathbf{x}(t|\boldsymbol{\vartheta}^j(\epsilon)) + \mathbf{B}(\mathbf{x}(t|\boldsymbol{\vartheta}^j(\epsilon)))\gamma_k^j\right) \mathrm{d}\tau
\end{aligned} \tag{3.47}$$

Furthermore, the first variation in the state vector $\mathbf{x}$ can be computed as follows

$$\begin{aligned}
\Delta\mathbf{x}(t) \;\triangleq\; & \frac{\mathrm{d}\mathbf{x}(t|\boldsymbol{\vartheta}^j(\epsilon))}{\mathrm{d}\epsilon}\Big|_{\epsilon=0} \\
=\; & \int_0^t \frac{\partial\left(\mathbf{A}(\mathbf{x}(\tau|\mathbf{v}))\mathbf{x}(\tau|\mathbf{v}) + \mathbf{B}(\mathbf{x}(\tau|\mathbf{v}))\mathbf{u}(\tau|\mathbf{v})\right)}{\partial\mathbf{x}} \Delta\mathbf{x}(\tau)\,\mathrm{d}\tau \\
& + \int_0^t \sum_{k=0}^{M_j} \left(\mathbf{A}(\mathbf{x}(\tau^-|\mathbf{v}))\mathbf{x}(\tau^-|\mathbf{v}) + \mathbf{B}(\mathbf{x}(\tau^-|\mathbf{v}))\mathbf{u}(\tau^-|\mathbf{v})\right) \\
& \times s_k^j \delta(\tau - t_k^j)\,\mathrm{d}\tau \\
& - \int_0^t \sum_{k=0}^{M_j} \left(\mathbf{A}(\mathbf{x}(\tau^+|\mathbf{v}))\mathbf{x}(\tau^+|\mathbf{v}) + \mathbf{B}(\mathbf{x}(\tau^+|\mathbf{v}))\mathbf{u}(\tau^+|\mathbf{v})\right) \\
& \times s_k^j \delta(\tau - t_k^j)\,\mathrm{d}\tau
\end{aligned} \tag{3.48}$$

where $\delta(\cdot)$ is the Dirac delta function while the right and left limit are defined as $\mathbf{x}(t^+|\mathbf{v}) = \lim_{\tau\to t^+}\mathbf{x}(\tau|\mathbf{v})$ and $\mathbf{x}(t^-|\mathbf{v}) = \lim_{\tau\to t^-}\mathbf{x}(\tau|\mathbf{v})$, respectively. The derivative of the first variation of the state vector $\mathbf{x}$ can be computed as follows

$$\begin{aligned}\Delta\dot{\mathbf{x}}(t) &= \frac{\partial\left(\mathbf{A}(\mathbf{x}(t|\mathbf{v}))\mathbf{x}(t|\mathbf{v}) + \mathbf{B}(\mathbf{x}(t|\mathbf{v}))\mathbf{u}(t|\mathbf{v})\right)}{\partial\mathbf{x}}\Delta\mathbf{x}(t) \\ &\quad + \sum_{k=0}^{M_j}\left(\mathbf{A}(\mathbf{x}(t^-|\mathbf{v}))\mathbf{x}(t^-|\mathbf{v}) + \mathbf{B}(\mathbf{x}(t^-|\mathbf{v}))\mathbf{u}(t^-|\mathbf{v})\right)s_k^j\delta(t-t_k^j) \\ &\quad - \sum_{k=0}^{M_j}\left(\mathbf{A}(\mathbf{x}(t^+|\mathbf{v}))\mathbf{x}(t^+|\mathbf{v}) + \mathbf{B}(\mathbf{x}(t^+|\mathbf{v}))\mathbf{u}(t^+|\mathbf{v})\right)s_k^j\delta(t-t_k^j)\end{aligned} \tag{3.49}$$

The first variation in the objective function J can be computed as follows

$$\begin{aligned}\frac{\mathrm{d}J(\vartheta^j(\epsilon))}{\mathrm{d}\epsilon}\Big|_{\epsilon=0} &= \frac{\partial\psi(\mathbf{x}(t|\mathbf{v}))}{\partial\mathbf{x}}\Delta\mathbf{x}(T) + \int_0^T\frac{\partial\mathcal{L}(\mathbf{x}(t|\mathbf{v}),\mathbf{u}(t|\mathbf{v}))}{\partial\mathbf{x}}\Delta\mathbf{x}(t)\,\mathrm{d}t \\ &\quad + \int_0^T\sum_{k=0}^{M_j}\left(\mathcal{L}(\mathbf{x}(t^-|\mathbf{v}),\mathbf{u}(t^-|\mathbf{v}))\right)s_k^j\delta(t-t_k^j)\,\mathrm{d}t \\ &\quad - \int_0^T\sum_{k=0}^{M_j}\left(\mathcal{L}(\mathbf{x}(t^+|\mathbf{v}),\mathbf{u}(t^+|\mathbf{v}))\right)s_k^j\delta(t-t_k^j)\,\mathrm{d}t\end{aligned} \tag{3.50}$$

Using the definition of H, (3.49), and the following integration by parts

$$\begin{aligned}\int_0^T(\boldsymbol{\lambda}(t|\mathbf{v}))^T\Delta\dot{\mathbf{x}}(t)\,\mathrm{d}t &= \frac{\partial\Phi(\mathbf{x}(T|\mathbf{v}))}{\partial\mathbf{x}}\Delta\mathbf{x}(T) \\ &\quad + \int_0^T\frac{\partial H(\mathbf{x}(t|\mathbf{v}),\mathbf{u}(t|\mathbf{v}),\boldsymbol{\lambda}(t|\mathbf{v}))}{\partial\mathbf{x}}\Delta\mathbf{x}(t)\,\mathrm{d}t\end{aligned} \tag{3.51}$$

The second term of the right hand side of the above equation can be computed as follows

$$\begin{aligned}&\int_0^T\frac{\partial\mathcal{L}(\mathbf{x}(t|\mathbf{v}),\mathbf{u}(t|\mathbf{v}))}{\partial\mathbf{x}}\Delta\mathbf{x}(t)\mathrm{d}t \\ = &-\frac{\partial\psi(\mathbf{x}(T|\mathbf{v}))}{\partial\mathbf{x}}\Delta\mathbf{x}(T) \\ &+ \int_0^T\boldsymbol{\lambda}^\intercal(t|\mathbf{v})\sum_{k=1}^{M_j}\left(\mathbf{A}(\mathbf{x}(t^-|\mathbf{v}))\mathbf{x}(t^-|\mathbf{v}) + \mathbf{B}(\mathbf{x}(t^-|\mathbf{v}))\mathbf{u}(t^-|\mathbf{v})\right)s_k^j\delta(t-t_k^j)\,\mathrm{d}t \\ &- \int_0^T\boldsymbol{\lambda}^\intercal(t|\mathbf{v})\sum_{k=1}^{M_j}\left(\mathbf{A}(\mathbf{x}(t^+|\mathbf{v}))\mathbf{x}(t^+|\mathbf{v}) + \mathbf{B}(\mathbf{x}(t^+|\mathbf{v}))\mathbf{u}(t^+|\mathbf{v})\right)s_k^j\delta(t-t_k^j)\,\mathrm{d}t\end{aligned} \tag{3.52}$$

Because

$$\frac{\mathrm{d}J(\vartheta^j(\epsilon))}{\mathrm{d}\epsilon}|_{\epsilon=0} = \frac{\mathrm{d}J(\mathbf{v})}{\mathrm{d}\mathbf{v}^j}\mathbf{s}^j \tag{3.53}$$

substituting (3.52) into (3.50) yields

$$\frac{\partial J(\mathbf{v})}{\partial \mathbf{v}^j}\mathbf{s}^j = \begin{bmatrix} H(\mathbf{x}(t_1^-|\mathbf{v}), \mathbf{u}(t_1^-|\mathbf{v}), \boldsymbol{\lambda}(t_1^-|\mathbf{v})) \\ -H(\mathbf{x}(t_1^+|\mathbf{v}), \mathbf{u}(t_1^+|\mathbf{v}), \boldsymbol{\lambda}(t_1^+|\mathbf{v})) \\ \vdots \\ H(\mathbf{x}(t_{M_j}^-|\mathbf{v}), \mathbf{u}(t_{M_j}^-|\mathbf{v}), \boldsymbol{\lambda}(t_{M_j}^-|\mathbf{v})) \\ -H(\mathbf{x}(t_{M_j}^+|\mathbf{v}), \mathbf{u}(t_{M_j}^+|\mathbf{v}), \boldsymbol{\lambda}(t_{M_j}^+|\mathbf{v})) \end{bmatrix}^\mathsf{T} \mathbf{s}^j \tag{3.54}$$

Hence, for each $j = 1, \cdots, N_w$, the gradient of the function J with respect to $\mathbf{v}^j$ is given by

$$\frac{\partial J(\mathbf{v})}{\partial \mathbf{v}^j} = \begin{bmatrix} H(\mathbf{x}(t_1^-|\mathbf{v}), \mathbf{u}(t_1^-|\mathbf{v}), \boldsymbol{\lambda}(t_1^-|\mathbf{v})) \\ -H(\mathbf{x}(t_1^+|\mathbf{v}), \mathbf{u}(t_1^+|\mathbf{v}), \boldsymbol{\lambda}(t_1^+|\mathbf{v})) \\ \vdots \\ H(\mathbf{x}(t_{M_j}^-|\mathbf{v}), \mathbf{u}(t_{M_j}^-|\mathbf{v}), \boldsymbol{\lambda}(t_{M_j}^-|\mathbf{v})) \\ -H(\mathbf{x}(t_{M_j}^+|\mathbf{v}), \mathbf{u}(t_{M_j}^+|\mathbf{v}), \boldsymbol{\lambda}(t_{M_j}^+|\mathbf{v})) \end{bmatrix} \tag{3.55}$$

where the right and left limit are defined as

$$H(t^+|\mathbf{v}) = \lim_{\tau \to t^+} H(\tau|\mathbf{v}) \tag{3.56}$$

$$H(t^-|\mathbf{v}) = \lim_{\tau \to t^-} H(\tau|\mathbf{v}) \tag{3.57}$$

3.4 The Halving Interval Method

The switching time gradient obtained from (3.55) is used to determine the optimal switching time control. Here, we use the halving interval method because it's convergence is guaranteed. The basic idea is to shrink the interval of the time horizon by one-half. The algorithm is presented below.

Because the method is gradient based, the solution is locally optimal when it converges. An illustration of the halving interval method can be observed in **Fig. 3.1**, where the solution converges in 8 iterations.

3.5 Issues on Practical Implementation

It has been shown that for regular linear and nonlinear optimal control problems involving n^{th} order systems, the optimal solution has at most n switching times (Bellman, 1956; Sussmann, 1979). Because in practice the number of grid blocks might be in the millions and the

Input: t_0, t_f, ϵ
Output: t_s
while $|t_f - t_0| \geq \epsilon$ **do**
    $t_s = \frac{t_f - t_0}{2}$;
    Compute $\frac{\partial J(t_s)}{\partial t}$;
    if $\frac{\partial J(t_s)}{\partial t} < 0$ **then**
        $t_0 = t_s$;
    else
        $t_f = t_s$;
    end
end

Algorithm 1: The halving interval method algorithm.

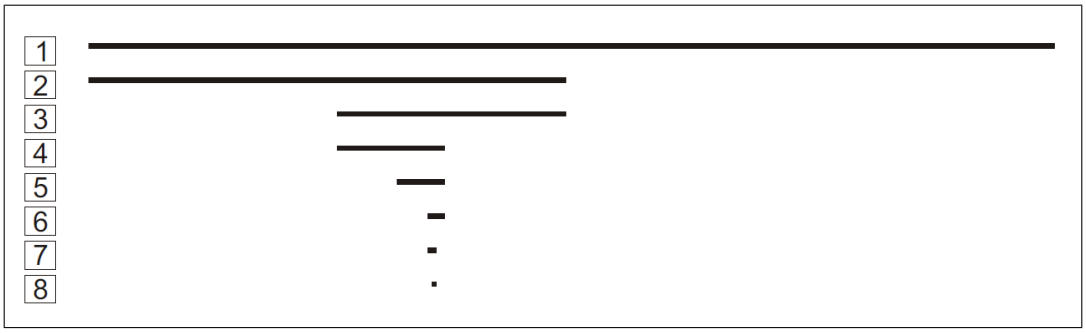

Figure 3.1: Ilustration of the halving interval method. The interval shrinks by half at each iteration. Here, the iterations are from 1 to 8.

number of wells might be in the dozens, the method does not appear to have much practical usefulness. Therefore, a pragmatic approach appears to be possible by setting the number of switching time to a reasonable number in comparison to the computational time.

Another limitation occurs when computing the left and right limit of the Hamiltonian sufficiently small time steps are required. On the other hand, one step of the reservoir simulation will require a significant amount of computational time, hence, in practice, larger time steps are usually used. To overcome this issue, in each simulation, the quality of the gradient should be checked by the finite difference.

3.6 Numerical Examples

Two cases are presented. The first is a simple two-dimensional case with a two-phase oil-water system, while the other is a three-dimensional reservoir that has realistic grids and well settings for a two-phase oil-water system. The aim is to maximize the following NPV

$$\max_{\mathbf{v}} J_{NPV} = \int_0^T \left(\sum_{j \in \mathcal{N}_{prod}} r_o^p(t) q_o^j(t) - \sum_{j \in \mathcal{N}_{prod}} r_w^p q_w^j(t) + \sum_{j \in \mathcal{N}_{inj}} r_w^i q_w^j(t) \right) \times \frac{1}{\left(1 + \frac{I}{100}\right)^{ct}} \, \mathrm{d}t \tag{3.58}$$

subject to the dynamical system described in (3.34)-(3.35) and the control constraint (3.38). The simulations were run using the MRST simulator (Lie et al., 2012).

3.6.1 Case 1

Consider a two-dimensional oil reservoir with one injection well and two production wells given in **Fig. 3.2**. The permeability distribution is composed of high and low permeability channels (**Fig. 3.3**). Intuitively, to retrieve as much oil as possible, production well no. 2 will initially be closed, while production well no. 1 will be fully open. In this example, our aim is to find the optimal switching times of both production wells such that (3.58) is maximized.

The injection rates are set to be constant for the injection wells at 500 $\mathrm{Sm}^3/\mathrm{day}$. The oil and water viscosity are set at 5×10^{-3} Pa.s and 1×10^{-3} Pa.s, while their density is 859 $\mathrm{kg/m}^3$ and 1014 $\mathrm{kg/m}^3$, respectively. The reservoir pressure p_R is 400 bara. The oil and water production price are $r_o^p = 630$ $\mathrm{USD/m}^3$ and $r_w^p = 63$ $\mathrm{USD/m}^3$, while the water injection price is $r_w^i = -63$ $\mathrm{USD/m}^3$. The discount factor is $I = 10\%$.

The control variables are the switching times of the valve opening in both production wells, namely t_1^1 and t_1^2. The optimization is run for 512 days. The result is compared with the reactive control method, in which the well is operated at maximum production rates and will be shut after the well is no longer profitable. In this case, the water cut threshold is 0.82. Reactive control is commonly used in the petroleum industry.

The saturation result can be observed from **Fig. 3.4** and **Fig. 3.5**. Here, the switching time method gives a better sweep efficiency compared to the reactive control method. The well control profile can be observed in **Fig. 3.6**. It should be noted that, at each iteration, the gradient quality of the objective function is checked with the finite difference method. **Fig. 3.7** shows the evolution of the objective function from the halving interval method. The NPV after 512 days from the switching time method is USD 2.84×10^8 while from reactive control, it is USD 2.35×10^8.

3.6.2 Case 2

For the second case, consider the realistic three-dimensional oil reservoir given in **Fig. 3.8**. The reservoir is taken from Lie et al. (2012). The number of active grid blocks is 13,420. The reservoir is completed with two injection wells and one multi-lateral production well. The multi-lateral production well is connected to two horizontal wells. Each horizontal well is installed with inflow control devices that can be used to control the flow rates or BHPs, i.e., both horizontal wells are controllable via the valves opening. The permeability distribution is given in **Fig. 3.9**.

The injection rates are set to be constant for both of the injection wells, at the value of $500\ \mathrm{m}^3/\mathrm{day}$. All of the reservoir properties and prices are set to be the same with case no. 1. The control variables are the switching times of the valve opening in both of the horizontal production wells, namely t_1^1, t_2^1, t_1^2, and t_2^2, i.e., $M_1 = M_2 = 2$. The optimization is run for 512 days.

In practice, the wells will be produced at maximum production rates in the first weeks to clean up the well from the brine set during completion and to obtain a good clean-up of the nearby well reservoir. Therefore, in the switching time method the wells will initially be fully open. In this case, the initial switching times are: $t_1^1 = 128$ days, $t_2^1 = 384$ days, $t_1^2 = 256$ days, and $t_2^2 = 384$ days, i.e., the well is closed between 128 days and 384 days for horizontal well no. 1 and between 256 days and 384 days for horizontal well no. 2. From this initial condition, the switching time algorithm will be used to find the optimal switching time.

Fig. 3.10 shows the optimal switching time control for both horizontal wells. Using the proposed method, we obtain $t_1^1 = 222$ days, $t_2^1 = 342$ days, $t_1^2 = 342$ days, and $t_2^2 = 510$ days, i.e., the well is shut between 222 days and 342 days for horizontal well no. 1 and between 342 days and 510 days for horizontal well no. 2. The reactive control method is shown by the dashed line. **Fig. 3.11** shows the comparison of the objective function of the switching time method and the reactive control method. It can be observed that the switching time method yields a higher NPV. A typical run-time was 4 minutes on an Intel core duo processor 1.66 GHz computer.

3.7 Conclusions

In this chapter, an optimal switching time method for an oil reservoir, given that the optimal settings of the wells are to be bang-bang controls, was presented. The bang-bang control has a major practical advantage because it can be implemented with simple on-off valves. The reservoir model is written in a state space representation and was assumed to be free from uncertainty. The optimal control settings are obtained based on a gradient calculation using the adjoint method combined with the halving interval method. Two examples of realistic reservoirs show that the proposed method can be used to increase oil revenue significantly.

Nomenclature

Symbols

$\mathbf{A}$	=	state matrix
$\mathbf{B}$	=	input matrix
H	=	Hamiltonian
J	=	objective function
$\mathbf{u}$	=	control vector
$\mathcal{U}$	=	control space
$\mathbf{v}$	=	switching time vector
$\mathbf{x}$	=	state vector
$\boldsymbol{\lambda}$	=	Lagrange multiplier
c	=	compressibility
f	=	fraction
I	=	discount factor
k	=	permeability
p	=	pressure
q	=	source or sink term
r	=	price
s	=	saturation
u	=	fluid velocity
N	=	number of well
$\mathcal{N}$	=	set of positive integer
μ	=	viscosity
ϕ	=	porosity
ρ	=	density

Scripts

0	=	initial
o	=	oil
g	=	gas
w	=	water
r	=	relative
inj	=	injection
$prod$	=	production
bh	=	bottom hole
T	=	transpose

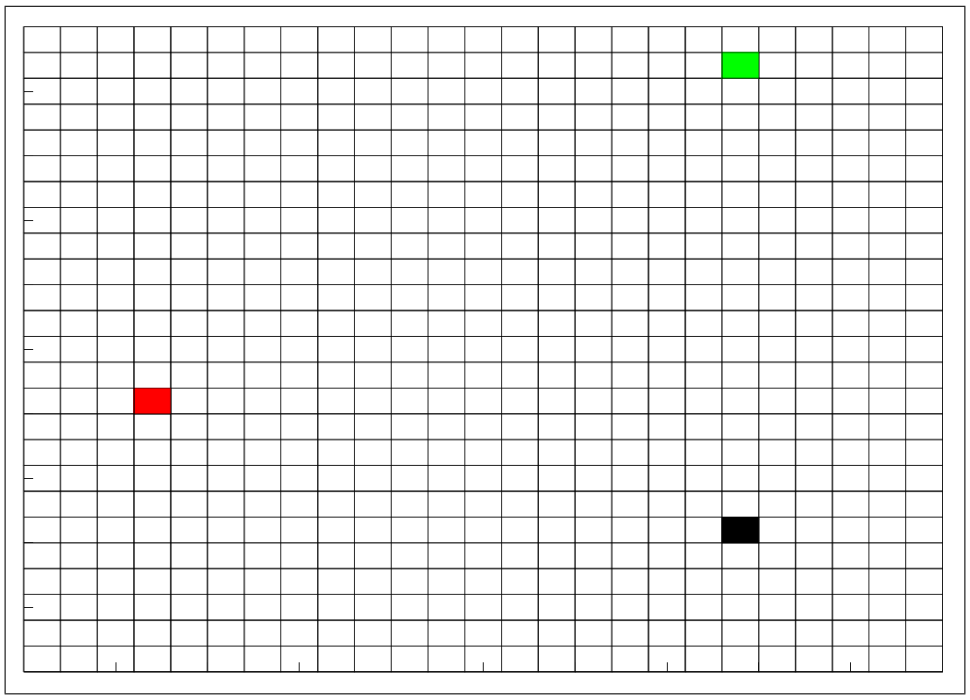

Figure 3.2: Position of the injection well (red), production well no. 1 (green) and production well no. 2 (black).

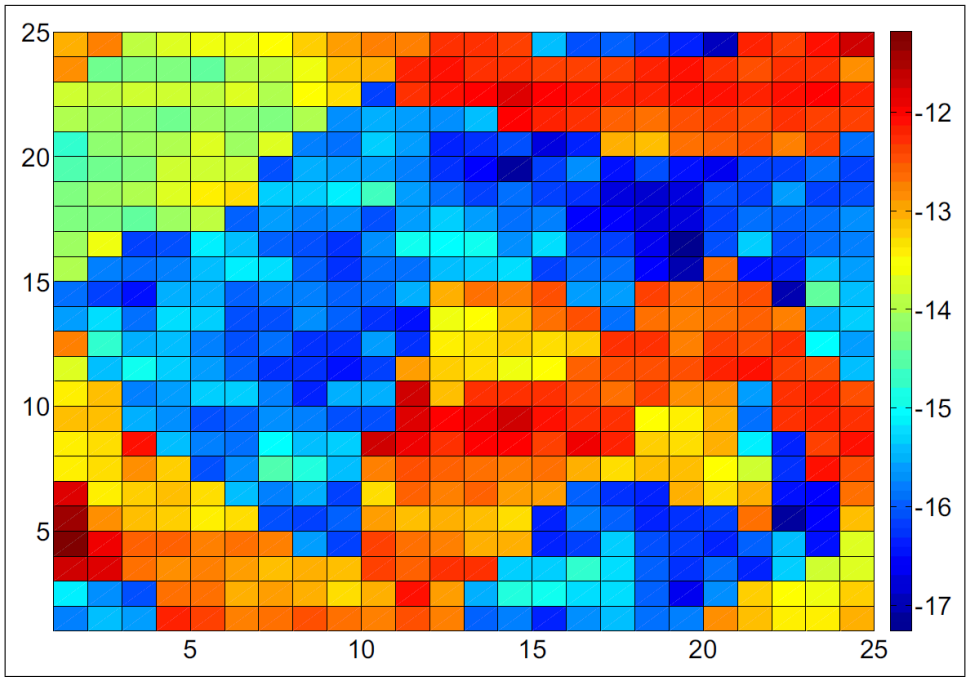

Figure 3.3: Permeability distribution of the reservoir comprising high and low permeability regions.

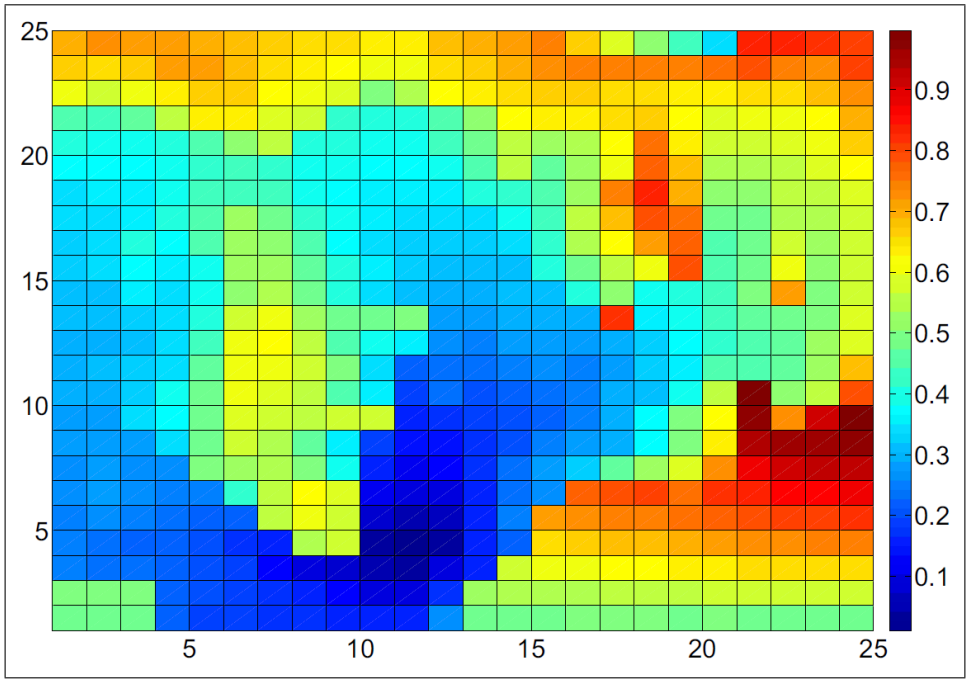

Figure 3.4: Final oil saturation using the reactive control method.

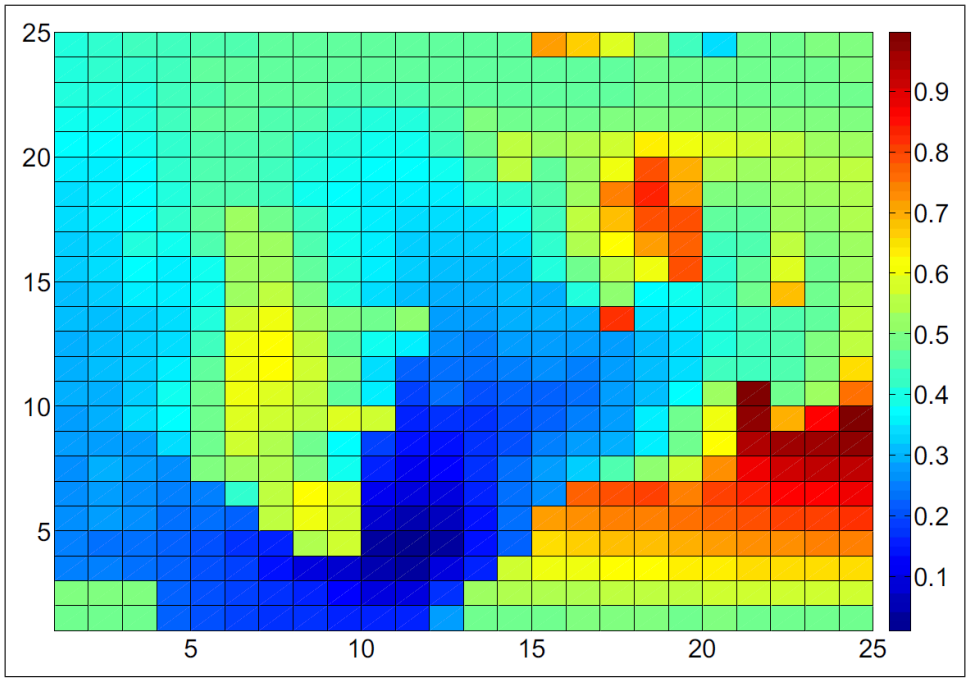

Figure 3.5: Final oil saturation using the switching time method.

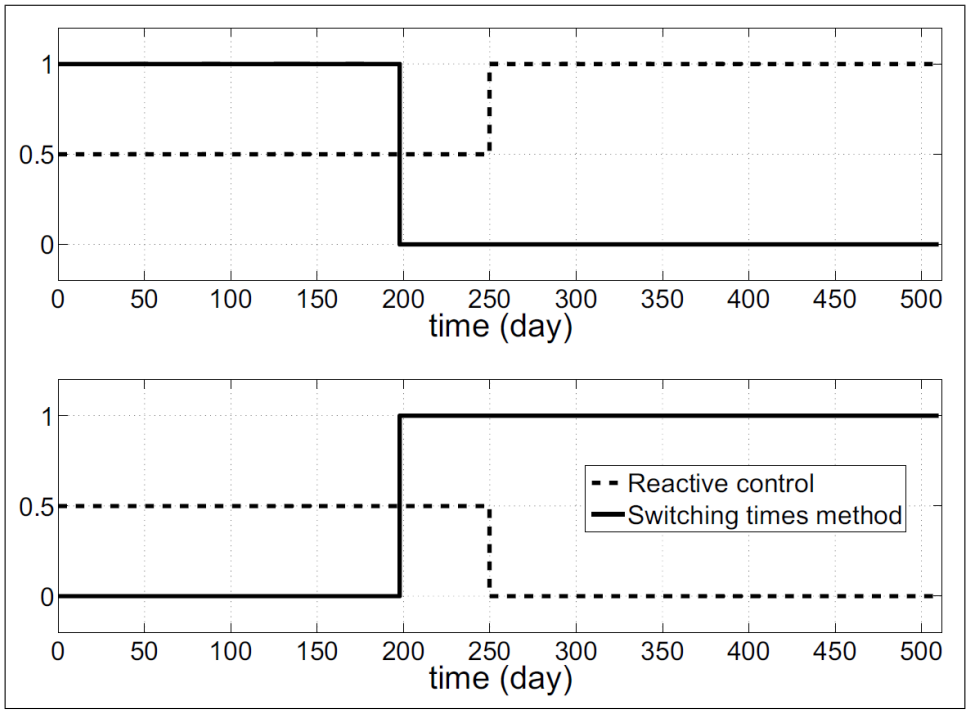

Figure 3.6: Rate profile from the switching times method for production well no. 1 (up) and production well no. 2 (down).

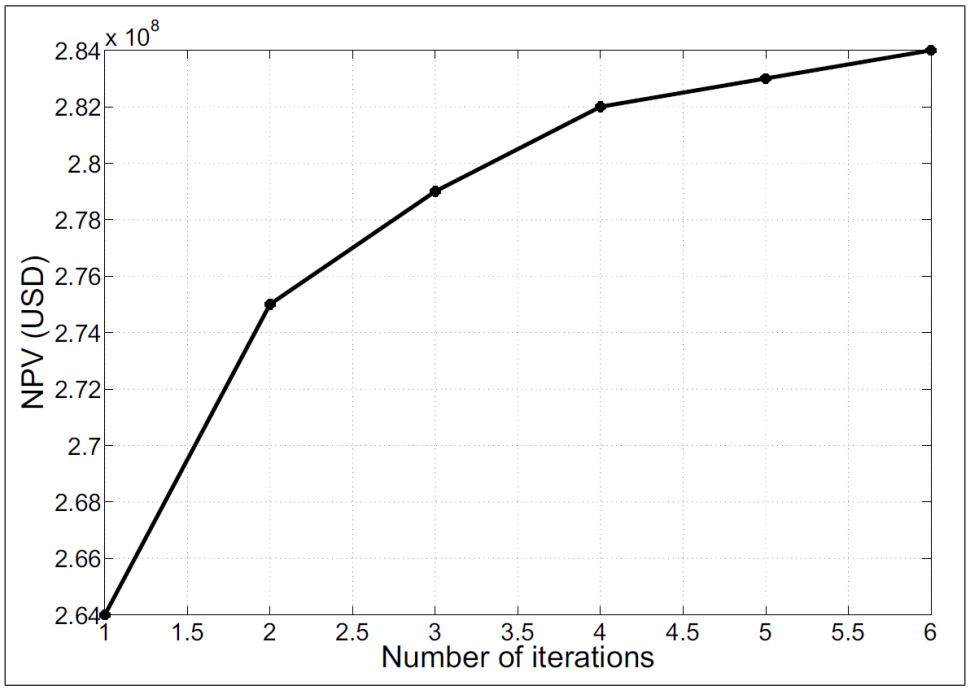

Figure 3.7: Evolution of the objective function using the halving interval method.

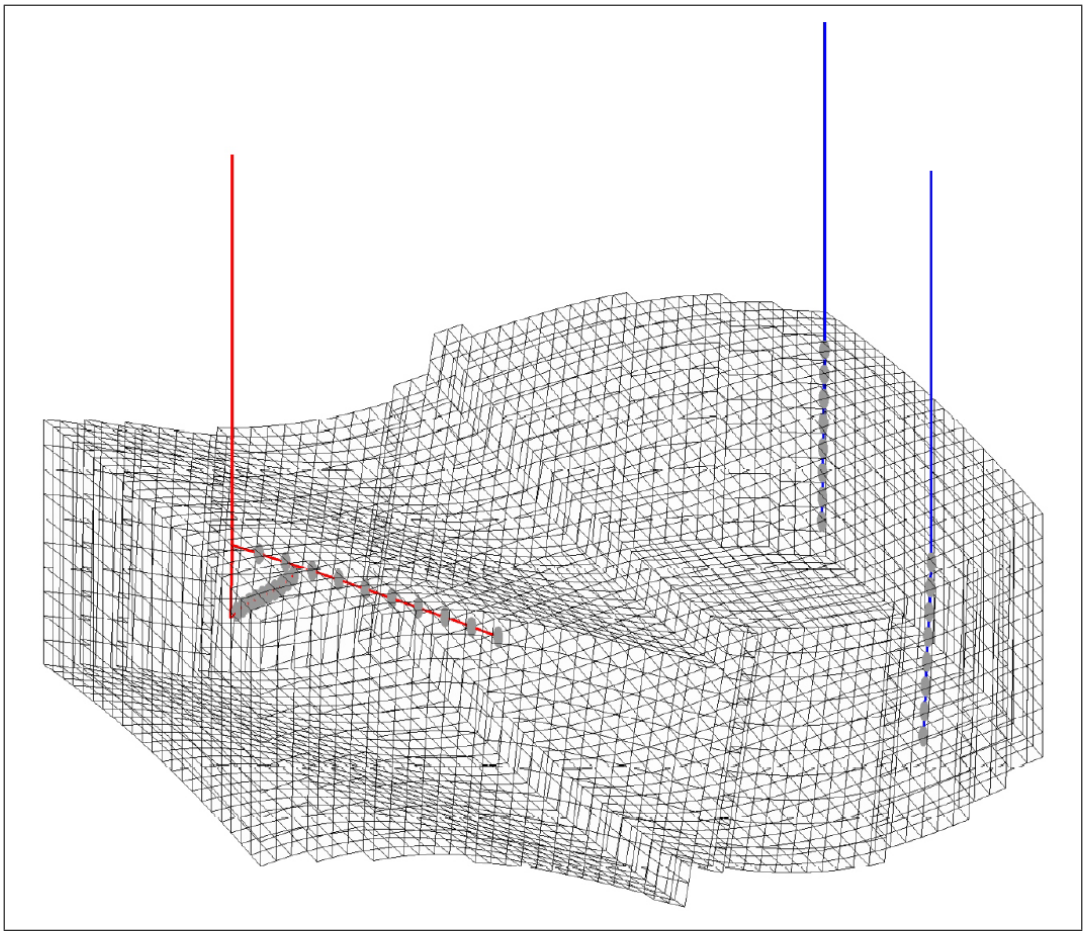

Figure 3.8: Grid and well positions for case 2.

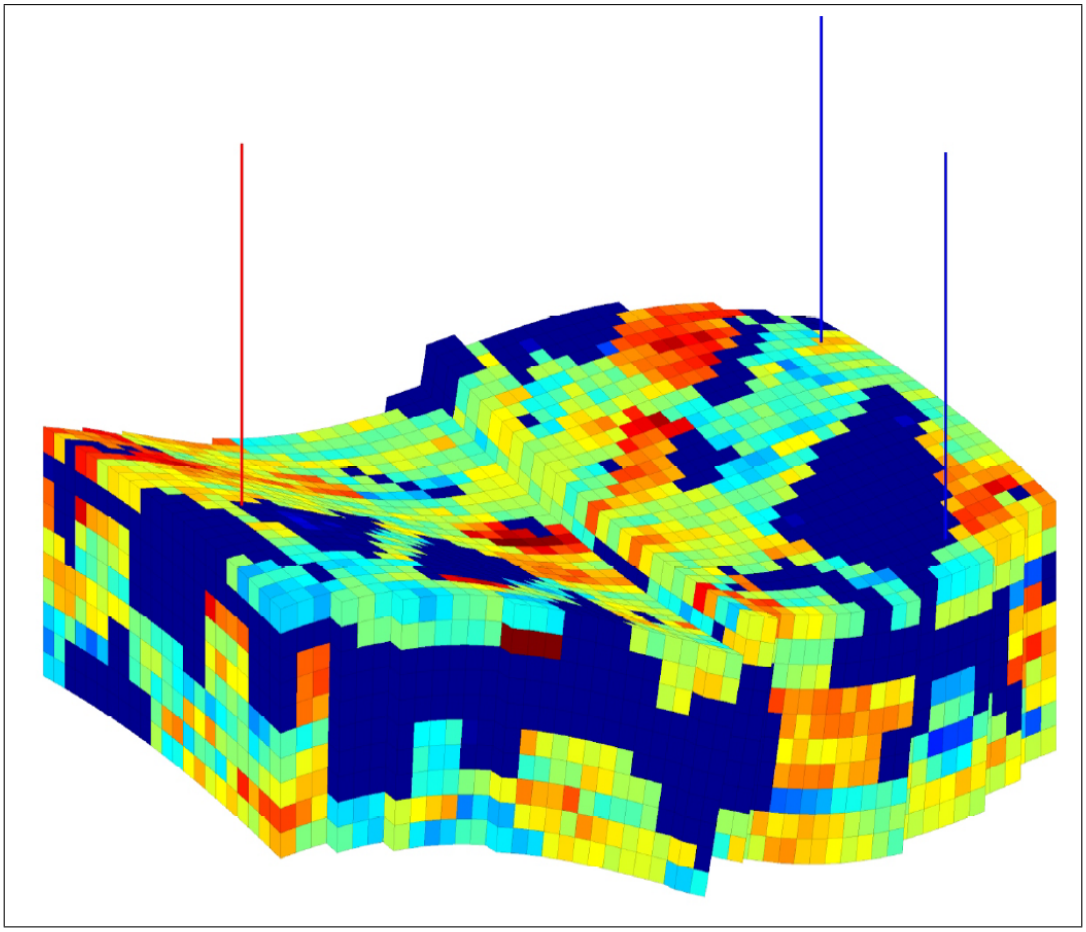

Figure 3.9: Permeability distribution for case 2.

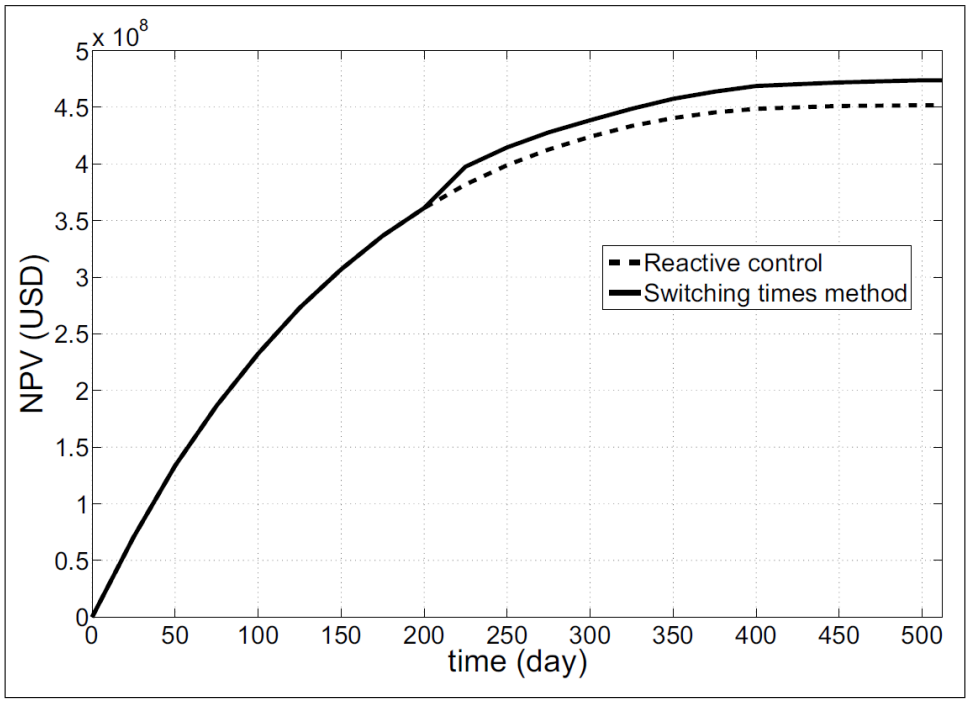

Figure 3.10: Comparison of the objective function. The dashed line is from the switching method while the straight line is from the reactive control.

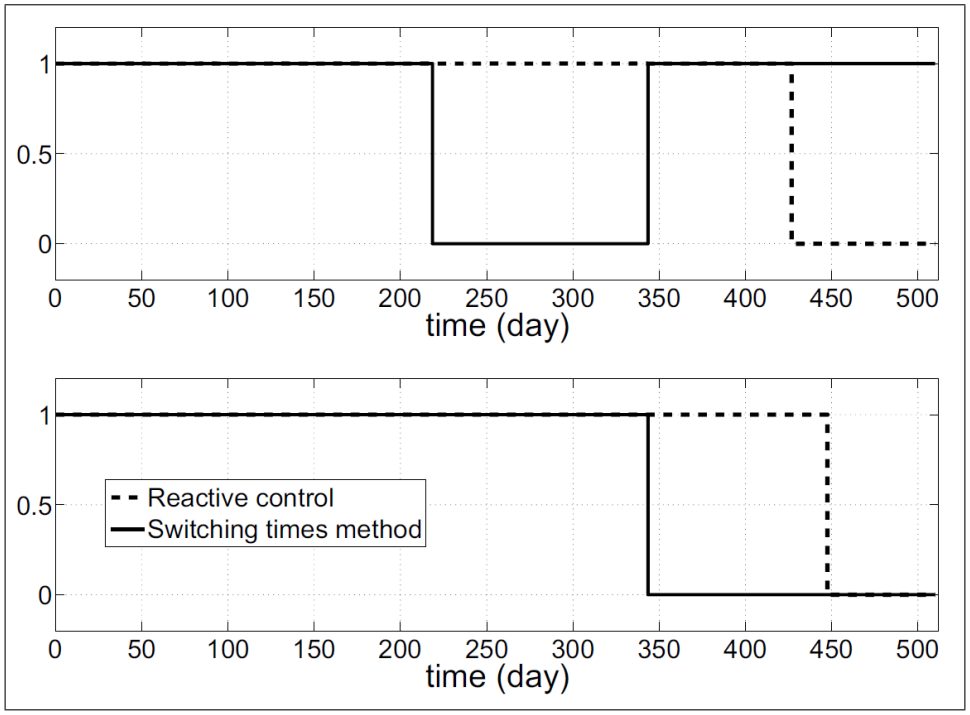

Figure 3.11: Rate profile from the switching time method for the first horizontal well.

Chapter 4

Decision Analysis for Long-term and Short-term Production Optimization

This chapter is based on a paper which has been submitted to the SPE Reservoir Characterisation and Simulation Conference and Exhibition 2013.

4.1 Introduction

Technically speaking, on average, less than half of the oil in reservoirs that can be produced, mainly due to low permeability regions and strength of the natural drives. With technological advances, however, the remaining oil in the reservoirs that have been difficult to produce is now accessible. The use of secondary recovery techniques such as gas lift and water injection have increased oil recovery significantly. A more advanced method like enhanced oil recovery (EOR) is even better (Lakatos, 2005). These methods are now supported by the installation of inflow control devices (ICD) in horizontal wells to control the production and injection rates (Fernandes et al., 2009). Since technologies are expensive, the question is how to use these technologies in an optimal manner.

Optimization may be performed in different field development stages using different kind of methods by different people. An optimization problem may involve many variables, parameters, and constraints where the result eventually leads to a decision. In reality, the decision is often a trade-off where we can't increase the value of one objective without decreasing the value of the other. As an example, in an early stage of field development when drilling a new well, in order to reduce formation damages and thus increasing well productivity, one may use underbalanced drilling instead of conventional (overbalanced) drilling. However, underbalanced drilling is much more expensive since more people are involved and some additional equipments need to be installed (Eck-Olsen et al., 2004). In this case, an economical analysis which includes risk analysis needs to be done.

From an operational point of view, a decision on how to operate the wells is also critical. Optimization is performed by both the reservoir and the production engineers. There is a sig-

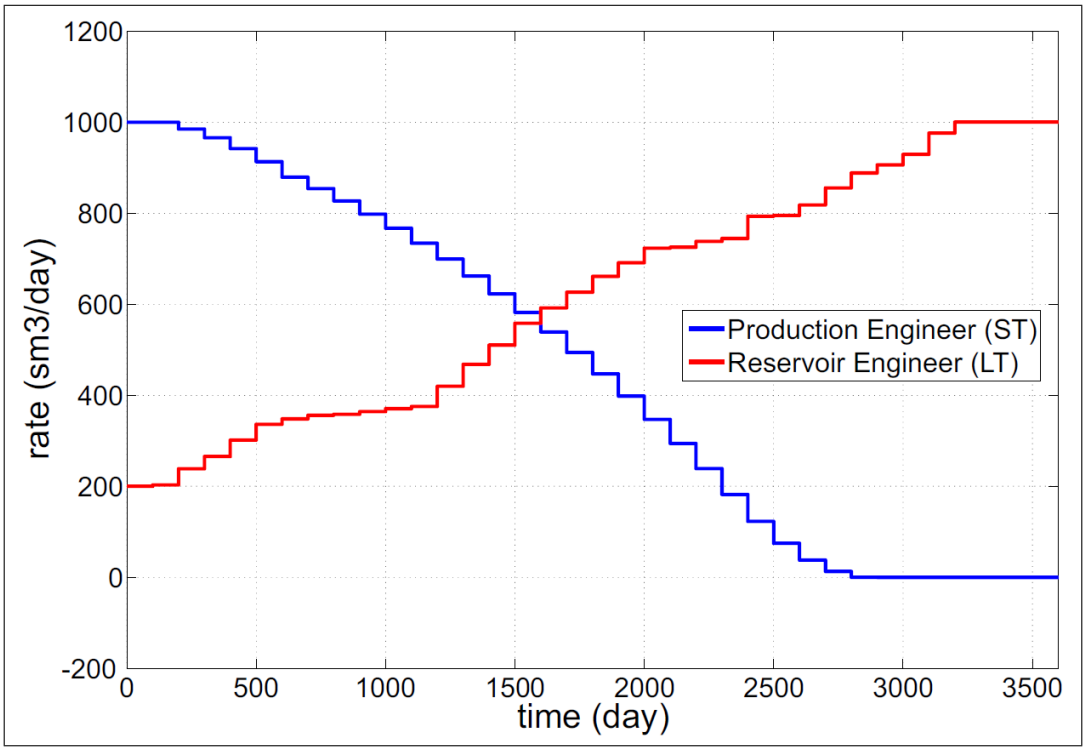

Figure 4.1: Illustration of oil production rate from different approaches.

nificant difference between the two approaches regarding the solution strategy. The reservoir engineers aim to obtain an optimization strategy for the whole reservoir life time, while the production engineers tend to optimize the production on a daily basis. The different solution strategies can be illustrated in **Fig. 4.1**. Here, the production engineer strategy is to produce the oil at the maximum rate in the beginning of the production and as the time goes by, the oil production will decrease. On the other hand, the reservoir engineer strategy is to produce the oil at a lower rate in the beginning and gradually increase the rate towards the end. The question is which strategy is the best? Since there are so many and large uncertainties present, for instance from the oil price, one may prefer to choose the short-term strategy. However, a significant amount of oil may be left in the reservoir at the end of production. Using the long-term strategy, one may gain more oil from the reservoir at the end of the production; however, this will require good information about the reservoir. Therefore, a systematical decision analysis is needed to balance the short-term and long-term strategy (van Essen and Van den Hof, 2011; Chen et al., 2012; Stenger et al., 2009).

In this chapter, we present a novel approach to systematically integrate long-term and short-term production optimization. The approach is based on a priori articulation of preferences, i.e., the decision maker is allowed to specify preferences which may be articulated in terms of goals or the relative importance of long-term and short-term objective. The approach is applied to a simplified model of the south wing of the Voador field in the Campos basin,

Brazil. The results are presented as surface Pareto-like plots which can be used for decision support to balance long-term and short-term goals.

4.2 The Voador Field

The Voador field is located in the Campos basin about 100 miles off the coast of Brazil at an average water depth of 565 m. The reservoir is a friable Marlim Sandstone known as the Carapebus Formation (Oligo-Miocene age). It is a solution gas drive reservoir that has been evenly depleted to below the bubble point pressure. It has two non-communicating reservoirs, namely the north and south wings (Lorenzatto et al., 2004).

The south wing started to produce in November 1992 via production well PROD1. In order to maintain the reservoir pressure, an injection well INJ1 was drilled in 1999. The injection well is a multilateral well and has been reported to be the first level five multilateral well (based on Technology Advancement for Multilaterals (TAML) standard) completed from a semi-submersible rig (Pasicznyk et al., 1999). The injection well installation was a big success as it boosted the oil production to 6000 Sm^3/day. However, the peak production did not last long. To increase the oil production, several production wells PROD2, PROD3, and PROD4 were drilled sequentially.

Today, the field is in its mature stage. The total oil production is less than 800 Sm^3/day and the water cut is above 0.9 for some production wells. After the reservoir pressure depleted below its bubble point pressure, the reservoir is also producing free gas. In 2011, the GOR for every production well is less than 80 Sm^3/Sm^3.

4.3 Mathematical Model

In this section, we present the simulator used in this research. Further, the concept of the adjoint method is also briefly discussed. The simulator is part of the Matlab Reservoir Simulator Toolbox (MRST). It is developed by SINTEF and is available online for free download under the terms of the GNU General Public License (GPL) (Lie et al., 2012).

4.3.1 Reservoir Model.

The simulator employed here uses the following basic assumptions:

1. Two-phase incompressible flow
2. Neglecting gravity
3. Zero capillary force
4. No-flow at the outer boundary of the reservoir

Since the presence of gas is not significant is the example, assumption 1 is assumed to hold. The pressure equation for the model may be given by

$$\vec{v} = -\Lambda(s)\mathbf{K}\nabla p \tag{4.1}$$

$$\nabla \cdot \vec{v} = q \tag{4.2}$$

where $\vec{v}$ denotes the Darcy velocity, Λ is the total mobility, s is the water saturation, $\mathbf{K}$ is the permeability tensor, and q is the fluid source term. The corresponding saturation equation is given by

$$\phi \frac{\partial s}{\partial t} + \nabla \cdot [f(s)\vec{v}] = q_w \tag{4.3}$$

where ϕ denotes the effective porosity, f is the water fractional flow function, and q_w is the water source term. Let $\mathbf{v}$ denote the outward face fluxes and well-perforation rates, $\mathbf{s}$ is the saturation cell, $\mathbf{p}$ is the pressure cell, and $\boldsymbol{\pi}$ is the face pressures and well pressures. The system corresponding to the pressure equation (4.1) at time t^n can be written in the form

$$\begin{bmatrix} \mathbf{B}(\mathbf{s}^{n-1}) & \mathbf{C} & \mathbf{D} \\ \mathbf{C}^\top & \mathbf{0} & \mathbf{0} \\ \mathbf{D}^\top & \mathbf{0} & \mathbf{0} \end{bmatrix} \begin{bmatrix} \mathbf{v}^n \\ -\mathbf{p}^n \\ \boldsymbol{\pi}^n \end{bmatrix} = \begin{bmatrix} \mathbf{0} \\ \mathbf{0} \\ \mathbf{v}_\Gamma^n \end{bmatrix} \tag{4.4}$$

where $\mathbf{B}(\mathbf{s}^{n-1})$ and $\mathbf{C}$ are block diagonal matrices. The block in $\mathbf{B}$ corresponds to a cell i is $\left[\Lambda(\mathbf{s}_i^{n-1})\mathbf{T}_i\right]^{-1}$ with an extended diagonal entry $\left[\Lambda(\mathbf{s}_i^{n-1})\mathbf{WI}_i\right]^{-1}$ for every well perforating cell i. Here, $\mathbf{T}_i$ denotes the transmissibility matrix while $\mathbf{WI}_i$ is the well productivity index. Each block in matric $\mathbf{C}$ has an $n_i \times 1$ vector of ones, where n_i is the number of faces plus the number well perforations in cell i. Further, each column of the matrix $\mathbf{D}$ corresponds to a unique face or well face and has unit entries in the positions of the face/well face in the cell wise ordering. The vector $\mathbf{v}_\Gamma^n$ has a zero entry corresponding to every face. Splitting the vector $\boldsymbol{\pi}^{n\top} = \begin{bmatrix} (\hat{\boldsymbol{\pi}}^n)^\top & \boldsymbol{\pi}_D^{n\top} \end{bmatrix}$ and the matrix $\mathbf{D} = \begin{bmatrix} \hat{\mathbf{D}} & \mathbf{D}_D \end{bmatrix}$, the system becomes

$$\begin{bmatrix} \mathbf{B}(\mathbf{s}^{n-1}) & \mathbf{C} & \hat{\mathbf{D}} \\ \mathbf{C}^\top & \mathbf{0} & \mathbf{0} \\ \hat{\mathbf{D}}^\top & \mathbf{0} & \mathbf{0} \end{bmatrix} \begin{bmatrix} \mathbf{v}^n \\ -\mathbf{p}^n \\ \hat{\boldsymbol{\pi}}^n \end{bmatrix} = \begin{bmatrix} \mathbf{A}_D^n \mathbf{u} + \mathbf{b}_D^n \\ \mathbf{0} \\ \mathbf{A}_N^n \mathbf{u} + \mathbf{b}_N^n \end{bmatrix} \tag{4.5}$$

where $\mathbf{A}_D^n$ and $\mathbf{A}_N^n$ are sparse matrices and $\mathbf{u}$ denotes a control input vector of piecewise constant pressures or rates for a given set of the wells at timestep t^n. The subscript D corresponds to bhp-controlled wells (Dirichlet boundary condition) while the subscript N corresponds to rate-controlled wells (Neumann boundary condition). The vectors $\mathbf{b}_D^n$ and $\mathbf{b}_N^n$ are all zeros except at entries corresponding to non-controllable boundary conditions. For more detail see Krogstad et al. (2011).

Next, using the standard upstream weighted implicit finite-volume method, the saturation equation (4.3) may be written in the following form

$$\mathbf{s}^n = \mathbf{s}^{n-1} + \delta t^n \mathbf{D}_{PV}^{-1} \left[\mathbf{A}(\mathbf{v}^n) f(\mathbf{s}^n) + \mathbf{q}(\mathbf{v}^n)_+\right] \tag{4.6}$$

where δt^n is the timestep, $\mathbf{D}_{PV}$ is the diagonal matrix containing the cell pore volumes, $\mathbf{A}(\mathbf{v}^n)$ is the sparse flux matrix, and $\mathbf{q}(\mathbf{v}^n)_+$ is the vector of positive cell sources (injection rates).

4.3.2 Adjoint Method.

The adjoint method is the most efficient way to compute gradients for reservoir models (see, e.g., Foss (2012)) which later will be used for optimization purposes.

The adjoint model for a simulator consisting of a multi-scale pressure solver and a saturation solver that works on flow-adapted grids is implemented in the MRST (Krogstad et al., 2011). Let $\mathbf{x}^n = (\mathbf{v}^n, \mathbf{p}^n, \boldsymbol{\pi}^n, \mathbf{s}^n)$ and $\mathbf{u}^n$ as the control input variables. Each time step of (4.5)-(4.6) can be re-written in a compact form as

$$F^n(\mathbf{x}^n, \mathbf{x}^{n-1}, \mathbf{u}^n) = 0 \tag{4.7}$$

where $\mathbf{x}$ and $\mathbf{u}$ are the stacked state and control inputs for all time steps. The pressure and saturation equations (4.5)-(4.6) may be written in a compact form as $F(\mathbf{x}, \mathbf{u})$. Let $J(\mathbf{x}, \mathbf{u})$ be an objective function and denoted by $\nabla_{\mathbf{u}} J$ the gradient of J with respect to $\mathbf{u}$. Introducing an auxiliary function $J_{\boldsymbol{\alpha}}$ as

$$J_{\boldsymbol{\alpha}}(\mathbf{x}, \mathbf{u}) = J(\mathbf{x}, \mathbf{u}) + \boldsymbol{\alpha}^\intercal F(\mathbf{x}, \mathbf{u}) \tag{4.8}$$

where $\boldsymbol{\alpha} = \boldsymbol{\alpha}\left(\boldsymbol{\alpha}_{\mathbf{v}}, \boldsymbol{\alpha}_{\mathbf{p}}, \boldsymbol{\alpha}_{\hat{\boldsymbol{\pi}}}, \boldsymbol{\alpha}_{\mathbf{s}}\right)$ is a vector of Lagrange multipliers. The gradient $\nabla_{\mathbf{u}} J_{\boldsymbol{\alpha}}$ is given by

$$(\nabla_{\mathbf{u}} J_{\boldsymbol{\alpha}})^\intercal = \frac{\partial J}{\partial \mathbf{u}} + \frac{\partial J}{\partial \mathbf{x}} \frac{\mathrm{d}\mathbf{x}}{\mathrm{d}\mathbf{u}} + \boldsymbol{\alpha}^\intercal \frac{\partial F}{\partial \mathbf{u}} + \boldsymbol{\alpha}^\intercal \frac{\partial F}{\partial \mathbf{x}} \frac{\mathrm{d}\mathbf{x}}{\mathrm{d}\mathbf{u}} + F^\intercal \frac{\mathrm{d}\boldsymbol{\alpha}}{\mathrm{d}\mathbf{u}} \tag{4.9}$$

which reduces to

$$(\nabla_{\mathbf{u}} J_{\boldsymbol{\alpha}})^\intercal = \frac{\partial J}{\partial \mathbf{u}} + \boldsymbol{\alpha}^\intercal \frac{\partial F}{\partial \mathbf{u}} \tag{4.10}$$

when $\boldsymbol{\alpha}$ obeys the adjoint equations

$$\frac{\partial F^\intercal}{\partial \mathbf{x}} \boldsymbol{\alpha} = -\frac{\partial J^\intercal}{\partial \mathbf{x}} \tag{4.11}$$

Remark that in (4.7), the matrix $\frac{\partial F}{\partial \mathbf{x}}$ has a block structure with blocks $\frac{\partial F^n}{\partial \mathbf{x}^n}$ on the main diagonal and $\frac{\partial F^{n+1}}{\partial \mathbf{x}^n}$ on the lower diagonal. Applying this to (4.11), the adjoint equations for time step n are given as

$$\frac{\partial F^{n\intercal}}{\partial \mathbf{x}^n} \boldsymbol{\alpha}^n + \frac{\partial F^{n+1\intercal}}{\partial \mathbf{x}^n} \boldsymbol{\alpha}^{n+1} = -\frac{\partial J^{n\intercal}}{\partial \mathbf{x}^n} \tag{4.12}$$

The above equation is solved backward in time to obtain $\boldsymbol{\alpha}$. Now the gradient with respect to time step n can be computed by the following equation

$$\nabla_{\mathbf{u}^n} J_{\boldsymbol{\alpha}} = \frac{\partial J^\intercal}{\partial \mathbf{u}^n} + \frac{\partial F^{n\intercal}}{\partial \mathbf{u}^n} \boldsymbol{\alpha}^n \tag{4.13}$$

For ease of notation, define

$$g(\mathbf{v},\mathbf{s}) = \delta t \mathbf{D}_{PV}^{-1}\left[\mathbf{A}(\mathbf{v})f(s) + \mathbf{q}(\mathbf{v})_+\right] \tag{4.14}$$

Finally, substituting (4.5) and (4.6) into (4.12), the adjoint equation for timestep n are obtained as follow

$$\left[\mathbf{I} - \frac{\partial g(\mathbf{v}^n,\mathbf{s}^n)}{\partial \mathbf{s}^n}\right]^\top \boldsymbol{\alpha}_s^n = \boldsymbol{\alpha}_s^{n+1} - \frac{\partial J^{n\top}}{\partial \mathbf{s}^n} - \left[\frac{\partial \mathbf{B}(\mathbf{s}^n)v^{n+1}}{\partial \mathbf{s}^n}\right]^\top \boldsymbol{\alpha}_v^{n+1} \tag{4.15}$$

$$\begin{bmatrix} \mathbf{B}(\mathbf{s}^{n-1}) & \mathbf{C} & \hat{\mathbf{D}} \\ \mathbf{C}^\top & \mathbf{0} & \mathbf{0} \\ \hat{\mathbf{D}}^\top & \mathbf{0} & \mathbf{0} \end{bmatrix} \begin{bmatrix} \boldsymbol{\alpha}_v^n \\ \boldsymbol{\alpha}_p^n \\ \boldsymbol{\alpha}_{\hat{\pi}}^n \end{bmatrix} = \begin{bmatrix} -\frac{\partial J^{n\top}}{\partial \mathbf{v}^n} + \frac{\partial g(\mathbf{v}^n,\mathbf{s}^n)^\top}{\partial \mathbf{v}^n}\boldsymbol{\alpha}_s^n \\ \mathbf{0} \\ \mathbf{0} \end{bmatrix} \tag{4.16}$$

Once the adjoint equations have been solved, the gradient of the objective function J at timestep n is given by

$$\nabla_{\mathbf{u}^n} J = \frac{\partial J^\top}{\partial \mathbf{u}^n} - \mathbf{A}_D^{n\top}\boldsymbol{\alpha}_v^n - \mathbf{A}_N^{n\top}\boldsymbol{\alpha}_{\hat{\pi}}^n \tag{4.17}$$

4.4 Long-term and Short-term Optimization

In this section, the notation $J_{NPV}(\mathbf{x},\mathbf{u};b)$ will be used to describe an objective function that depends on the state variable $\mathbf{x}$, control variable $\mathbf{u}$, and parameter b. This objective function will be maximized (or minimized) using piecewise constant functions of flow rates or well pressures as the control variables. Suppose the control variable is the flow rate $\mathbf{q}$.

The objective takes the following form of the net present value (NPV)

$$\begin{aligned} J_{NPV}(\mathbf{x},\mathbf{q};b) = & \int_0^T \left(\sum_{j\in\mathcal{N}_{prod}} r_o^{prod} q_o^j(\mathbf{x}(t)) - \sum_{j\in\mathcal{N}_{prod}} r_w^{prod} q_w^j(\mathbf{x}(t)) - \sum_{j\in\mathcal{N}_{inj}} r_w^{inj} q_w^j(\mathbf{x}(t)) \right) \\ & \frac{1}{\left(1+\frac{b}{100}\right)^{ct}}\,\mathrm{d}t \end{aligned} \tag{4.18}$$

where r_o^{prod}, r_w^{prod}, and r_w^{inj} denote the oil production price, water production cost, and water injection cost, respectively. The discount factor is denoted by b and consider as the parameter, while c is the time constant. Due to production constraints, the flow rate vector $\mathbf{q}$ has an upper and lower bound

$$\mathbf{q}_{LB} \le \mathbf{q} \le \mathbf{q}_{UB} \tag{4.19}$$

To solve the optimization problem of (4.18) with respect to the dynamical system (4.5)-(4.6) and the bound constraints (4.19) on the interval $[0,T]$, the gradient is calculated by the

adjoint method described in the previous section. Further, the gradient is used in a line search algorithm to find an optimal control setting $\mathbf{q}$.

The discount factor b will be used to move emphasis between short-term and long-term optimization. Setting $b = 0$ focuses on recovery while large b values stresses high production on a short-term horizon. There is clear analogy to the reservoir management and reservoir engineers who focus on long-term effects, and daily operations and production engineers who emphasize short-term effects. In the following $\mathbf{q}_{LT}$ and $\mathbf{q}_{ST}$ will denote strategies which focus on long-term and short-term horizons, respectively.

As a consequence of the long-term versus short-term planning horizons, the production profiles may differ quite substantially, i.e., $\mathbf{q}_{LT}$ and $\mathbf{q}_{ST}$ differs. In the short-time horizon, the $J_{NPV}(\mathbf{x}, \mathbf{q}_{ST}; b)$ is usually higher than $J_{NPV}(\mathbf{x}, \mathbf{q}_{LT}; b)$, while in the long-time horizon it is vice versa. When it comes to decision making, one may prefer to choose $\mathbf{q}_{ST}$ instead of $\mathbf{q}_{LT}$ since there is a lot of uncertainties in the long term prediction provided by the model and from the future oil price. However, a decision based only on $\mathbf{q}_{ST}$ might not be well founded in a life cycle perspective. Therefore, a method to balance these objectives is justified.

In the following, the method will be introduced in a stepwise manner.

1. The NPV (4.18) is maximized using the adjoint method for a reasonable b value; e.g., $b = 10\%$ along the time horizon. This will be called our "true" long-term NPV and the rate strategy will be denoted by $\mathbf{q}_{LT}$.

2. The same NPV (4.18) with $b = 10\%$, is evaluated using the strategy obtained from the reactive control, where the strategy is defined for an appropriate water cut value, and plotted in the same figure as the NPV in the first step. This will be called our "true" short-term NPV and the rate strategy will be denoted by $\mathbf{q}_{ST}$.

3. Define two NPVs using two different discount factors; e.g., $b_{UB} = 0\%$ and $b_{LB} = 75\%$, where UB and LB stand for upper and lower bound, respectively. The idea here is to introduce a heuristic for some upper and lower bound of the NPV, where the upper bound represents the long-term objective while the lower bound represents a short-term perspective.

4. Next, we define a new objective which basically is the convex combination between the heuristic upper bound (long-term) and the heuristic lower bound (short-term) in step 3 and perform an optimization, e.g., using the adjoint method. Using this approach, the long-term and short-term optimization can be solved simultaneously using an optimization method. For every convex combination, a new production profile $\mathbf{q}_\lambda$ will be obtained. This method is called the weighted-sum and will be presented in the next section.

5. Every $\mathbf{q}_\lambda$ will be used to generate NPV with $b = 10\%$. Remark that the NPV from step 1, step 2, and this step have the same discount factor and each of them will represent a trade-off between long-term and short-term optimization.

6. Finally, a Pareto-like plot is generated. The vertical axis shows the NPV on the horizon T while the horizontal axis shows NPV on a much shorter horizon. This visualizes the trade-off between long-term and short-term considerations.

It is important to note that the choice of the upper and the lower bound is subjective. However, to simplify the problem, in this chapter the upper and the lower bound is created from (4.18) by changing the discount factor b.

4.5 Weighted-Sum Method

Let's consider the following augmented function

$$J_{NPV}(\mathbf{x}, \mathbf{q}_\lambda; b_{UB}, b_{LB}) = \lambda * \underbrace{J_{NPV}(\mathbf{x}, \mathbf{q}; b_{UB})}_{\text{long-term NPV}} + (1-\lambda) * \underbrace{J_{NPV}(\mathbf{x}, \mathbf{q}; b_{LB})}_{\text{short-term NPV}} \tag{4.20}$$

Here, the function $J_{NPV}(\mathbf{x}, \mathbf{q}_\lambda; b_{UB}, b_{LB})$ is a convex combination of the heuristic upper bound $J_{NPV}(\mathbf{x}, \mathbf{q}; b_{UB})$ and lower bound $J_{NPV}(\mathbf{x}, \mathbf{q}; b_{LB})$ of the NPV. The parameter λ varies from zero to one. Solving an optimal control problem with (4.20) as the objective yields a new input solution (strategy) $\mathbf{q}_\lambda$. By varying λ, a set of input solutions can be obtained. The input solution $\mathbf{q}_\lambda$ will be used to compute the actual $J_{NPV}(\mathbf{x}, \mathbf{q}_\lambda; b)$. It can be observed from (4.20) that the choice of λ represents the priori articulation preference of the decision maker.

This approach is adopted from multi-objective optimization (MOO). In MOO, the solution is not a single point but rather a collection of solutions known as the Pareto frontier (Marler and Arora, 2004). For bi-objective optimization problems, the frontier may be obtained by plotting both objectives in x and y Cartesian coordinates. It has been shown that for positive coefficients of the weighted-sum method, the solution is always Pareto optimal (Zadeh, 1963). Therefore, any solution of (4.20) is a Pareto solution in the design space. However, since the method presented here in not using the actual objective functions and since no global solution is guaranteed, we do not claim that our solution is Pareto optimal. In fact, since the choice of the upper and lower bounds may be different, a solution may be dominated by the other and hence the solution may not Pareto optimal. In spite of these shortcomings, the solutions may still be used by the decision maker since it considers a trade-off between short-term and long-term strategies. Using the weighted-sum method, the computational effort to find a set of solutions can be performed by parallel computation.

4.6 Numerical Simulations

The simulation uses data from the south wing of the Voador field. The permeability and porosity field are shown in **Fig. 4.2** and **Fig. 4.3**, respectively. The time horizon for this simulation is 10 years. In this study, we first observed the difference between the long-term and short-term optimization strategy in term of the NPV. To this end, the long-term strategy

will be computed using the adjoint-based optimization while the short-term strategy will be computed by the reactive control.

We consider the actual discount factor as $b = 10\%$ while the upper and lower bound of the NPV may be obtained by using $b_{UB} = 0\%$ and $b_{LB} = 75\%$. The oil production price is chosen at 630 USD/Sm^3, water production cost is 63 USD/Sm^3, and water injection cost is 63 USD/Sm^3. The water cut threshold is 0.82.

In this simulation, all values presented in the figures have been normalized. As can be seen from **Fig. 4.4**, using a 10% discount factor, in the short time horizon (less than 700 days) the NPV of the short-term strategy $J_{NPV}(\mathbf{q}_{ST}; 10\%)$ is significantly higher than the NPV of the long-term strategy $J_{NPV}(\mathbf{q}_{LT}; 10\%)$. The solution after 10 years, however, is the opposite. Keep in mind that $\mathbf{q}_{ST}$ is obtained from reactive control while $\mathbf{q}_{LT}$ is obtained from the long-term adjoint-based optimization.

Next, we introduce the upper and the lower bound of the NPV as can be seen from **Fig. 4.5**. In this case, the upper bound $J_{NPV}(\mathbf{q}; 0\%)$ and the lower bound $J_{NPV}(\mathbf{q}; 75\%)$ are computed by the adjoint-based optimization. By varying λ, a set of strategies is obtained. A small λ means that the decision maker places more weight to the short-term strategy and vice versa. As an example, **Fig. 4.6** and **Fig. 4.7** show that using $\lambda = 0.1$, we can gain a higher oil revenue in the short time horizon (500 days) without losing too much revenue after 10 years. It can be observed also as λ increases, the NPV approaches the long-term objective. This is consistent with (4.20) where increasing λ means we increase the weight to the long-term objective.

Fig. 4.8 shows the oil production rate from production well PROD3. It can be observed that the weighting method solution with $\lambda = 0.1$ lies between the long-term and short-term strategy. This can be interpreted as an intermediate solution between the production engineer and the reservoir engineer. According to this solution, at the beginning, the oil production needs to be higher than for the long-term strategy, so that at the end of the production we can still produce some oil from the well with water cut below its threshold. On the other hand, using reactive control the well is closed after 8 years of production. To facilitate the decision maker to choose the desirable strategy, we plot the NPV for the short-term strategy in a short time horizon and the long-term strategy in a long time horizon as a Pareto-like curve (**Fig. 4.9**). As we have explained before, this solution is not Pareto optimal since we didn't solve the actual short-term and long-term objectives. The solution, however, shows a trade-off between the two optimization approaches. It is possible also to use a non-constant convex coefficient in the augmented function (4.20). To this end, let's consider the following augmented function

$$J_{NPV}(\mathbf{q}; b_{UB}, b_{LB}; c) = \left(1 - e^{-\mu t}\right) * J_{NPV}(\mathbf{q}; b_{UB}) + e^{-\mu t} * J_{NPV}(\mathbf{q}; b_{LB}) \tag{4.21}$$

In this case $\mu > 0$ acts as a time scale constant. Using the augmented function (4.21), in the beginning of the production we give more weight to the short-term strategy, while as time goes by, the weight is shifted to the long-term strategy. However, as can be observed from **Fig. 4.10**, using two different time scale constants, no improvement can be made compared to the constant convex coefficient. Even though it seems the solution resulting from the

weighed sum method is non-dominated solution, it's not Pareto optimal. There is a slight improvement in the oil saturation using the adjoint-based optimization and the weighted-sum method compared with the conventional reactive control method, as can be seen from **Fig. 4.11**.

It is also possible to consider b_{UB} and b_{LB} as parameters instead of λ. In this case, λ is fixed. To this end, we set $b_{UB} = 0$ while varying b_{LB}. The result for short-term and long-term optimization is shown in **Fig. 4.12** and **Fig. 4.13**, respectively. Using smaller b_{LB} the NPV approaches the long-term objective since the bound becomes tighter. Finally, **Fig. 4.14** shows the NPV surface plot for different λ and b_{LB}.

4.7 Conclusions

In this chapter, we have presented a novel approach to short-term and long-term production optimization problem. The approach, called the weighed sum method, is adopted from multi-objective optimization method where the solution is not a single solution but rather a collection of points. To this end, we introduce upper and lower bounds of the objective function. The reason to introduce these functions is that the objective function can be written in a different form, while in reality the short-term and long-term optimization is performed with the same objective but different methods. The idea is then to solve a bi-objective optimization problem for the upper and lower objective functions and project the solution onto the original objective. Further, the method is tested on a simplified reservoir model of the South wing of the Voador field located in the Campos basin of Brazil. The result is presented in a Pareto-like plot and surface plot decision where the decision makers may choose different strategies based on their articulation of preferences.

Nomenclature

Symbols

$\vec{v}$	=	Darcy velocity
Λ	=	total mobility
λ	=	weighted coefficient
$\mathbf{K}$	=	permeability tensor
q	=	source term
ϕ	=	porosity
f	=	water fractional flow
$\mathbf{v}$	=	outward face fluxes and well-perforation rate
$\mathbf{s}$	=	saturation cell
$\mathbf{p}$	=	pressure cell
$\boldsymbol{\pi}$	=	face and well pressures
$\boldsymbol{\alpha}$	=	vector of Langrangian multiplier
J	=	objective function
k	=	isotropic permeability
T	=	final time
b	=	discount factor
r	=	price
s	=	saturation

Scripts

o	=	oil
g	=	gas
w	=	water
inj	=	injection
$prod$	=	production
NPV	=	net present value
$\intercal$	=	transpose

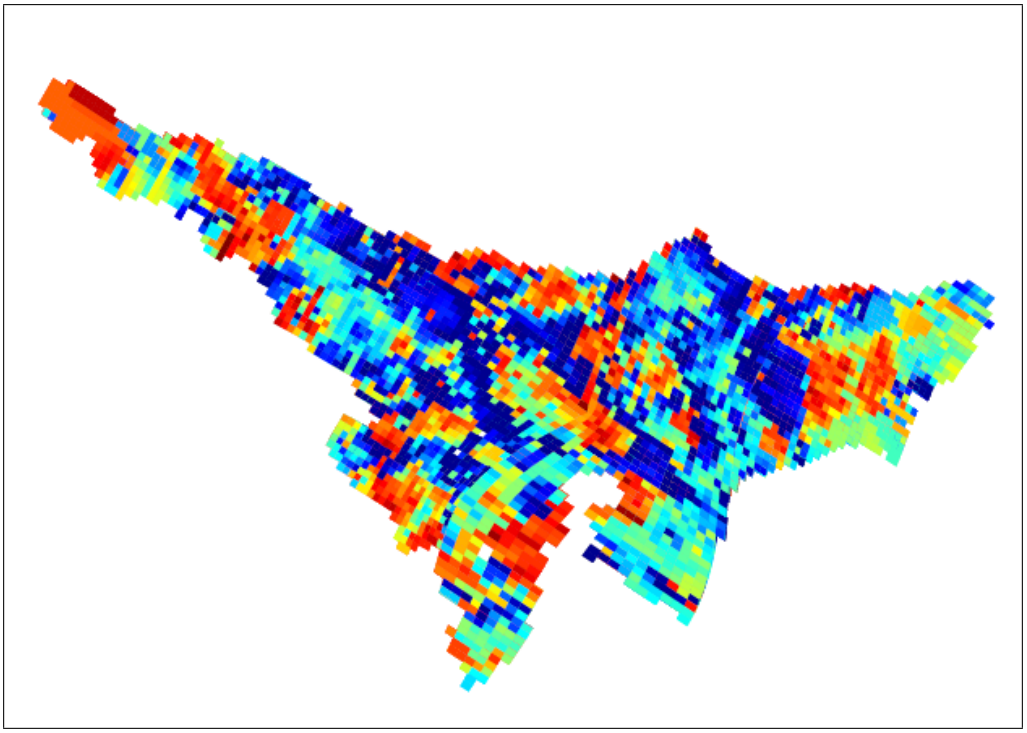

Figure 4.2: Permeability distributions.

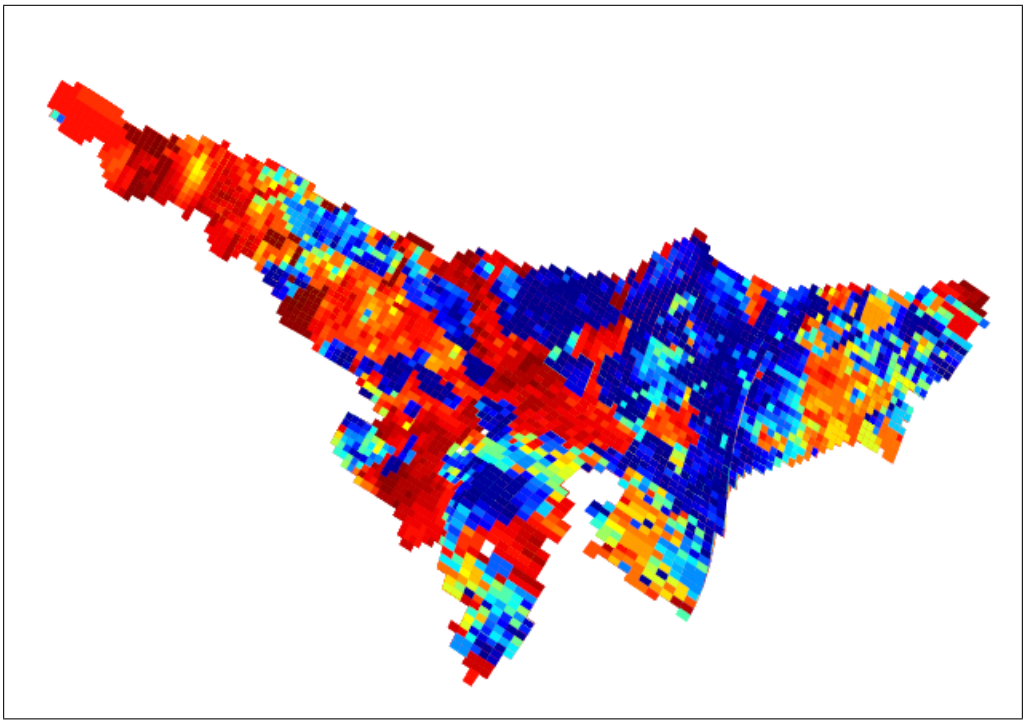

Figure 4.3: Porosity distributions.

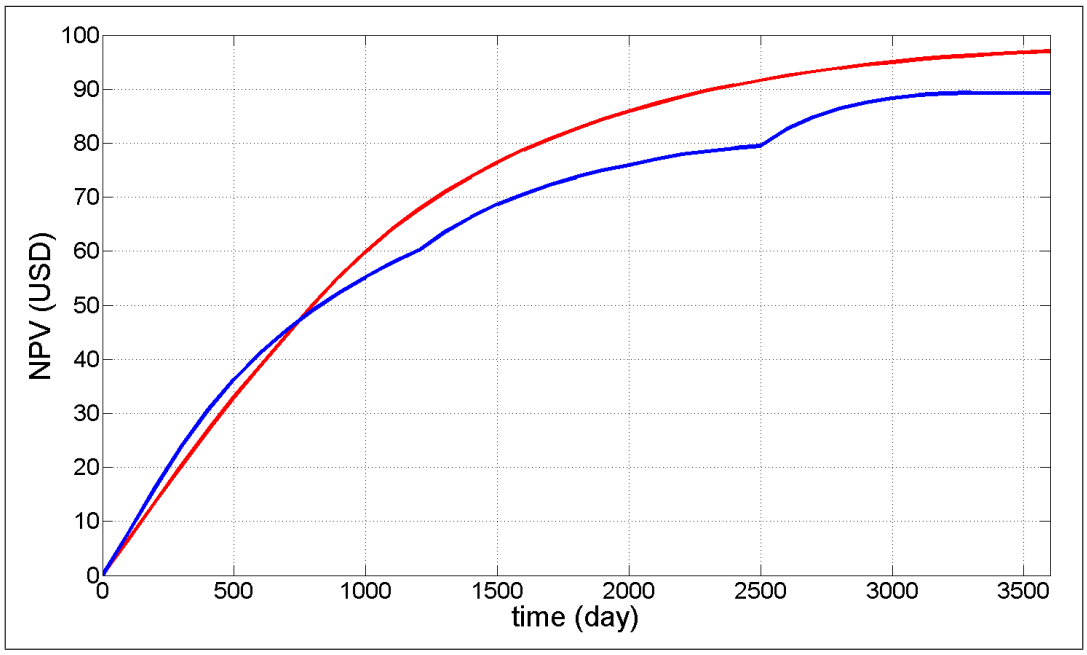

Figure 4.4: Normalized NPV of the long-term optimization (red) using adjoint-based optimization and short-term optimization (blue) using reactive control.

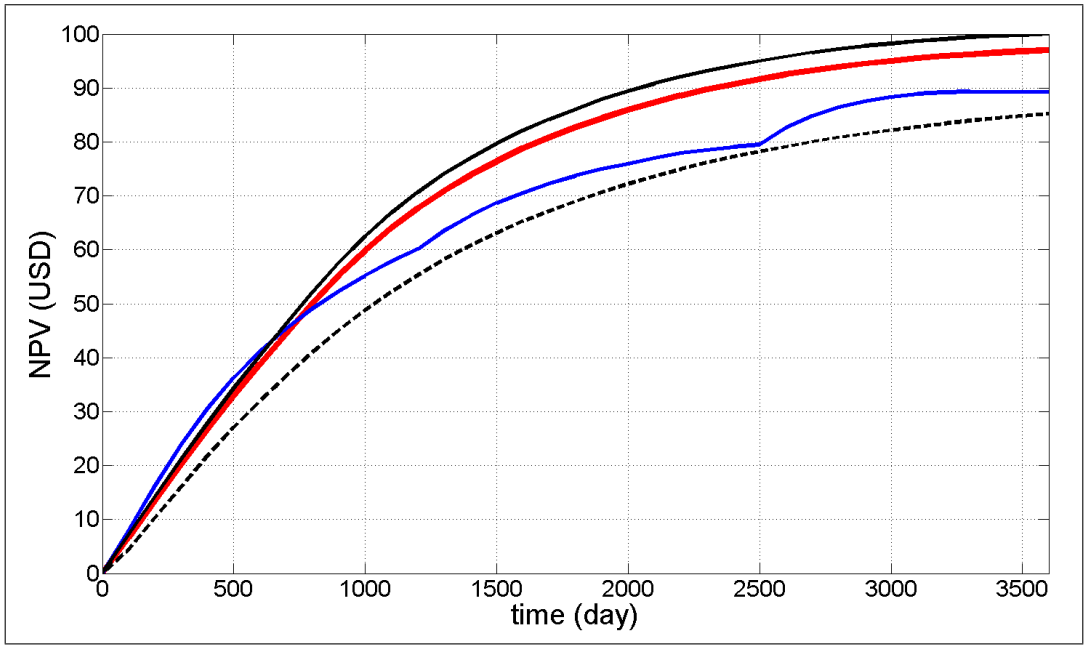

Figure 4.5: Normalized upper bound (black line) and lower bound (dashed line) of the NPV. The long-term and short-term strategy are computed with 10 % discount factor while the upper and lower bound are computed with 0% and 75% discount factors, respectively.

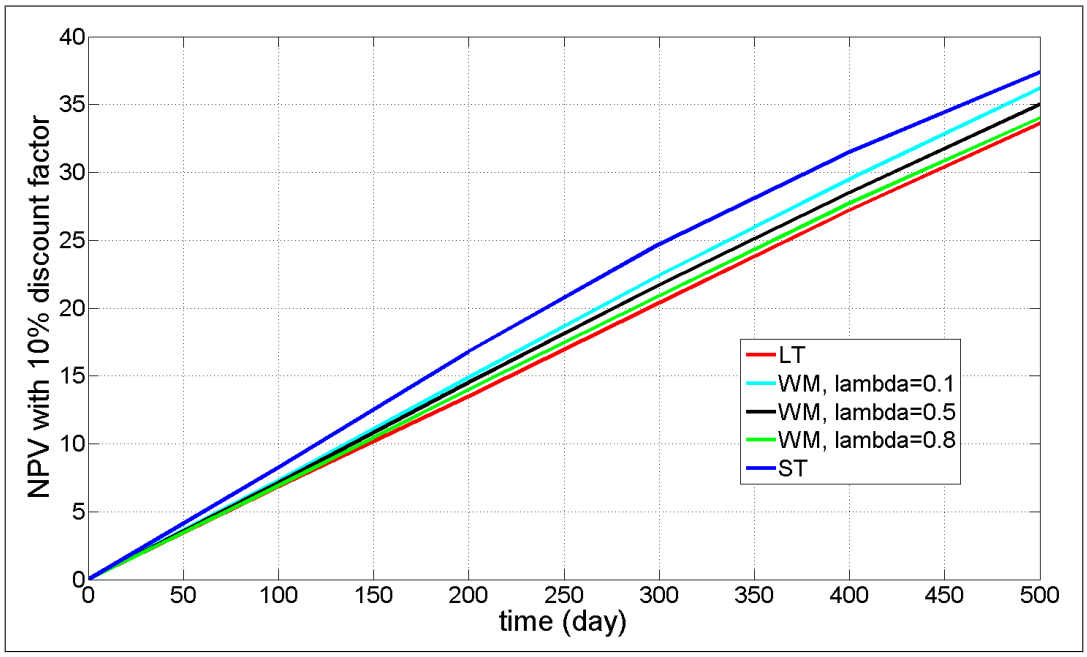

Figure 4.6: Normalized NPV in a short time horizon (500 days) for different λ. The weighted-sum method (WM) solutions are lies between the long-term and short-term NPV.

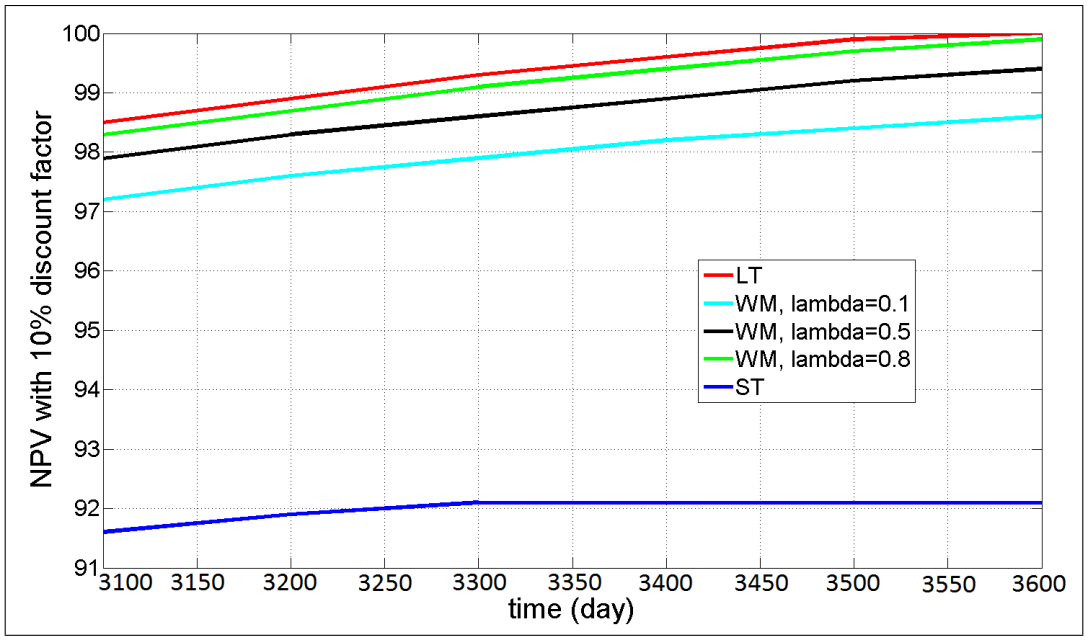

Figure 4.7: Normalized NPV in a long time horizon (10 years) for different λ. The weighted-sum method (WM) solutions are also lies between the long-term and short-term NPV.

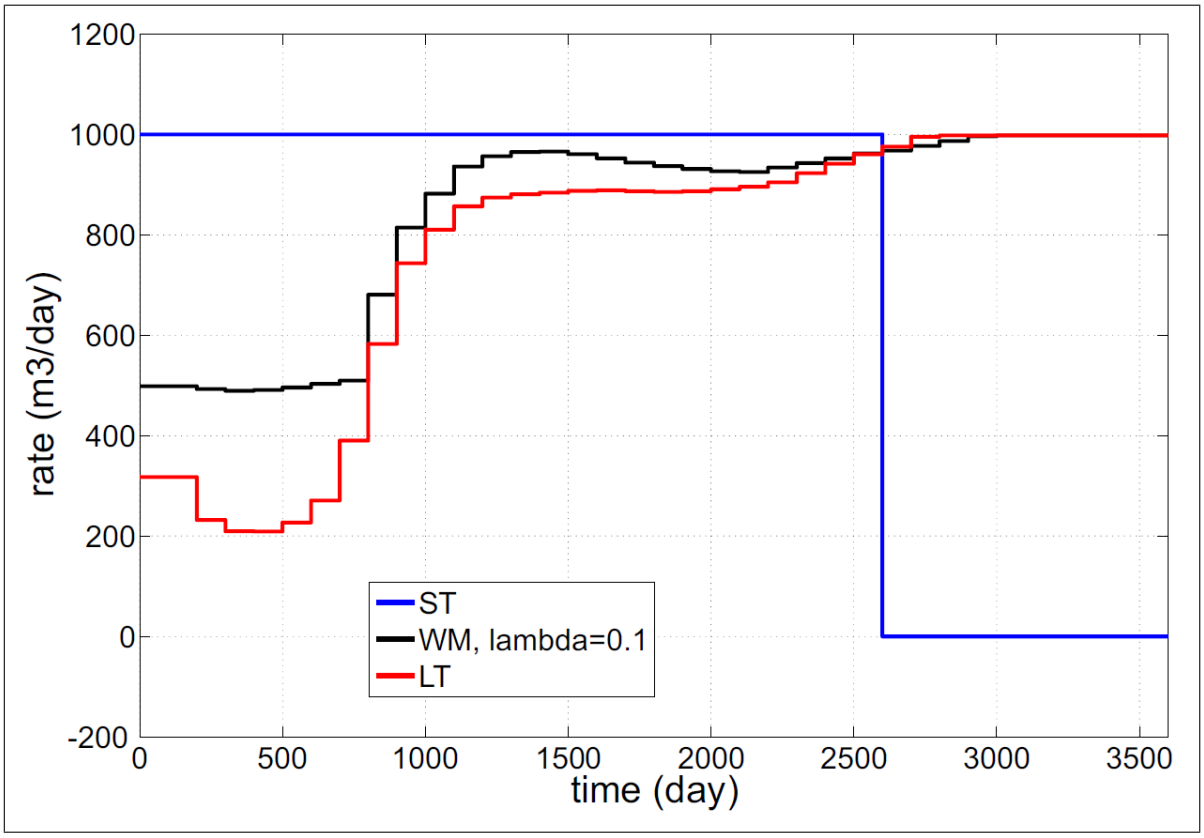

Figure 4.8: Oil rate from production well PROD3 using different strategies; reactive control (blue), adjoint-based optimization (red), and the weighted-sum method (black).

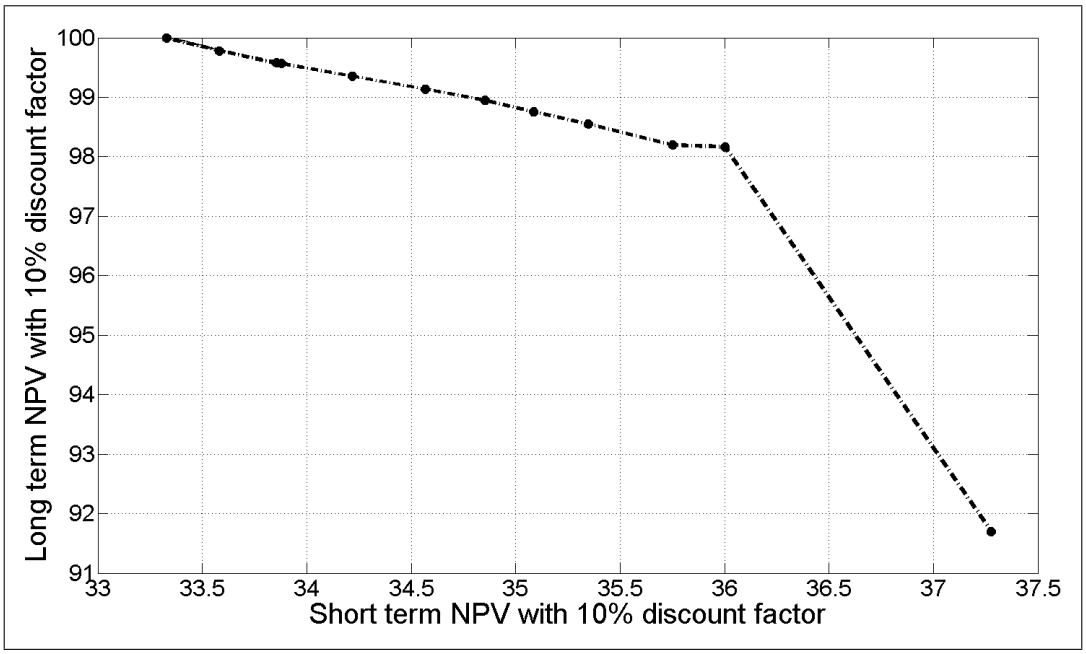

Figure 4.9: Pareto-like plot of NPV of the long-term and short-term optimization for $b_{UB} = 0\%$ and $b_{LB} = 75\%$.

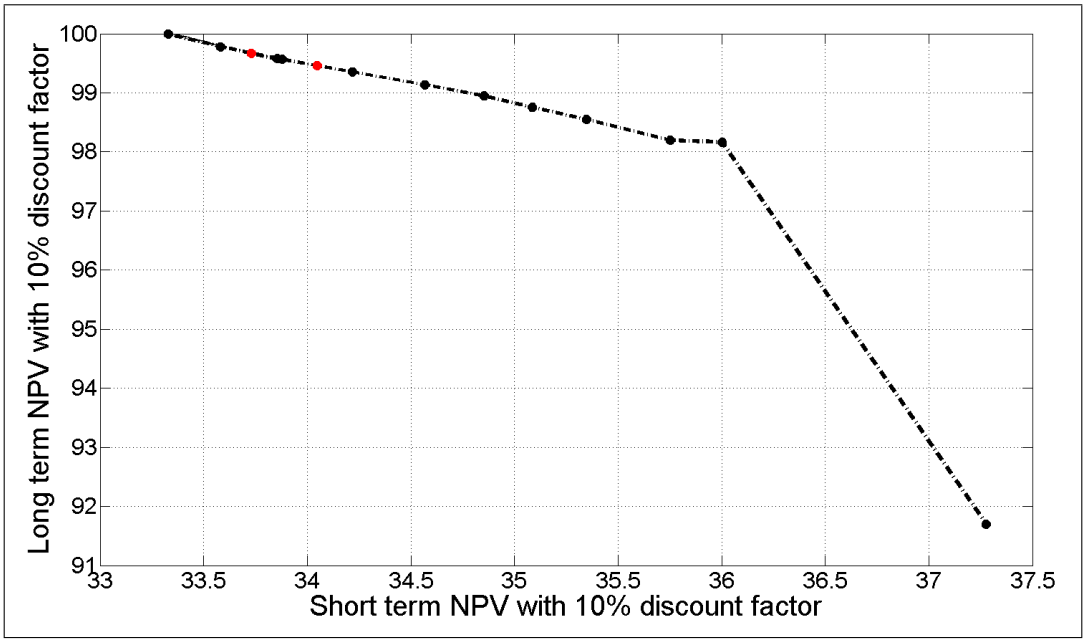

Figure 4.10: Pareto-like plot of NPV of the long-term and short-term optimization with red dots indicated the use of non constant coefficient in the weighted-sum method.

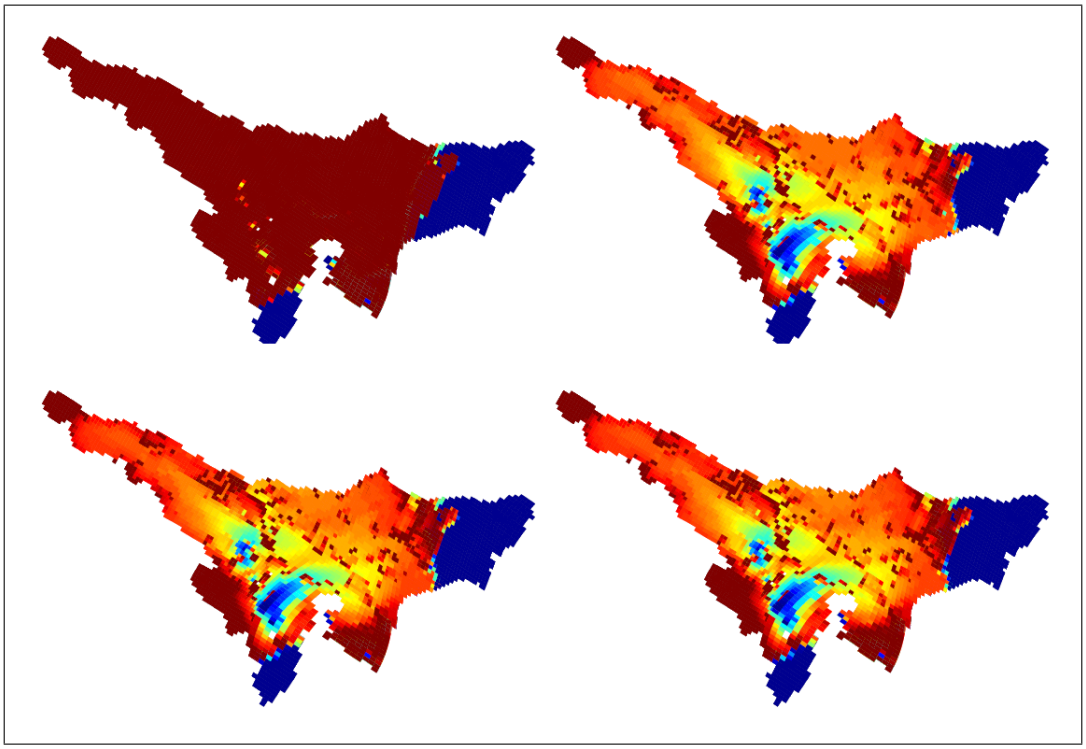

Figure 4.11: Initial saturation (upper left), final saturation using the reactive control (upper right), final saturation using the weighted-sum method with $\lambda = 0.1$, $b_{UB} = 0\%$, and $b_{LB} = 75\%$ (lower left), and final saturation using the adjoint-based optimization (lower right).

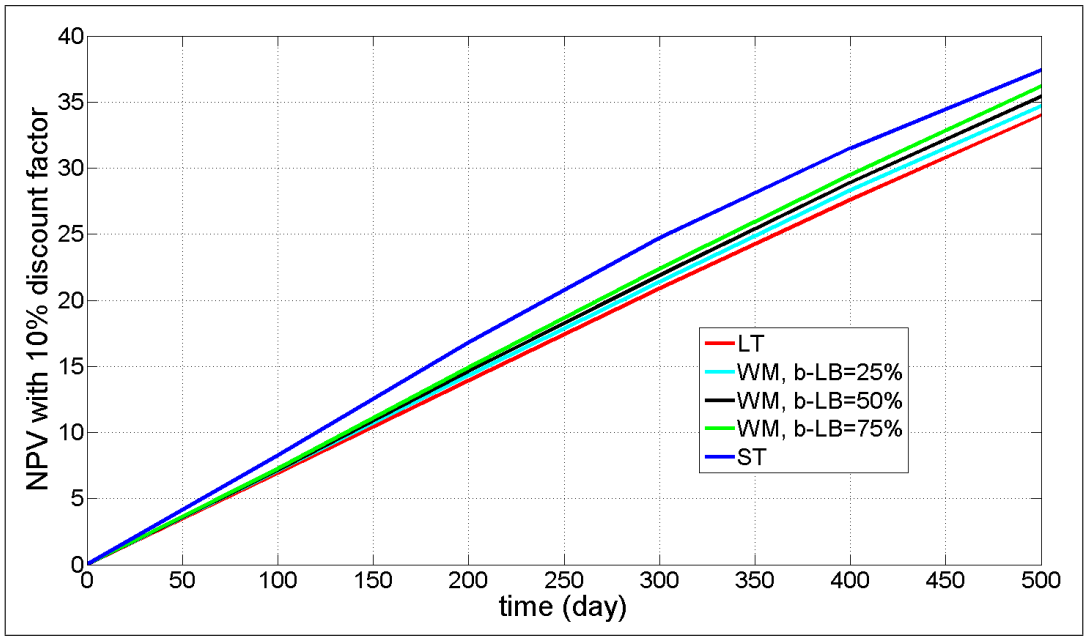

Figure 4.12: Normalized NPV in a short time horizon (500 days) for different b_{LB}. The weighted-sum method (WM) solutions are lies between the long-term and short-term NPV.

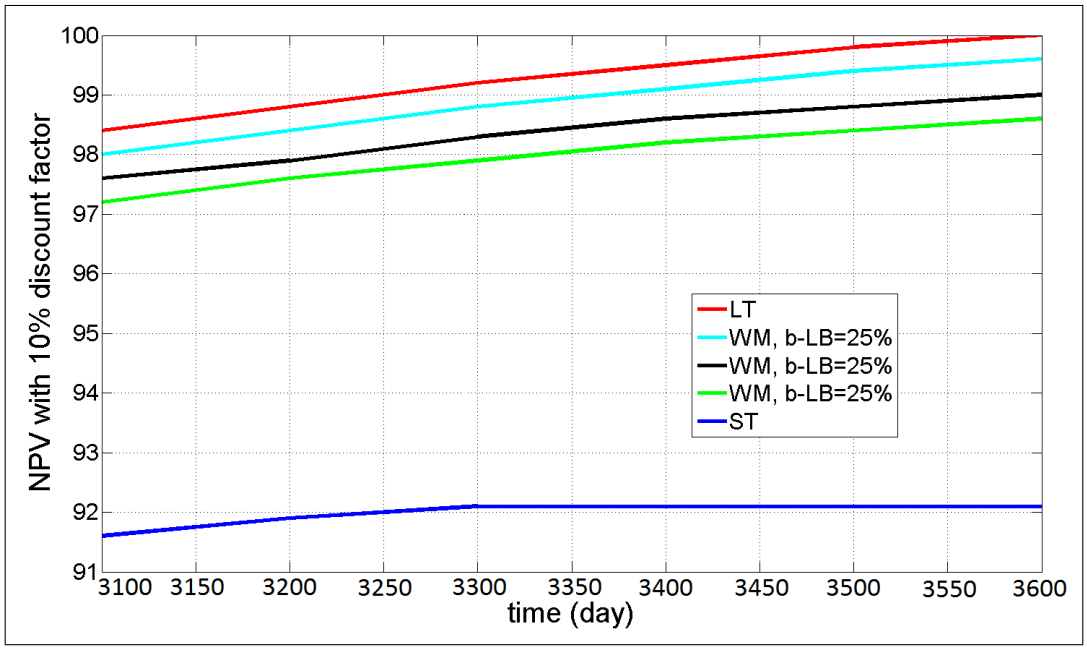

Figure 4.13: Normalized NPV in a long time horizon (10 years) for different b_{LB}. The weighted-sum method (WM) solutions are lies between the long-term and short-term NPV.

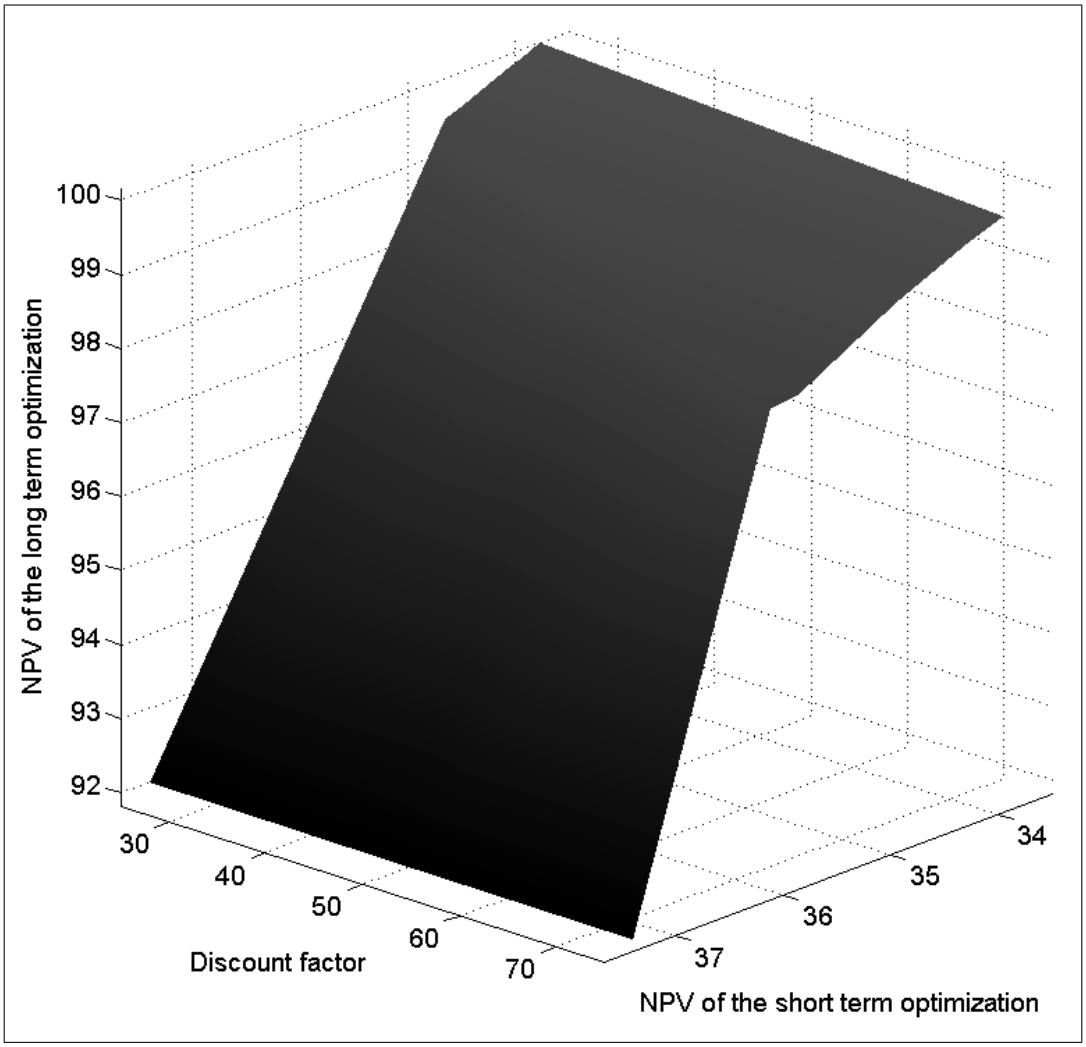

Figure 4.14: Surface plot decision of the long-term and short-term NPV. It was created by varying the weight coefficient λ and the lower bound of the discount factor b_{LB}.

Chapter 5

Boundary Stabilization of the Wave Equations

This chapter is based on Hasan and Foss (2011) which has been published in the proceedings of the 18th IFAC World Congress, ISBN 978-3-902661-93-7, pp. 6771-6776 and Hasan et al. (2013a) which has been published in Systems and Control Letters, vol 62:1, 2013.

5.1 Introduction

Two equations are usually used as models of waves on shallow water surfaces. The Benjamin-Bona-Mahony (BBM) equation, sometimes known as the regularized long wave equation, can be used to approximate the unidirectional propagation of long waves in certain nonlinear dispersive systems (Benjamin et al., 1972). The equation was proposed as an alternative to the well-known Korteweg-de Vries (KdV) equation (Korteweg and de Vries, 1895). The main motivation for introducing the BBM equation is the fact that the local Cauchy problem in the energy space is much easier for the BBM equation than for the KdV equation, whereas the BBM equation describes a relevant physical situation as does the KdV equation. However, while the KdV equation is a completely integrable model, the BBM equation is not. This limitation prohibits extension of the inverse scattering theory developed for the KdV equation to the BBM equation. To this point, the difficulty of the KdV equation and the BBM equation seem to be comparable Martel et al. (2010).

Despite several complications in the mathematical analysis, it is well known that both equations perform well as mathematical models for long time evolution of the nonlinear waves phenomenon. The applications are mostly found in the area of fluid dynamics, such as: surface water waves in a uniform channel (Bona et al., 1980a), near shore surface waves with sandbar formation (Socha, 2002), and tsunami propagation from the ocean toward the beach and toward river channels (Tsuji et al., 1991).

In order to obtain good agreement between experimental observations and the prediction of the theoretical models, a Burgers-type dissipative mechanism is often appended to the KdV

and the BBM models to form the KdV-Burgers and the BBM-Burgers equations (Bona et al., 1980b, 1996). In a bounded domain, these two models are given in the following forms

$$u_t - \epsilon u_{xx} + (\delta u_{xx} + u^p)_x = 0,\ 0 < x < 1,\ t > 0 \tag{5.1}$$
$$u_t - \epsilon u_{xx} - (\delta u_{xt} - u^p)_x = 0,\ 0 < x < 1,\ t > 0 \tag{5.2}$$

where (5.1) is the KdV-Burgers equation, and (5.2) is the BBM-Burgers equation. Here, $\epsilon, \delta > 0$ denote dissipation and dispersion coefficients, respectively, and $p \geq 2$ is a positive integer. Both equations can be considered as models of unidirectional long waves of Boussinesq-type, and can be applied for instance to describe Tsunami waves in an ocean (Dutykh, 2007).

In the application of surface water waves, the dependent variable u is a real-valued function which denotes the elevation of the free surface waves relative to its undisturbed position. The independent variables x and t denote the distance along the channel and the elapsed time, respectively. The parameter ϵ expresses the effect of dissipative mechanisms of the waves medium. This quantity can be interpreted as the medium viscosity. The exponent $p \geq 1$ is presented in the equation to model surface waves with highly nonlinear effects, e.g., internal wave over a continental slope with arbitrary vertical stratification of ocean density and background shear flow is modeled by (5.1) with $p = 2$ (Talipova et al., 1997). Increasing the exponent can be considered as a generalization of (5.1) and (5.2). Unfortunately, for higher orders of the nonlinearity ($p \geq 4$), and ϵ less than its critical value ϵ_c, the solutions form singularities in finite time, i.e., solutions blow up in finite time (Bona et al., 1996).

Numerous works have been conducted to investigate the applicability as well as the theoretical analysis (well possedness problem) of the initial-boundary value problem for both (5.1) and (5.2), see e.g., Bona and Dougalis (1980); Coleman and Noll (1960). While the issue of controllability and stability of the KdV-Burgers, or the simpler KdV equation, has received much attention since it was introduced in 1895 (Balogh and Krstic, 2000b; Krstic and Smyshlyaev, 2008), there are to date few results concerning controllability and stability of the BBM-Burgers equation. Moreover, to the best of our knowledge there are no publications concerning stabilization of the BBM-Burgers equation by boundary control.

In fluid flow systems, stabilization using boundary control is more preferred than using distributed control. The reason is that it would be more practically feasible to put sensors and actuators at the boundary of the system rather than mid-flow. One may imagine wave generation in a water tank where the generator is placed at the boundary of the tank. Hence, the contribution of this chapter is to analyze and provide a set of boundary conditions (control laws) which guarantees stability for systems modeled by the generalized KdV-Burgers and BBM-Burgers equations. The case when the dispersive effect dominates the nonlinear effect for the generalized KdV-Burgers equation is also discussed. The existence and uniqueness of the solution in this chapter for the given systems with the proposed boundary conditions are conjectured. However, one may consider results by Colin and Ghidaglia (2001) and Bona et al. (2008) where the well-posedness problem of the generalized KdV-Burgers and BBM-Burgers equations posed in a bounded domain is solved using the contraction mapping theorem.

5.2 Notation and Definitions

Definition 2. *(Bona and Luo, 1995) Denoted by $C^k(0,1)$ is a Banach space of k-times continuously differentiable functions defined on $[0,1]$. This space is completed with the norm*

$$\|u(t)\|_{C^k(0,1)} = \sup_{x\in[0,1],\, j\in\mathbb{Z}=\{0,1,\cdots,k\}} |u^{(j)}(x)|. \tag{5.3}$$

Definition 3. *The L^2-norm of a function u is denoted by*

$$\|u(t)\|_{L^2}^2 = \int_0^1 u^2(x,t)\,\mathrm{d}x, \tag{5.4}$$

while $\forall k \geq 0$, the Sobolev norms are defined as

$$\|u(t)\|_{H^k}^2 \triangleq \sum_{i=0}^{k} \int_0^1 \left(\frac{\partial^i u}{\partial x^i}\right)^2 \mathrm{d}x, \tag{5.5}$$

and $u \in H^k(0,1)$ when $\|u(t)\|_{H^k}$ is finite.

Definition 4. *(Balogh and Krstic, 2000b) The trivial solution ($u \equiv 0$) of a dynamical system is said to be globally asymptotically stable in an $\mathcal{L}$ spatial norm if*

$$\|u(t)\|_{\mathcal{L}} \leq \mathcal{B}\left(\|u_0\|_{\mathcal{L}}, t\right), \quad \forall t \geq 0, \forall u_0 \in \mathcal{L}, \tag{5.6}$$

where $\mathcal{B}(\cdot,\cdot)$ is a function with the properties that

- *for fixed t, $\mathcal{B}(r,t)$ is a monotonically increasing continuous function of r such that $\mathcal{B}(0,t) \equiv 0$,*
- *for fixed r, $\mathcal{B}(r,t)$ is a monotonically decreasing continuous function of t such that $\lim_{t\to\infty} \mathcal{B}(r,t) \equiv 0$.*

The trivial solution is globally exponentially stable when

$$\mathcal{B}(r,t) = kre^{-\delta t}, \tag{5.7}$$

for some $k, \delta > 0$ independent of r and t, and it is semi-globally exponentially stable when

$$\mathcal{B}(r,t) = \mathcal{D}(r)e^{-\delta t}, \tag{5.8}$$

where $\mathcal{D}(r)$ is a continuous non-decreasing function with $\mathcal{D}(0) = 0$.

5.3 The Korteweg-de Vries-Burgers Equation

Consider the boundary stabilization problem of the generalized KdV-Burgers equation in the following form

$$\begin{aligned} u_t - \epsilon u_{xx} + (\delta u_{xx} + u^p)_x &= 0,\ 0 < x < 1,\ t > 0 && (5.9)\\ u(x,0) &= u_0(x),\ 0 \le x \le 1 && (5.10)\\ u(0,t) &= 0,\ t \ge 0 && (5.11)\\ u_x(1,t) &= f_1(u(1,t)),\ t \ge 0 && (5.12)\\ u_{xx}(1,t) &= f_2(u(1,t)),\ t \ge 0 && (5.13) \end{aligned}$$

The generalized KdV-Burgers equation is a nonlinear mathematical model describing both dispersion and dissipation phenomenon. In the case of $\epsilon = 0$, this equation is reduced to the generalized KdV equation. The KdV equation together with the nonlinear Schrodinger equation are considered as universal models for Hamiltonian systems in infinite dimension (Martel and Merle, 2001b). Bona and Luo (1993) have shown that the KdV is well posed in certain function spaces.

In this section, the boundary $u(1,t)$ is considered as the measurement while $u_x(1,t)$ and $u_{xx}(1,t)$ are considered as the manipulated control inputs. Thus, we consider the case of co-located sensing and actuation at the boundary $x = 1$. The functions f_1 and f_2 are to be designed and constitutes our static output feedback control laws.

A fundamental feature of the KdV equation is the existence of a family of traveling waves (soliton) solutions. It has been shown analytically that if $2 \le p < 5$ (sub-critical case), all solutions are global and uniformly bounded in H^1 (Martel and Merle, 2001a). When $p = 5$ (critical case), it has been shown by Merle (2001) the existence of finite time blow-up solution. For $p > 5$ (super-critical case), blow-up had been predict numerically (Bona et al., 1995).

In the case when $\epsilon = 0$ and $p = 2$, the equation becomes the original KdV equation, a nonlinear partial differential equation (PDE) which describes waves on shallow water surfaces (Korteweg and de Vries, 1895). The KdV equation is an example of a nonlinear PDE whose solutions can be exactly specified. This equation may also be used to model acoustic waves on plasma and crystal lattices. In the case when $\delta = 0$ and $p = 2$, the equation is reduced to the Burgers equation, a nonlinear PDE which describes gas dynamics and traffic flow. Further, if $\epsilon = 0$ the equation becomes the Inviscid Burgers equation. Mathematical analysis regarding controllability and boundary controllability of the KdV equation may be found in Russell and Zhang (1996) and Rosier (1997), while an initial-boundary-value problem of the KdV equation posed on a finite interval has been resolved recently by Bona et al. (2009) and Colin and Ghidaglia (2001).

As a next step in the analysis of the system, it is natural to consider boundary stabilization on a bounded domain. Boundary control stabilization of the KdV-Burgers equation has been studied by Liu and Krstic (2002) and an improved version by Balogh and Krstic (2000a). Gao and Deng (2007) consider a case where the dissipation coefficient of the KdV-Burgers

equation is unknown and a case of the KdV-Burgers equation with time delay. Smaoui and Al-Jamal (2008) proposed a set of control laws for generalized KdV-Burgers equation using a Lyapunov approach. However, they used zero Neumann boundary condition which has been shown by Balogh and Krstic (2000a) to have a poor performance. The control inputs (5.11)-(5.13) for the initial value problem (5.9) and (5.10) are proposed in the following form

$$u(0,t) = 0 \tag{5.14}$$

$$u_x(1,t) = -\frac{1}{\epsilon}\Big(c + \tfrac{p^2}{c(p+1)^2}u^{2p-2}(1,t) \Big)u(1,t) \tag{5.15}$$

$$u_{xx}(1,t) = \frac{1}{\epsilon^2}\Big(c + \tfrac{p^2}{c(p+1)^2}u^{2p-2}(1,t) \Big)^2 u(1,t) \tag{5.16}$$

where $c > 0$ is a constant.

The main result of this section can be stated in the following theorem.

Theorem 1. *For any initial conditions $u_0 \in H^3(0,1)$, if the initial value problem of the generalized KdV-Burgers equation (5.9) with boundary conditions (5.14)-(5.16) has a global classical solution $u(x,t) \in \mathbb{C}(0,\infty;L^2(0,1))$, than the equilibrium $u(x,t) \equiv 0$ is globally exponentially stable in L^2-sense.*

Proof. Lets take the L^2 inner product of the generalized KdV-Burgers equation (5.9) with u, this yields

$$\int_0^1 (uu_t - \epsilon u u_{xx} + \delta u u_{xxx} + p u^p u_x)\,\mathrm{d}x = 0 \tag{5.17}$$

Using integration by parts and boundary control laws (5.14)-(5.16), each terms of (5.17) may be computed as

$$\int_0^1 uu_t\,\mathrm{d}x = \frac{\mathrm{d}}{\mathrm{d}t}\Big(\tfrac{1}{2}\textstyle\int_0^1 u^2\,\mathrm{d}x \Big) = \frac{\mathrm{d}}{\mathrm{d}t}\|u\|_{L^2}^2 \tag{5.18}$$

$$\begin{aligned} -\epsilon\int_0^1 uu_{xx}\,dx &= -\epsilon u u_x|_0^1 + 2\epsilon\Big(\tfrac{1}{2}\textstyle\int_0^1 u_x^2\,\mathrm{d}x \Big) \\ &= -\epsilon u(1,t)u_x(1,t) + 2\epsilon\|u_x\|_{L^2}^2 \\ &= \Big(c + \tfrac{p^2}{c(p+1)^2}u^{2p-2}(1,t) \Big)u^2(1,t) + 2\epsilon\|u_x\|_{L^2}^2 \end{aligned} \tag{5.19}$$

$$\begin{aligned} \delta\int_0^1 uu_{xxx}\,\mathrm{d}x &= \delta u u_{xx}|_0^1 - \delta\int_0^1 u_x u_{xx}\,\mathrm{d}x \\ &= \delta u(1,t)u_{xx}(1,t) - \frac{\delta}{2}u_x^2|_0^1 \\ &= \frac{\delta}{2\epsilon^2}\Big(c + \tfrac{p^2}{c(p+1)^2}u^{2p-2}(1,t) \Big)^2 u^2(1,t) + \frac{\delta}{2}u_x^2(0,t) \end{aligned} \tag{5.20}$$

$$p\int_0^1 u^p u_x\,\mathrm{d}x = \frac{p}{p+1}u^{p+1}(1,t) \tag{5.21}$$

Applying the Young inequality to the last term gives

$$\frac{p}{p+1}u^{p+1}(1,t) \leq \frac{p^2}{2c(p+1)^2}u^{2p}(1,t) + \frac{c}{2}u^2(1,t) \tag{5.22}$$

Putting together all terms above, yields

$$\frac{\mathrm{d}}{\mathrm{d}t}\|u\|^2 + 2\epsilon\|u_x\|^2 + \left(\ \tfrac{\delta c^2}{2\epsilon^2} + \tfrac{c}{2}\ \right)u^2(1,t) + \left(\ \tfrac{p^2}{2c(p+1)^2} + \tfrac{\delta p^2}{\epsilon^2(p+1)^2}\ \right)u^{2p}(1,t) + \frac{\delta p^4}{2\epsilon^2 c^2(p+1)^4}u^{4p-2}(1,t) \leq 0 \tag{5.23}$$

With the help of Poincare inequality, (5.23) becomes

$$\frac{\mathrm{d}}{\mathrm{d}t}\|u\|_{L^2}^2 \leq -2\epsilon\|u_x\|_{L^2}^2 \leq -2\epsilon\|u\|_{L^2}^2 \tag{5.24}$$

which implies that the generalized KdV-Burgers equation (5.9) is globally exponentially stable in the L^2 norm, i.e.

$$\|u(t)\| \ \leq \ \|u_0\|_{L^2}e^{-\epsilon t} \tag{5.25}$$

□

The boundary control laws (5.15)-(5.16) only require measurement at the boundary of the systems, in this case $u(1,t)$. Thus, they are easy to implement. This is an advantage from a practical point of view where the sensors and actuators are often placed at the boundary. One may consider water wave propagation where actuation would normally be mounted at the walls of the flow domain. Further, remark that the control laws (5.15) and (5.16) are invertible functions, i.e., there are functions g and h such that

$$u(1,t) = g(u_x(1,t)) = h(u_{xx}(1,t)) \tag{5.26}$$

and therefore they can be used via any of the following three variables actuated at $x = 1$; $(u, u_x), (u, u_{xx})$, and (u_x, u_{xx}). As we mention earlier, the existence of a classical solution $u(x,t) \in \mathbb{C}(0,\infty; L^2(0,1))$ to the generalized KdV-Burgers equation (5.9) together with boundary control laws (5.14)-(5.16) is conjectured. The L^2 stability is not sufficient because it does not guarantee boundedness of the solutions, i.e., the L^2 energy can be bounded even though the solution $u(x)$ can take infinite values on a subset of [0, 1]. Therefore, stability in higher norms (e.g., H^1) may be pursued. The viscosity parameter ϵ in (5.9) can take an arbitrary positive value. In reality, the value of this parameter sometimes is unknown. Since the control laws (5.15)-(5.16) depend on ϵ, an adaptive controller which incorporates parameter estimation as a dynamic component of the control laws may need to be designed.

5.3.1 Adaptive Control

Suppose that the dissipation coefficient ϵ in (5.9) is unknown. In this section, an adaptive boundary control will be constructed for this case.

Let ψ denote an estimate for $\frac{1}{\epsilon}$. Define a Lyapunov function

$$W(t) = \frac{1}{2}\int_0^1 u^2\,\mathrm{d}x + \frac{\epsilon}{2\gamma}\Big(\ \psi - \tfrac{1}{\epsilon}\ \Big)^2 \tag{5.27}$$

and compute its time derivative

$$\begin{aligned}
\dot{W}(t) &= \int_0^1 u u_t\,\mathrm{d}x + \frac{\epsilon}{\gamma}\Big(\ \psi - \tfrac{1}{\epsilon}\ \Big)\dot{\psi} \\
&= \int_0^1 u\Big(\ \epsilon u_{xx} - \delta u_{xxx} - p u^{p-1}u_x\ \Big)\,\mathrm{d}x + \frac{\epsilon}{\gamma}\Big(\ \psi - \tfrac{1}{\epsilon}\ \Big)\dot{\psi} \\
&\le -\epsilon\int_0^1 u_x^2\,\mathrm{d}x - \delta u(1,t)u_{xx}(1,t) + \frac{\delta}{2}u_x^2(1,t) \\
&\quad +\epsilon u(1,t)u_x(1,t) + \frac{p^2}{2c(p+1)^2}u^{2p}(1,t) + \frac{c}{2}u^2(1,t) + \frac{\epsilon}{\gamma}\Big(\ \psi - \tfrac{1}{\epsilon}\ \Big)\dot{\psi}
\end{aligned} \tag{5.28}$$

Using algebraic manipulation, the above inequality yields

$$\begin{aligned}
\dot{W}(t) &\le -\epsilon\int_0^1 u_x^2\,\mathrm{d}x - \delta u(1,t)u_{xx}(1,t) + \frac{\delta}{2}u_x^2(1,t) + \epsilon u(1,t)u_x(1,t) \\
&\quad +\epsilon\psi u(1,t)\Big(\ \tfrac{p^2}{2c(p+1)^2}u^{2p-1}(1,t) + \tfrac{c}{2}u(1,t)\ \Big) \\
&\quad +\Big(\ \tfrac{p^2}{2c(p+1)^2}u^{2p}(1,t) + \tfrac{c}{2}u^2(1,t) - \tfrac{\dot{\psi}}{\gamma}\ \Big)\epsilon\Big(\ -\psi + \tfrac{1}{\epsilon}\ \Big)
\end{aligned} \tag{5.29}$$

Take the feedback control laws

$$\dot{\psi}(t) = \frac{\gamma}{2}\Big(\ c + \tfrac{p^2}{c(p+1)^2}u^{2p-2}(1,t)\ \Big)u^2(1,t) \tag{5.30}$$

$$u_x(1,t) = -\frac{\psi}{2}\Big(\ c + \tfrac{p^2}{c(p+1)^2}u^{2p-2}(1,t)\ \Big)u(1,t) \tag{5.31}$$

$$u_{xx}(1,t) = \frac{\psi^2}{8}\Big(\ c + \tfrac{p^2}{c(p+1)^2}u^{2p-2}(1,t)\ \Big)^2 u(1,t) \tag{5.32}$$

where $c > 0$, (5.29) yields

$$\dot{W}(t) \le -\epsilon\int_0^1 u_x^2\,\mathrm{d}x \tag{5.33}$$

Thus, (5.9) is globally L^2 stable and the closed-loop system (5.9)-(5.10)-(5.14)-(5.30)-(5.31)-(5.32) and the initial condition of the estimate

$$\psi(0) = \psi_0 \tag{5.34}$$

The result of this section can be stated in the following theorem.

Theorem 2. *Suppose that $\gamma > 0$, $\psi_0 \geq 0$ and the initial conditions $u_0 \in H^3(0,1)$. If the initial value problem of the generalized KdV-Burgers equation (5.9) with boundary conditions (5.30)-(5.32) has a global classical solution $u(x,t) \in \mathbb{C}(0,\infty;L^2(0,1))$, then the equilibrium $u(x,t) \equiv 0$ is globally L^2 stable, i.e.*

$$\|u\|^2 + \frac{\epsilon}{2\gamma}\Big(\psi - \tfrac{1}{\epsilon} \Big)^2 \leq \|u_0\|^2 + \frac{\epsilon}{2\gamma}\Big(\psi_0 - \tfrac{1}{\epsilon} \Big)^2 \tag{5.35}$$

Further, $\psi(t)$ could be written in the form

$$\psi(t) = \psi_0 + \frac{\gamma}{2}\int_0^t \Big(c + \tfrac{p^2}{c(p+1)^2} u^{2p-2}(1,\tau) \Big) u^2(1,\tau)\,\mathrm{d}\tau \tag{5.36}$$

Remark that the feedback design (5.30)-(5.32) is decentralized, which means the feedback calculation at each end of the domain would use measurements only from that end.

5.3.2 The Korteweg-de Vries Equation

Now consider the case when the dissipation coefficient $\epsilon = 0$. The generalized KdV-Burgers equation (5.9) reduces to the generalized KdV equation, and the initial-boundary value problem can be stated as follows

$$\begin{aligned}
u_t + (\delta u_{xx} + u^p)_x &= 0,\ 0 < x < 1,\ t > 0 && (5.37)\\
u(x,0) &= u_0(x),\ 0 \leq x \leq 1 && (5.38)\\
u(0,t) &= 0,\ t \geq 0 && (5.39)\\
u_x(1,t) &= g_1(u(1,t)),\ t \geq 0 && (5.40)\\
u_{xx}(1,t) &= g_2(u(1,t)),\ t \geq 0 && (5.41)
\end{aligned}$$

Clearly, the boundary control laws (5.15) and (5.16) cannot be used. In this case, the boundary stabilization of (5.37) can be approached using the following control laws

$$\begin{aligned}
u(0,t) &= 0 && (5.42)\\
u_x(1,t) &= 0 && (5.43)\\
u_{xx}(1,t) &= \frac{1}{2\delta}\Big(c + \tfrac{p^2}{c(p+1)^2} u^{2p-2}(1,t) \Big) u(1,t) && (5.44)
\end{aligned}$$

where $c > 0$. Define the Lyapunov function as the L^2-norm (5.4). With the help of the Young inequality, its time derivative is given by

$$\begin{aligned}
\dot{V}(t) &= \int_0^1 u\Big(-\delta u_{xxx} - p u^{p-1} u_x \Big)\,\mathrm{d}x\\
&= -\delta\Big(u(1,t)u_{xx}(1,t) - \tfrac{1}{2}u_x^2\big|_0^1 \Big) - \frac{p}{p+1}u^{p+1}\big|_0^1\\
&\leq -\delta\Big(u(1,t)u_{xx}(1,t) - \tfrac{1}{2}u_x^2(1,t) \Big) + \frac{p^2}{2c(p+1)^2}u^{2p}(1,t) + \frac{c}{2}u^2(1,t) \qquad (5.45)
\end{aligned}$$

Substituting the boundary control laws (5.42)-(5.44) into (5.45), yields

$$\dot{V}(t) \leq 0 \tag{5.46}$$

Hence, the following theorem can be stated

Theorem 3. *For any initial conditions $u_0 \in H^3(0,1)$, if the the generalized KdV equation (5.37) with boundary conditions (5.42)-(5.44) has a global classical solution $u(x,t) \in \mathbb{C}(0,\infty;L^2(0,1))$, then the equilibrium $u \equiv 0$ is globally asymptotically stable in the L^2-sense.*

We need to mention that the choice of the control laws is not unique. A more aggressive control law that achieves better performance in terms of stabilization time could be made by using an active Neumann boundary condition as follows:

$$u(0,t) = 0 \tag{5.47}$$

$$u_x(1,t) = \sqrt{\frac{cu^2(1,t)}{\delta} + \frac{p^2}{c\delta(p+1)^2}u^{2p}(1,t)} \tag{5.48}$$

$$u_{xx}(1,t) = \frac{u(1,t)}{\delta}\Big(\; c + \tfrac{p^2}{c(p+1)^2}u^{2p-2}(1,t) \; \Big) \tag{5.49}$$

5.3.3 The Burgers Equation

The generalized Burgers equation is the case when the generalized KdV-Burgers equation (5.9) with δ=0.

Neumann Boundary Control for The Generalized Burgers Equation

Consider the following initial-boundary value problem of the generalized Burgers equation

$$u_t - \epsilon u_{xx} + (u^p)_x = 0,\ 0 < x < 1,\ t > 0 \tag{5.50}$$

$$u(x,0) = u_0(x),\ 0 \leq x \leq 1 \tag{5.51}$$

$$u_x(0,t) = v_0(u(0,t)),\ t \geq 0 \tag{5.52}$$

$$u_x(1,t) = v_1(u(1,t)),\ t \geq 0 \tag{5.53}$$

Here, the manipulated control inputs are in the form of Neumann boundary conditions at the both ends of the system. Recall the Lyapunov function (5.4) and compute its time derivative.

$$\begin{aligned}
\dot{V}(t) &= \int_0^1 u\Big(\; \epsilon u_{xx} - pu^{p-1}u_x \; \Big)\,\mathrm{d}x \\
&= \epsilon u u_x|_0^1 - \epsilon\int_0^1 u_x^2\,dx - \frac{p}{p+1}u^{p+1}|_0^1 \\
&= +u(1,t)\Big(\; \epsilon v_1(u(1,t)) - \tfrac{p}{p+1}u^p(1,t) \; \Big) \\
&\quad -u(0,t)\Big(\; \epsilon v_0(u(0,t)) - \tfrac{p}{p+1}u^p(0,t) \; \Big) - \epsilon\int_0^1 u_x^2\,\mathrm{d}x
\end{aligned} \tag{5.54}$$

Choose the control laws as

$$v_0(u(0,t)) = \frac{1}{\epsilon}\Big(c_0 u(0,t) + \tfrac{p}{p+1} u^p(0,t) \Big) \tag{5.55}$$

$$v_1(u(1,t)) = -\frac{1}{\epsilon}\Big(c_1 u(1,t) + \tfrac{p}{p+1} u^p(1,t) \Big) \tag{5.56}$$

where $c_0, c_1 > 0$. This yields

$$\dot{V}(t) = -\epsilon \int_0^1 u_x^2 \, \mathrm{d}x - c_1 u^2(1,t) - c_0 u^2(0,t) \tag{5.57}$$

By Poincare's inequality, (5.57) yields

$$\dot{V}(t) \leq -\min\Big(\tfrac{\epsilon}{2}, c_1, c_0 \Big) V \tag{5.58}$$

This implies that the equilibrium $u(x,t) = 0$ is globally exponentially stable in L^2-sense. The control laws (5.55)-(5.56) are not invertible for even p, thus one may seek an invertible control laws for the generalized Burgers equation (5.64). From (5.54) we have

$$\begin{aligned} \dot{V}(t) = {} & \epsilon u(1,t) v_1(u(1,t)) - \frac{p}{p+1} u^{p+1}(1,t) \\ & -\epsilon u(0,t) v_0(u(0,t)) + \frac{p}{p+1} u^{p+1}(0,t) - \epsilon \int_0^1 u_x^2 \, \mathrm{d}x \end{aligned} \tag{5.59}$$

Using Young's inequality, this yields

$$\begin{aligned} \dot{V}(t) \leq {} & \epsilon u(1,t) v_1(u(1,t)) + \frac{p^2}{2c(p+1)^2} u^{2p}(1,t) + \frac{c}{2} u^2(1,t) \\ & -\epsilon u(0,t) v_0(u(0,t)) + \frac{p^2}{2c(p+1)^2} u^{2p}(0,t) + \frac{c}{2} u^2(0,t) - \epsilon \int_0^1 u_x^2 \, \mathrm{d}x \end{aligned} \tag{5.60}$$

Select the control laws

$$v_0(u(0,t)) = \frac{1}{2\epsilon} u(0,t) \Big(c + \tfrac{p^2}{c(p+1)^2} u^{2p-2}(0,t) \Big) \tag{5.61}$$

$$v_1(u(1,t)) = -\frac{1}{2\epsilon} u(1,t) \Big(c + \tfrac{p^2}{c(p+1)^2} u^{2p-2}(1,t) \Big) \tag{5.62}$$

where $c > 0$. With the help of the Poincare inequality, the following expression is derived

$$\dot{V}(t) \leq -\epsilon \int_0^1 u_x^2 \, \mathrm{d}x \leq -\epsilon \int_0^1 u^2 \, \mathrm{d}x = -2\epsilon V(t) \tag{5.63}$$

Hence, the following theorem can be stated.

Theorem 4. *For any initial conditions $u_0 \in H^2(0,1)$, if the generalized Burgers equation (5.64) with boundary conditions (5.61)-(5.62) has a global classical solution $u(x,t) \in \mathbb{C}(0,\infty;L^2(0,1))$, then the equilibrium $u \equiv 0$ is globally exponentially stable in the L^2-sense.*

Again, the Neumann boundary control laws (5.61)-(5.62) only require measurement at the boundary of the system. The situation would be different if Dirichlet boundary control laws are employed as can be seen in the following subsection. Further, if the viscosity parameter ϵ in (5.64) is unknown, one may design an adaptive controller as we discussed earlier.

Dirichlet Boundary Control for The Generalized Burgers Equation

Consider the following initial-boundary value problem of the generalized Burgers equation with two Dirichlet boundary conditions at both ends

$$\begin{aligned} u_t - \epsilon u_{xx} + (u^p)_x &= 0,\ 0 < x < 1,\ t > 0 && (5.64)\\ u(x,0) &= u_0(x),\ 0 \le x \le 1 && (5.65)\\ u_x(0,t) &= w_0(u(0,t)),\ t \ge 0 && (5.66)\\ u_x(1,t) &= w_1(u(1,t)),\ t \ge 0 && (5.67) \end{aligned}$$

First select

$$w_0(u(0,t)) = 0 \tag{5.68}$$

Young's inequality yields

$$\epsilon u(1,t)u_x(1,t) \le \frac{p}{2(p+1)}|u(1,t)|^{p+1} + \frac{p^2}{2(p+1)}\left|\ \tfrac{2\epsilon}{p}u_x(1,t)\ \right|^{\frac{p+1}{p}} \tag{5.69}$$

Substituting (5.68) and (5.69) to (5.54), yields

$$\begin{aligned} \dot{V}(t) \le\ & -\epsilon\int_0^1 u_x^2\,\mathrm{d}x + \frac{p}{2(p+1)}|u(1,t)|^{p+1}\\ & + \frac{p^2}{2(p+1)}\left|\ \tfrac{2\epsilon}{p}u_x(1,t)\ \right|^{\frac{p+1}{p}} - \frac{p}{p+1}u^{p+1}(1,t) \end{aligned} \tag{5.70}$$

Select

$$\begin{aligned} w_1(u(1,t)) =\ & \sqrt[p+1]{(p+1)\left|\ \tfrac{2\epsilon}{p}u_x(1,t)\ \right|^{\frac{p+1}{p}}} + \sqrt[p+1]{\mu|u_{xx}(1,t)|^{p+1}}\\ & + \sqrt[p+1]{\nu\int_0^1 u_x(x,t)^2\,\mathrm{d}x} \end{aligned} \tag{5.71}$$

where $\mu, \nu > 0$, which provides the following expression

$$\begin{aligned}\dot{V}(t) \;\leq\; & -\Big(\ \epsilon + \tfrac{p\nu}{2(p+1)}\ \Big)\int_0^1 u_x^2\,\mathrm{d}x - \frac{p}{2(p+1)}\Big|\ \tfrac{2\epsilon}{p}u_x(1,t)\ \Big|^{\frac{p+1}{p}} \\ & -\frac{p\mu}{2(p+1)}|u_{xx}(1,t)|^{p+1} \end{aligned} \tag{5.72}$$

Once more, the Poincare's inequality gives

$$\dot{V}(t) \leq -\Big(\ 2\epsilon + \tfrac{p\nu}{(p+1)}\ \Big)V(t) \tag{5.73}$$

which shows the equilibrium $u(x,t) \equiv 0$ globally exponentially stable in L^2-sense. Control law (5.71) requires measurements from the interior of the domain. Therefore, an observer which estimates $u_x(x,t)$ inside the domain should be constructed, as we can see in the next subsection.

Observer Based Dirichlet Control for The Generalized Burgers Equation

Consider the following system of nonlinear observer

$$\hat{u}_t - \epsilon\hat{u}_{xx} + p\hat{u}^{p-1}\hat{u}_x = 0,\ 0<x<1,\ t>0 \tag{5.74}$$
$$\hat{u}(x,0) = \hat{u}_0(x),\ 0\leq x\leq 1 \tag{5.75}$$
$$\hat{u}(0,t) = u(0,t),\ t\geq 0 \tag{5.76}$$
$$\hat{u}(1,t) = u(1,t),\ t\geq 0 \tag{5.77}$$

Select the control laws as

$$u(0,t) = 0 \tag{5.78}$$
$$\begin{aligned} u(1,t) = & \sqrt[p+1]{(p+1)\Big|\ \tfrac{2\epsilon}{p}\hat{u}_x(1,t)\ \Big|^{\frac{p+1}{p}}} + \sqrt[p+1]{\mu|\hat{u}_{xx}(1,t)|^{p+1}} \\ & + \sqrt[p+1]{\nu\int_0^1 \hat{u}_x(x,t)^2\,\mathrm{d}x} \end{aligned} \tag{5.79}$$

where $\mu, \nu > 0$. This controller guarantees

$$\begin{aligned}\frac{\mathrm{d}}{\mathrm{d}t}\Big(\ \tfrac{1}{2}\textstyle\int_0^1 \hat{u}(x,t)^2\,\mathrm{d}x\ \Big) \;\leq\; & -\Big(\ \epsilon + \tfrac{p\nu}{2(p+1)}\ \Big)\int_0^1 \hat{u}_x^2\,\mathrm{d}x - \frac{p}{2(p+1)}\Big|\ \tfrac{2\epsilon}{p}\hat{u}_x(1,t)\ \Big|^{\frac{p+1}{p}} \\ & -\frac{p\mu}{2(p+1)}|\hat{u}_{xx}(1,t)|^{p+1} \end{aligned} \tag{5.80}$$

Employing Poincare's inequality, the observer equilibrium $\hat{u}(x,t) \equiv 0$ has a globally exponentially L^2-stable.

The Inviscid Burgers Equation

Consider (5.64) with $\epsilon = 0$. The equation is called the Inviscid generalized Burgers equation, and the initial-boundary value problem becomes

$$\begin{aligned} u_t + (u^p)_x &= 0,\ 0 < x < 1,\ t > 0 && (5.81)\\ u(x,0) &= u_0(x),\ 0 \le x \le 1 && (5.82)\\ u(0,t) &= z_0(u(0,t)),\ t \ge 0 && (5.83)\\ u(1,t) &= z_1(u(1,t)),\ t \ge 0 && (5.84) \end{aligned}$$

Differentiating (5.4) for (5.81) yields

$$\dot{V}(t) = \int_0^1 u\Big(-pu^{p-1}u_x \Big)\,\mathrm{d}x = -\frac{p}{p+1}u^{p+1}|_0^1 \tag{5.85}$$

Choose

$$\begin{aligned} z_0(u(0,t)) &= 0 && (5.86)\\ z_1(u(1,t)) &= \sqrt[p+1]{\frac{c(p+1)}{p}\Big(\int_0^1 |u_x(x,t)|^{p+1}\,\mathrm{d}x \Big)} && (5.87) \end{aligned}$$

where $c > 0$ and (5.85) yields

$$\dot{V}(t) = -c\int_0^1 |u_x(x,t)|^{p+1}\,\mathrm{d}x \tag{5.88}$$

The Poincare and Holder inequalities gives

$$\begin{aligned} \int_0^1 u^2\,\mathrm{d}x &\le 2\int_0^1 u_x^2\,\mathrm{d}x\\ &\le 2\Big(\int_0^1 |u_x(x,t)|^{p+1}\,\mathrm{d}x \Big)^{\frac{2}{p+1}} \Big(\int_0^1 |1|^{\frac{p+1}{p-1}}\,\mathrm{d}x \Big)^{\frac{p-1}{p+1}}\\ &\le 2\Big(\int_0^1 |u_x(x,t)|^{p+1}\,\mathrm{d}x \Big)^{\frac{2}{p+1}} && (5.89) \end{aligned}$$

Substituting (5.89) into (5.88) gives

$$\dot{V}(t) \le -cV^{\frac{p+1}{2}}(t) \tag{5.90}$$

This shows that the equilibrium $u(x,t) = 0$ is globally asymptotically stable in the L^2-sense.

5.4 The Benjamin-Bona-Mahony-Burgers Equation

In this section, we discuss a boundary stabilization problem of the BBM-Burgers equation, however, in a more general form. Consider the boundary stabilization problem for a class of pseudo-parabolic differential equations in the following form

$$\begin{aligned} \frac{\partial}{\partial t}(\Delta u - u) + \epsilon \Delta u &= f(x,t,u,u_x),\ 0 < x < 1,\ t > 0 && (5.91)\\ u(x,0) &= u_0(x),\ 0 \le x \le 1 && (5.92)\\ u(0,t) &= 0,\ t \ge 0 && (5.93)\\ u_x(1,t) &= z(u(1,t)),\ t \ge 0 && (5.94) \end{aligned}$$

Here, $\Delta = \frac{\partial^2}{\partial x^2}$ denotes the Laplacian differential operator, $\epsilon > 0$ is the dissipation coefficient, while f is the source of nonlinearity. The boundary $u(1,t)$ is considered as the measurement and $u_x(1,t)$ as the manipulated control input. Thus, we consider the case of co-located sensing and actuation at the boundary $x = 1$. The function z is to be designed and constitutes our static output feedback control law.

The basic mathematical and physical theory of (5.91) has been the subject of numerous papers, see e.g., Ting (1969); Showalter and Ting (1970); Quarteroni (1987); Bona and Dougalis (1980); Bona and Luo (1995). The applications cover thermodynamic processes (Chen and Gurtin, 1968; Ting, 1974), fluid flow in porous media (Barenblatt et al., 1990; Cuesta and Hulshof, 2003), shear in second order fluids (Coleman and Noll, 1960; Ting, 1963), long waves in dispersive systems (Bona et al., 1980b; Socha, 2002), tsunami modeling (Tsuji et al., 1991; Dutykh, 2007), and option pricing (Itkin and Carr, 2011). An important case of (5.91) is represented by the BBM-Burgers equation given as

$$\frac{\partial}{\partial t}(\Delta u - u) + \epsilon \Delta u = \frac{\partial}{\partial x}\left(u + \frac{1}{2}u^2\right) \tag{5.95}$$

which was introduced in Benjamin et al. (1972) as a model for unidirectional propagation of long waves of small amplitude, an alternative model for the KdV-Burgers equation (Korteweg and de Vries, 1895). The boundary stabilization problem for (5.95) was solved in Hasan et al. (2011a).

The class of functions f considered in this chapter is of the following form

$$f(x,t,u,u_x) = \frac{\partial}{\partial x}\left(\sum_{k=1}^{p+1} \frac{a_k}{k} u^k(x,t)\right) \tag{5.96}$$

Here, p is a finite positive integer and $a_k \ge 0,\ \forall k \in \{1,2,\cdots,p\}$ while $a_{p+1} > 0$. If $p = 0$, then (5.91) is linear. This special form could be considered as a generalization of the BBM-Burgers equation. For higher orders of the nonlinearity, $p \ge 5$, (5.91) may have unstable solitary wave solutions Bona et al. (2000).

The existence and uniqueness of a classical solution satisfying the initial and boundary value problem (5.91)-(5.94) for general boundary conditions has been solved in Bona and Dougalis (1980) by converting the differential equation into an integral equation and then applying Banach's fixed point theorem to the integral equation. The proof requires that $u(1,t)$ be a continuously differentiable function of time, which is true, for instance in the case of homogeneous Dirichlet boundary conditions at $x = 1$. For the boundary condition (5.94) proposed in this chapter, however, the existence and uniqueness of a classical solution remains an open problem and hence will be assumed in the results of this chapter.

The contributions of this chapter are:

- development of control laws that stabilize systems governed by the linear and the nonlinear pseudo-parabolic equations,
- derivation of various bounds on the solution, and
- numerical simulations that illustrate the performance of the proposed control laws.

5.4.1 Linear System

This section starts by discussing boundary stabilization of the linear pseudo-parabolic differential equations. The analysis will be extended in the next section to a nonlinear system by introducing a compensating term in the control laws for handling the nonlinearity. The initial value problem of the linear pseudo-parabolic differential equation is simply written as

$$\frac{\partial}{\partial t}(\Delta u - u) + \epsilon \Delta u = a_1 \frac{\partial u}{\partial x},\ 0 < x < 1,\ t > 0 \tag{5.97}$$

$$u(x,0) = u_0(x) \in H^1(0,1) \tag{5.98}$$

A set of boundary control laws proposed for the linear pseudo-parabolic equation (5.97) is as follows

$$u(0,t) = 0 \tag{5.99}$$

$$u_x(1,t) = -\frac{c}{\epsilon} u(1,t) \tag{5.100}$$

where $c > 0$ is a positive control gain. Here, the parameter c can be seen as a tuning parameter that may affect the performance of the closed-loop. Applying the feedback controller (5.99)-(5.100) is unnecessary in the linear case, since (5.97) is an open loop stable system. However, (5.99)-(5.100) will serve as a starting point for developing boundary control laws in the nonlinear case, where open loop solutions may be unstable.

A result on the boundary stabilization problem of the linear pseudo-parabolic differential equation is stated in the following theorem.

Theorem 5. *Suppose the initial condition $u_0 \in H^1(0,1)$ is consistent with the boundary conditions* (5.99)-(5.100)*. If the initial value problem of the linear pseudo-parabolic equation*

(5.97)-(5.98) *with boundary conditions* (5.99)-(5.100) *possesses a unique classical solution* $u(x,t) \in C^{2,1}([0,1]\times[0,\infty))$*, then the trivial solution is globally exponentially stable in the* H^1*-norm.*

Proof. Computing the first derivative of the H^1 Sobolev norm for the linear pseudo-parabolic equation (5.97) with respect to time, yields

$$\frac{\mathrm{d}}{\mathrm{d}t}\|u(t)\|_{H^1}^2 = 2uu_{xt}|_0^1 + 2\epsilon u_x u|_0^1 - a_1 u^2|_0^1 - 2\epsilon\int_0^1 u_x^2\,\mathrm{d}x \tag{5.101}$$

Substituting (5.99)-(5.100) into (5.101) and using Wirtinger's inequality (5.162), yields

$$\begin{aligned}\frac{\mathrm{d}}{\mathrm{d}t}\left(\|u(t)\|_{H^1}^2 + \frac{c}{\epsilon}u^2(1,t)\right) &\leq -\epsilon\left(\int_0^1 u_x^2\,\mathrm{d}x + \int_0^1 u_x^2\,\mathrm{d}x + \frac{c}{\epsilon}u^2(1,t)\right)\\ &\leq -\epsilon\left(\int_0^1 u^2\,\mathrm{d}x + \int_0^1 u_x^2\,\mathrm{d}x + \frac{c}{\epsilon}u^2(1,t)\right)\\ &\leq -\epsilon\left(\|u(t)\|_{H^1}^2 + \frac{c}{\epsilon}u^2(1,t)\right)\end{aligned} \tag{5.102}$$

Integrating the above equation with respect to time, yields

$$\|u(t)\|_{H^1}^2 \leq \left(\|u_0\|_{H^1}^2 + \frac{c}{\epsilon}u^2(1,0)\right)e^{-\epsilon t} \tag{5.103}$$

Since

$$u(1,0) = u(0,0) + \int_0^1 u_x(x,0)\,\mathrm{d}x = \int_0^1 u_x(x,0)\,\mathrm{d}x \tag{5.104}$$

the Cauchy-Schwarz inequality gives

$$u^2(1,0) \leq \left(\int_0^1 u_x^2(x,0)\,\mathrm{d}x\right)\left(\int_0^1 1^2\,\mathrm{d}x\right) \leq \|u_0\|_{H^1}^2 \tag{5.105}$$

Hence, (5.103) yields

$$\|u(t)\|_{H^1}^2 \leq \left(1 + \frac{c}{\epsilon}\right)\|u_0\|_{H^1}^2 e^{-\epsilon t} \tag{5.106}$$

which shows that the trivial solution is globally exponentially stable in the H^1-sense. □

Since the control law $z(\cdot)$ inferred by (5.100) is invertible, the control law may also be implemented with $u_x(1,t)$ as the measurement and $u(1,t)$ as the manipulated control input. In general, the boundary control law (5.100) is called the Robin boundary condition.

5.4.2 Nonlinear System

Suppose the initial value problem of the nonlinear pseudo-parabolic equation (5.91) has the following form

$$\frac{\partial}{\partial t}(\Delta u - u) + \epsilon \Delta u - \frac{\partial}{\partial x}\left(\sum_{k=2}^{p+1} \frac{a_k}{k} u^k\right) = a_1 \frac{\partial u}{\partial x},\ 0 < x < 1,\ t > 0 \tag{5.107}$$

$$u(x,0) = u_0(x) \in H^1(0,1) \tag{5.108}$$

A set of boundary control laws is proposed as follows

$$u(0,t) = 0 \tag{5.109}$$

$$u_x(1,t) = -\frac{c}{\epsilon} p u(1,t) - \frac{1}{\epsilon} \sum_{k=1}^{p} \frac{(k+1)}{(k+2)^2 c} a_{k+1}^2 u^{2k+1}(1,t) \tag{5.110}$$

A result on the boundary stabilization problem of the nonlinear pseudo-parabolic differential equation is stated in the following theorem.

Theorem 6. *Suppose the initial condition $u_0 \in H^1(0,1)$ is consistent with the boundary conditions* (5.109)-(5.110)*. If the initial value problem of the nonlinear pseudo-parabolic equation* (5.107)-(5.108) *with boundary conditions* (5.109)-(5.110) *possesses a unique classical solution $u(x,t) \in C^{2,1}([0,1]\times[0,\infty))$, then the trivial solution is semi-globally exponentially stable in the H^1-norm, i.e., there exists a non-decreasing positive constant $\mathcal{D}$ that depends on the initial condition, such that*

$$\|u(t)\|_{H^1}^2 \le \mathcal{D}(\|u_0\|_{H^1}) e^{-\epsilon t}, \quad \forall t \ge 0 \tag{5.111}$$

Furthermore, the solution is bounded in the H^2-norm i.e., there exists a positive constant $\mathcal{G}$ that depends on the initial condition, such that

$$\|u(t)\|_{H^2}^2 \le \mathcal{G}(\|u_0\|_{H^2}), \quad \forall t \ge 0 \tag{5.112}$$

Proof. The proof is similar to the proof of theorem 1 in Balogh and Krstic (2000a). Computing the first derivative of the H^1 Sobolev norm for the nonlinear pseudo-parabolic equation with respect to time, yields

$$\begin{aligned}\frac{\mathrm{d}}{\mathrm{d}t}\|u(t)\|_{H^1}^2 = {} & 2u u_{xt}|_0^1 + 2\epsilon u_x u|_0^1 - a_1 u^2|_0^1 - 2\sum_{k=1}^{p} \frac{a_{k+1}}{k+2} u^{k+2}|_0^1 \\ & -2\epsilon \int_0^1 u_x^2 \,\mathrm{d}x \end{aligned} \tag{5.113}$$

Substituting (5.109)-(5.110) into (5.113), the first and the second terms of the right hand side of (5.113) are

$$2uu_{xt}|_0^1 = -\frac{\mathrm{d}}{\mathrm{d}t}\left(\frac{c}{\epsilon}pu^2(1,t)+\sum_{k=1}^{p}\frac{(2k+1)}{(k+2)^2c\epsilon}a_{k+1}^2u^{2k+2}(1,t)\right) \tag{5.114}$$

$$2\epsilon u_x u|_0^1 = -2cpu^2(1,t)-2\sum_{k=1}^{p}\frac{(k+1)}{(k+2)^2c}a_{k+1}^2u^{2k+2}(1,t) \tag{5.115}$$

while a bound for the 4^{th} term of the right hand side of (5.113) is obtained through the following steps. First, note that

$$\sum_{k=1}^{p}\frac{a_{k+1}}{k+2}u^{k+2}(1,t)=\frac{a_2}{3}u^3(1,t)+\frac{a_3}{4}u^4(1,t)+\cdots+\frac{a_{p+1}}{p+2}u^{p+2}(1,t) \tag{5.116}$$

Applying Young's inequality (5.161) to each term in the right hand side gives

$$\frac{a_2}{3}u^3(1,t) \leq \frac{c}{2}u^2(1,t)+\frac{a_2^2}{3^2 2c}u^4(1,t) \tag{5.117}$$

$$\frac{a_3}{4}u^4(1,t) \leq \frac{c}{2}u^2(1,t)+\frac{a_3^2}{4^2 2c}u^6(1,t) \tag{5.118}$$

$$\vdots \tag{5.119}$$

$$\frac{a_{p+1}}{p+2}u^{p+2}(1,t) \leq \frac{c}{2}u^2(1,t)+\frac{a_{p+1}^2}{(p+2)^2 2c}u^{2p+2}(1,t) \tag{5.120}$$

Finally, adding the above terms and multiplying by 2 gives

$$2\sum_{k=1}^{p}\frac{a_{k+1}}{k+2}u^{k+2}(1,t)\leq cpu^2(1,t)+\sum_{k=1}^{p}\frac{a_{k+1}^2}{(k+2)^2c}u^{2k+2}(1,t) \tag{5.121}$$

Hence, (5.113) becomes

$$\begin{aligned}\frac{\mathrm{d}}{\mathrm{d}t}\|u(t)\|_{H^1}^2 \leq & -\frac{\mathrm{d}}{\mathrm{d}t}\left(\frac{c}{\epsilon}pu^2(1,t)+\sum_{k=1}^{p}\frac{(2k+1)}{(k+2)^2c\epsilon}a_{k+1}^2u^{2k+2}(1,t)\right)\\ & -cpu^2(1,t)-\sum_{k=1}^{p}\frac{(2k+1)}{(k+2)^2c}a_{k+1}^2u^{2k+2}(1,t)\\ & -a_1u^2(1,t)-2\epsilon\int_0^1 u_x^2\,\mathrm{d}x\end{aligned} \tag{5.122}$$

Using Wirtinger's inequality, (5.122) yields

$$\begin{aligned}
&\frac{\mathrm{d}}{\mathrm{d}t}\left(\|u(t)\|_{H^1}^2+\frac{c}{\epsilon}pu^2(1,t)+\sum_{k=1}^{p}\frac{(2k+1)}{(k+2)^2c\epsilon}a_{k+1}^2u^{2k+2}(1,t)\right)\\
\leq\ &-\epsilon\left(\|u(t)\|_{H^1}^2+\frac{c}{\epsilon}pu^2(1,t)+\sum_{k=1}^{p}\frac{(2k+1)}{(k+2)^2c\epsilon}a_{k+1}^2u^{2k+2}(1,t)\right)
\end{aligned}\tag{5.123}$$

Integrating the above inequality with respect to time, yields

$$\|u(t)\|_{H^1}^2\leq\left(\|u_0\|_{H^1}^2+\frac{c}{\epsilon}pu^2(1,0)+\sum_{k=1}^{p}\frac{(2k+1)}{(k+2)^2c\epsilon}a_{k+1}^2u^{2k+2}(1,0)\right)e^{-\epsilon t}\tag{5.124}$$

Using (5.105), this yields

$$\begin{aligned}
\|u(t)\|_{H^1}^2\ &\leq\ \left(\left(1+\frac{c}{\epsilon}p\right)\|u_0\|_{H^1}^2+\sum_{k=1}^{p}\frac{(2k+1)}{(k+2)^2c\epsilon}a_{k+1}^2\|u_0\|_{H^1}^{2k+2}\right)e^{-\epsilon t}\\
&=\ \mathcal{D}(\|u_0\|_{H^1})e^{-\epsilon t}
\end{aligned}\tag{5.125}$$

where $\mathcal{D}$ is a non-decreasing function of $\|u_0\|_{H^1}$. For brevity, let $\mathcal{D}=\mathcal{D}(\|u_0\|_{H^1})$. Integrating (5.122) on $\tau\in[0,t]$, yields

$$\begin{aligned}
&\int_0^1u^2\,\mathrm{d}x+\int_0^1u_x^2\,\mathrm{d}x+\frac{c}{\epsilon}pu^2(1,t)\\
&+\sum_{k=1}^{p}\frac{(2k+1)}{(k+2)^2c\epsilon}a_{k+1}^2u^{2k+2}(1,t)+2\epsilon\int_0^t\int_0^1u_x^2(x,\tau)\,\mathrm{d}x\,\mathrm{d}\tau\\
&+\int_0^t\left(cpu^2(1,\tau)+\sum_{k=1}^{p}\frac{(2k+1)}{(k+2)^2c}a_{k+1}^2u^{2k+2}(1,\tau)\right)\mathrm{d}\tau\\
\leq\ &\int_0^1u_0^2\,\mathrm{d}x+\int_0^1u_{0x}^2\,\mathrm{d}x+\frac{c}{\epsilon}pu^2(1,0)+\sum_{k=1}^{p}\frac{(2k+1)}{(k+2)^2c\epsilon}a_{k+1}^2u^{2k+2}(1,0)\\
\leq\ &\mathcal{D}
\end{aligned}\tag{5.126}$$

Inequality (5.126) produces the following estimates

$$\|u(\cdot,t)\|_{L^2}^2\leq\mathcal{D}\tag{5.127}$$

$$\|u_x(\cdot,t)\|_{L^2}^2\leq\mathcal{D}\tag{5.128}$$

$$2\epsilon\int_0^t\int_0^1u_x^2(x,\tau)\,\mathrm{d}x\,\mathrm{d}\tau\leq\mathcal{D}\tag{5.129}$$

$$\int_0^t\left(cpu^2(1,\tau)+\sum_{k=1}^{p}\frac{(2k+1)}{(k+2)^2c}a_{k+1}^2u^{2k+2}(1,\tau)\right)\mathrm{d}\tau\leq\mathcal{D}\tag{5.130}$$

$\forall t \in \mathbb{R} > 0$. Applying Agmon's inequality (5.164), (5.127) and (5.128) yields

$$\|u(\cdot,t)\|_{L^\infty}^2 \leq 2\|u(\cdot,t)\|_{L^2}\|u_x(\cdot,t)\|_{L^2} \leq 2\mathcal{D} \tag{5.131}$$

Remark that using the first lemma in appendix (5.160)

$$\begin{aligned}\sum_{k=1}^{p+1} u^{2k}(1,t) &\leq \sum_{k=1}^{p}\left(\frac{1}{k}u^2(1,t) + \frac{k-1}{k}u^{2k+2}(1,t)\right) + u^{2p+2}(1,t) \\ &\leq pu^2(1,t) + u^{2p+2}(1,t) + \sum_{k=1}^{p} u^{2k+2}(1,t)\end{aligned} \tag{5.132}$$

Since $p \geq 1$, $c > 0$, $a_k \geq 0, \forall k \in \{1,2,\cdots,p\}$, and $a_{p+1} > 0$ are finite numbers, there exists a sufficiently large positive constant $\mu(p,c,a_1,\cdots,a_{p+1})$ such that

$$\sum_{k=1}^{p+1} u^{2k}(1,t) \leq \mu\left(cpu^2(1,t) + \sum_{k=1}^{p}\frac{(2k+1)}{(k+2)^2 c}a_{k+1}^2 u^{2k+2}(1,t)\right) \tag{5.133}$$

Therefore, integrating the above inequality with respect to t and using (5.130), yields

$$\int_0^t\left(\sum_{k=1}^{p+1} u^{2k}(1,\tau)\right)\mathrm{d}\tau \leq \mu\mathcal{D} \tag{5.134}$$

Next, taking the L^2 inner product of (5.107) with $-2u_{xx}$ and using boundary control laws (5.109) and (5.110), the various terms are

$$\begin{aligned}-2\int_0^1 u_{xx}u_t\,\mathrm{d}x &= \frac{\mathrm{d}}{\mathrm{d}t}\left(\int_0^1 u_x^2\,\mathrm{d}x + \frac{c}{\epsilon}pu^2(1,t)\right. \\ &\quad \left. + \sum_{k=1}^{p}\frac{a_{k+1}^2}{(k+2)^2 c\epsilon}u^{2k+2}(1,t)\right)\end{aligned} \tag{5.135}$$

$$\begin{aligned}-2a_1\int_0^1 u_{xx}u_x\,\mathrm{d}x &= -a_1\left(\frac{c}{\epsilon}pu(1,t)\right. \\ &\quad \left. + \sum_{k=1}^{p}\frac{(k+1)}{(k+2)^2 c\epsilon}a_{k+1}^2 u^{2k+1}(1,t)\right)^2 + a_1 u_x^2(0,t)\end{aligned} \tag{5.136}$$

$$2\epsilon\int_0^1 u_{xx}u_{xx}\,\mathrm{d}x = 2\epsilon\int_0^1 u_{xx}^2\,\mathrm{d}x \tag{5.137}$$

$$2\int_0^1 u_{xx}u_{xxt}\,\mathrm{d}x = \frac{\mathrm{d}}{\mathrm{d}t}\int_0^1 u_{xx}^2\,\mathrm{d}x \tag{5.138}$$

Using (5.131), the last term may be estimated as follows

$$\begin{aligned} & -2\int_0^1\left(\sum_{k=1}^{p} a_{k+1}u^k u_{xx}u_x\right)\mathrm{d}x \\ \geq\ & -2\left(\sum_{k=1}^{p} a_{k+1}\sup_{0\leq s\leq t}\|u(\cdot,s)\|_{L^\infty}^k\right)\int_0^1 |u_{xx}u_x|\,\mathrm{d}x \\ \geq\ & -\sum_{k=1}^{p} a_{k+1}2^{\frac{k}{2}+1}\mathcal{D}^{\frac{k}{2}}\int_0^1 |u_{xx}u_x|\,\mathrm{d}x \end{aligned} \tag{5.139}$$

With the help of Cauchy-Schwarz's inequality

$$\begin{aligned} & -\sum_{k=1}^{p} a_{k+1}2^{\frac{k}{2}+1}\mathcal{D}^{\frac{k}{2}}\int_0^1 |u_{xx}u_x|\,\mathrm{d}x \\ \geq\ & -\sum_{k=1}^{p} a_{k+1}2^{\frac{k}{2}+1}\mathcal{D}^{\frac{k}{2}}\left(\int_0^1 u_x^2\,\mathrm{d}x\right)^{\frac{1}{2}}\left(\int_0^1 u_{xx}^2\,\mathrm{d}x\right)^{\frac{1}{2}} \end{aligned} \tag{5.140}$$

Young's inequality gives

$$\begin{aligned} & \left(\int_0^1 u_x^2\,\mathrm{d}x\right)^{\frac{1}{2}}\left(\int_0^1 u_{xx}^2\,\mathrm{d}x\right)^{\frac{1}{2}} \\ \leq\ & \frac{1}{2}\left(\sum_{k=1}^{p}\frac{a_{k+1}}{\epsilon}2^{\frac{k}{2}-1}\mathcal{D}^{\frac{k}{2}}\right)\int_0^1 u_x^2\,\mathrm{d}x + \frac{1}{2}\left(\frac{1}{\sum_{k=1}^{p}\frac{a_{k+1}}{\epsilon}2^{\frac{k}{2}-1}\mathcal{D}^{\frac{k}{2}}}\right)\int_0^1 u_{xx}^2\,\mathrm{d}x \end{aligned} \tag{5.141}$$

Hence, the last term may be estimated as follows

$$\begin{aligned} & -2\sum_{k=1}^{p} a_{k+1}\int_0^1 u^k u_x u_{xx}\,\mathrm{d}x \\ \geq\ & -\frac{1}{2\epsilon}\left(\sum_{k=1}^{p} a_{k+1}2^{\frac{k}{2}}\mathcal{D}^{\frac{k}{2}}\right)^2\int_0^1 u_x^2\,\mathrm{d}x - 2\epsilon\int_0^1 u_{xx}^2\,\mathrm{d}x \end{aligned} \tag{5.142}$$

Using (5.125), the above inequality yields

$$2\sum_{k=1}^{p} a_{k+1}\int_0^1 u^k u_x u_{xx}\,\mathrm{d}x \leq \frac{1}{2\epsilon}\left(\sum_{k=1}^{p} a_{k+1}2^{\frac{k}{2}}\mathcal{D}^{\frac{k+1}{2}}\right)^2 e^{-\epsilon t} + 2\epsilon\int_0^1 u_{xx}^2\,\mathrm{d}x \tag{5.143}$$

Assembling (5.135)-(5.138) and (5.143) gives

$$\begin{aligned}
&\frac{\mathrm{d}}{\mathrm{d}t}\left(\int_0^1 u_x^2\,\mathrm{d}x+\int_0^1 u_{xx}^2\,\mathrm{d}x+\frac{c}{\epsilon}pu^2(1,t)+\sum_{k=1}^{p}\frac{a_{k+1}^2}{(k+2)^2c\epsilon}u^{2k+2}(1,t)\right)\\
\leq\ &\frac{1}{2\epsilon}\left(\sum_{k=1}^{p}a_{k+1}2^{\frac{k}{2}}\mathcal{D}^{\frac{k+1}{2}}\right)^2e^{-\epsilon t}+a_1\frac{c^2}{\epsilon^2}p^2u^2(1,t)\\
&+2a_1\frac{c}{\epsilon}p\sum_{k=1}^{p}\frac{(k+1)}{(k+2)^2c\epsilon}a_{k+1}^2u^{2k+2}(1,t)+a_1\sum_{k=1}^{p}\frac{(k+1)^2}{(k+2)^4c^2\epsilon^2}a_{k+1}^4u^{4k+2}(1,t)\\
&+2a_1\sum_{k=1}^{p-1}\sum_{l=k+1}^{p}\frac{(k+1)}{(k+2)^2c\epsilon}\frac{(l+1)}{(l+2)^2c\epsilon}a_{k+1}^2a_{l+1}^2u^{2(k+l)+2}(1,t)
\end{aligned}\tag{5.144}$$

To simplify the notation, define

$$\mathcal{X}(t) = \int_0^1 u_x^2\,\mathrm{d}x+\int_0^1 u_{xx}^2\,\mathrm{d}x+\frac{c}{\epsilon}pu^2(1,t)+\sum_{k=1}^{p}\frac{a_{k+1}^2}{(k+2)^2c\epsilon}u^{2k+2}(1,t)\tag{5.145}$$

$$\mathcal{E} = \frac{1}{2\epsilon}\left(\sum_{k=1}^{p}a_{k+1}2^{\frac{k}{2}}\mathcal{D}^{\frac{k+1}{2}}\right)^2\tag{5.146}$$

$$f(t) = \sum_{k=1}^{p+1}u^{2k}(1,t)\tag{5.147}$$

so that (5.144) can be written as

$$\begin{aligned}
\frac{\mathrm{d}}{\mathrm{d}t}\mathcal{X}(t) &\leq \mathcal{E}e^{-\epsilon t}+\lambda\left(\sum_{k=1}^{2p+1}u^{2k}(1,t)\right)\\
&\leq \mathcal{E}e^{-\epsilon t}+\lambda f(t)+\lambda f(t)u^{2p}(1,t)
\end{aligned}\tag{5.148}$$

where λ is a large number. By (5.160) in appendix, and the definition of $\mathcal{X}(t)$, there exists a sufficiently large number $\omega>\lambda>0$ such that (5.148) yields

$$\frac{\mathrm{d}}{\mathrm{d}t}\mathcal{X}(t) \leq \mathcal{E}e^{-\epsilon t}+\omega f(t)+\omega f(t)\mathcal{X}(t)\tag{5.149}$$

Integrating the above equation on $\tau\in[0,t]$ and using (5.134) give

$$\mathcal{X}(t) \leq \mathcal{X}(0)+\frac{1}{\epsilon}\mathcal{E}+\omega\mu\mathcal{D}+\int_0^t\omega f(\tau)\mathcal{X}(\tau)\,\mathrm{d}\tau\tag{5.150}$$

The Gronwall-Bellman inequality (5.167) gives

$$\mathcal{X}(t) \leq \left(\mathcal{X}(0) + \frac{1}{\epsilon}\mathcal{E} + \omega\mu\mathcal{D}\right)e^{\omega\mu\mathcal{D}} \tag{5.151}$$

Since

$$\mathcal{X}(0) \leq \left(1 + \frac{c}{\epsilon}p\right)\|u_0\|_{H^2}^2 + \sum_{k=1}^{p}\frac{1}{(k+2)^2 c\epsilon}a_{k+1}^2\|u_0\|_{H^2}^{2p+2} \tag{5.152}$$

and $\mathcal{D}$ and $\mathcal{E}$ are non-decreasing functions of $\|u_0\|_{H^1}$, and since $\|u_0\|_{H^1} \leq \|u_0\|_{H^2}$, it follows that

$$\frac{1}{2}\|u(t)\|_{H^2}^2 \leq \mathcal{X}(t) \leq \frac{1}{2}\mathcal{G}(\|u_0\|_{H^2}) \tag{5.153}$$

where $\mathcal{G}$ is a positive constant that depends on the initial condition as defined by (5.151), which completes the proof. □

Since the control law $z(\cdot)$ inferred by (5.110) is invertible, there exists a function $z^{-1}(\cdot)$ such that

$$u(1,t) = z^{-1}(u_x(1,t)) \tag{5.154}$$

From (5.123), we have

$$\frac{\mathrm{d}}{\mathrm{d}t}\left(\|u(t)\|_{H^1}^2 + \frac{c}{\epsilon}pu^2(1,t) + \sum_{k=1}^{p}\frac{(2k+1)}{(k+2)^2 c\epsilon}a_{k+1}^2 u^{2k+2}(1,t)\right) \leq 0 \tag{5.155}$$

while from (5.126), we have

$$\int_0^\infty\left(\|u(t)\|_{H^1}^2 + \frac{c}{\epsilon}pu^2(1,t) + \sum_{k=1}^{p}\frac{(2k+1)}{(k+2)^2 c\epsilon}a_{k+1}^2 u^{2k+2}(1,t)\right)\mathrm{d}t \leq \frac{\mathcal{D}}{\epsilon} \tag{5.156}$$

Hence, using 5.169

$$\lim_{t\to\infty} u^2(1,t) = 0 \tag{5.157}$$

5.4.3 Numerical Example

As an example, consider the nonlinear pseudo-parabolic equation (5.107). Let $p = 5$, $a_2 = \cdots = a_5 = 0$, and $a_1 = a_6 = 1$. Suppose the dissipation coefficient is known to be $\epsilon = 10^{-6}$, then the equation becomes the 5^{th}-order BBM-Burgers equation

$$u_t + u_x - 10^{-6}u_{xx} - u_{xxt} + u^5 u_x = 0 \tag{5.158}$$

The initial condition

$$u_0(x) = 7.67(1 - x^3)\text{sech}(2\pi x)\sin^2(2\pi x) \tag{5.159}$$

is chosen to be consistent with the boundary conditions (5.109)-(5.110) (**Fig. 5.1**).

The simulation is carried out by discretizing the equation using the finite difference method. The time step used in this simulation is $\Delta t = 0.001$ while the spatial grid size $\Delta x = 0.01$. In the controlled case, the control laws are computed by the proposed boundary control laws (5.109) and (5.110) while in the uncontrolled case, homogeneous Dirichlet boundary conditions are imposed at both ends. The results are presented below. **Fig. 5.2** shows that using the proposed control laws, the H^1 energy decays to zero, while in the uncontrolled case the energy increases without bound. In the uncontrolled case, **Fig. 5.3**, the solution shows an erratic behavior and eventually blows up after 258×10^{-3} s. This unsatisfactory behavior is remedied by applying boundary control, as shown in **Fig. 5.4** where the solution converges to the zero solution $u \equiv 0$.

5.5 Conclusions

Boundary control laws for the generalized KdV-Burgers equation have been presented in this chapter. The invertible control laws for different cases of generalized KdV-Burgers guarantee global (exponential and asymptotic) stability in the sense of the L^2 norm. Further, most of the control laws only require measurement at the boundary of the systems which is an advantage from a practical point of view. The only control law which uses measurement inside the domain is the Burgers equation with Dirichlet boundary conditions. In this case, an observer has been designed to estimate the in-domain state and again exponential stability is proved. An adaptive control laws has been constructed for the case when the dissipation parameter is unknown. The control laws are decentralized, which means the controller calculation at each end of the domain would use measurements only from that end. The controllers guarantee global L^2 stability.

The boundary stabilization problem for a class of pseudo-parabolic differential equations is solved in this chapter. Using the proposed control laws, the nonlinear closed-loop system is semi-globally exponentially stable in the H^1-norm. However, the problem of existence and uniqueness of a classical solution under the proposed control law remains open. A numerical example shows that the proposed control laws are able to prevent blow up in finite time.

Appendix

Lemma 1. *For any* $n \geq 1$

$$u^{2n}(1,t) \leq \left(\frac{n-1}{n}\right) u^{2n+2}(1,t) + \left(\frac{1}{n}\right) u^2(1,t) \tag{5.160}$$

Proof. The result is trivial for $n = 1$. For $n > 1$, Young's inequality can be applied, which states that if a and b are non-negative real-valued functions and p and q are positive real numbers such that $\frac{1}{p} + \frac{1}{q} = 1$, then

$$ab \leq \frac{a^p}{p} + \frac{b^q}{q} \tag{5.161}$$

Choosing $a = \left(u^{\frac{n-1}{n}(n+1)}(1,t)\right)^2, b = \left(u^{\frac{1}{n}}(1,t)\right)^2, p = \frac{n}{n-1}, q = n$, gives (5.160). □

Lemma 2. (Wirtinger's inequality) *For any* $u \in C^1(0,1)$*, then*

$$\int_0^1 u^2(x,t)\,\mathrm{d}x \leq u^2(0,t) + \frac{4}{\pi^2}\int_0^1 u_x^2(x,t)\,\mathrm{d}x \tag{5.162}$$

$$\int_0^1 u^2(x,t)\,\mathrm{d}x \leq u^2(1,t) + \frac{4}{\pi^2}\int_0^1 u_x^2(x,t)\,\mathrm{d}x \tag{5.163}$$

Lemma 3. (Agmon's inequality) *For any* $u \in C^1(0,1)$*, then*

$$\max_{x\in[0,1]} u^2(x,t) \leq u^2(0,t) + 2\sqrt{\int_0^1 u^2\,\mathrm{d}x}\sqrt{\int_0^1 u_x^2\,\mathrm{d}x} \tag{5.164}$$

$$\max_{x\in[0,1]} u^2(x,t) \leq u^2(1,t) + 2\sqrt{\int_0^1 u^2\,\mathrm{d}x}\sqrt{\int_0^1 u_x^2\,\mathrm{d}x} \tag{5.165}$$

Lemma 4. (Gronwall-Bellman's inequality) *Let* $\nu : [a,b] \to \mathbb{R}$ *be continuous and nonnegative. If a continuous function* $y : [a,b] \to \mathbb{R}$ *satisfies*

$$y(t) \leq \kappa + \int_a^t \nu(s)y(s)\,\mathrm{d}s \tag{5.166}$$

$\forall \kappa \in \mathbb{R}$*, then*

$$y(t) \leq \kappa e^{\int_a^t \nu(s)\,\mathrm{d}s} \tag{5.167}$$

Lemma 5. *Suppose that the function* $f(t)$ *defined on* $[0,\infty)$ *satisfies the following conditions*

1. $f(t) \geq 0, \forall t \in [0,\infty)$,

2. $f(t)$ *is differentiable on* $[0,\infty)$ *and there exist a constant* M *such that*

$$\frac{\mathrm{d}}{\mathrm{d}t}f(t) \leq M, \quad \forall t \geq 0 \tag{5.168}$$

3. $\int_0^\infty f(t)\,\mathrm{d}t < \infty$

Then

$$\lim_{t\to\infty} f(t) = 0 \tag{5.169}$$

Proofs of lemma 2 and lemma 3 can be found in Krstic (1999), lemma 4 is given in Khalil (2001), while lemma 5 is found in Krstic et al. (1995).

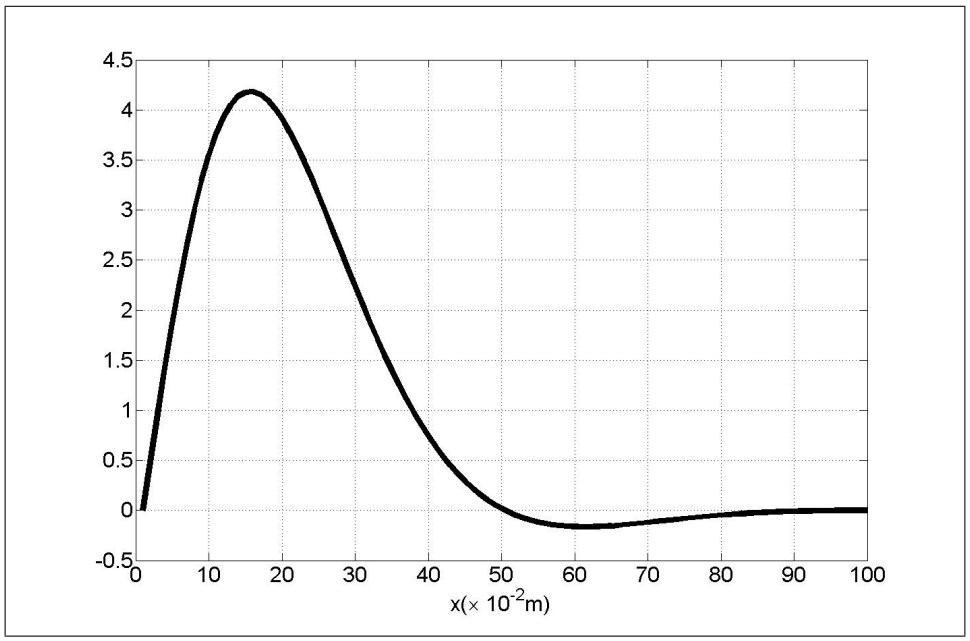

Figure 5.1: Initial condition $u_0(x)$.

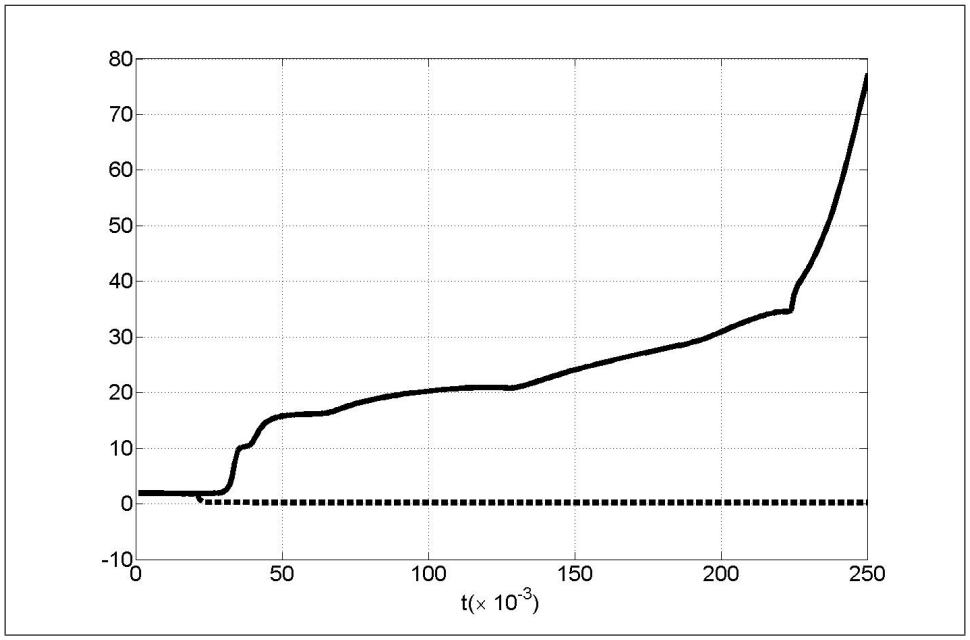

Figure 5.2: Plots of the H^1 norm. The dash line is from control laws (5.109)-(5.110) while the thick line is from the homogeneous Dirichlet boundary conditions in both ends.

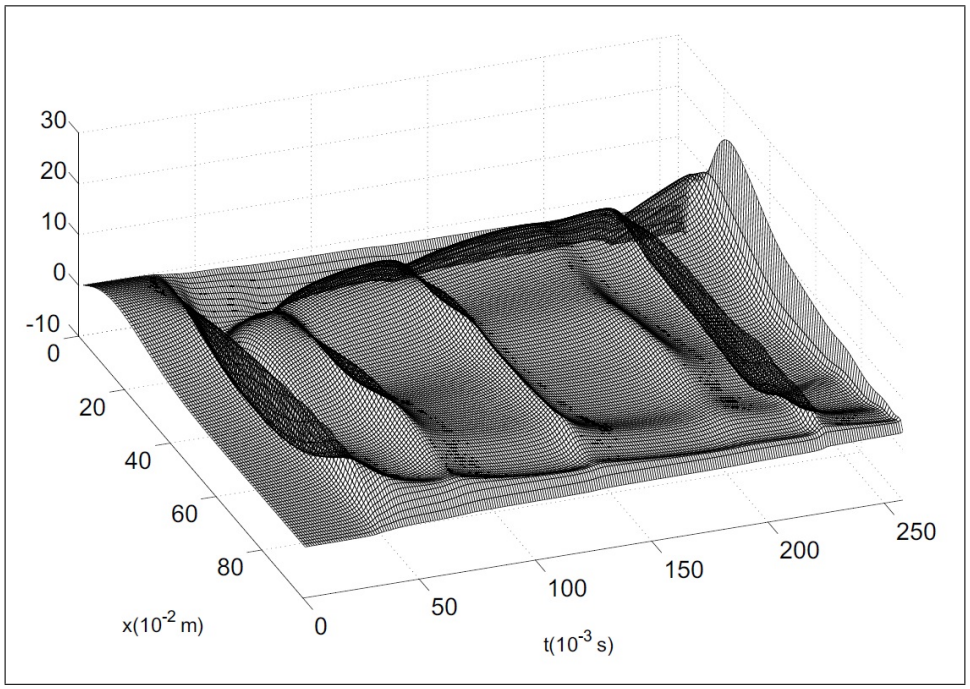

Figure 5.3: Uncontrolled case using homogeneous Dirichlet boundary conditions at both ends.

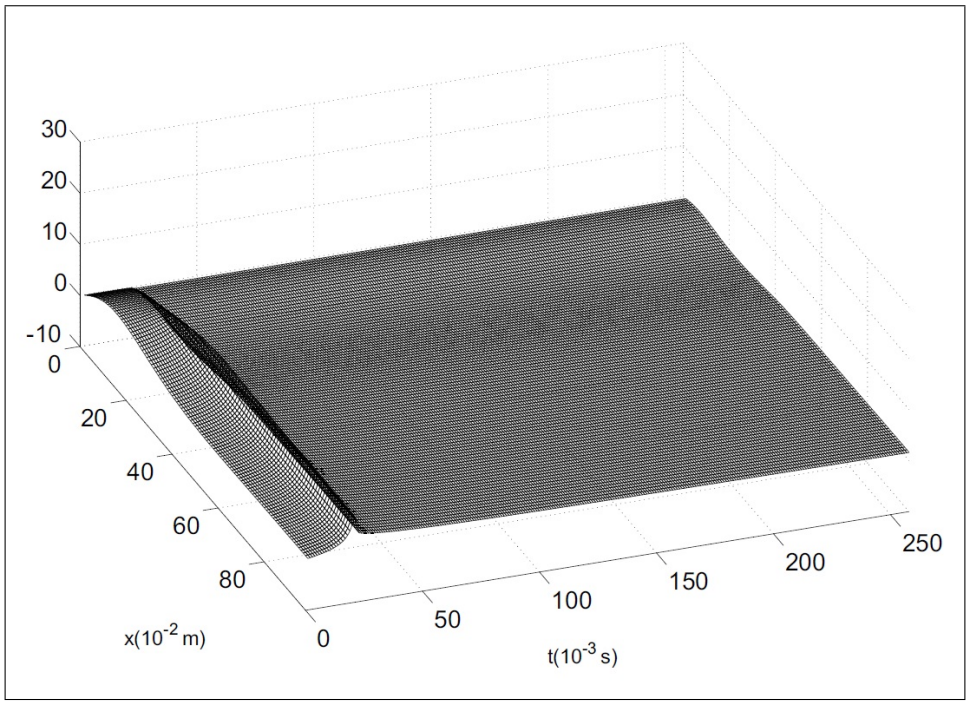

Figure 5.4: Controlled case using homogeneous Dirichlet boundary condition at $x = 0$ and the control law (5.110) at $x = 1$.

Chapter 6

Discussions and Recommendations

In this thesis, we present some control and optimization problems related to the sub-surface petroleum production systems and proposed some methods to solve them. To this end, we consider gas coning control and water-flooding control problems in a closed-loop reservoir management framework. We also discuss the effect of long-term and short-term optimization to the production strategies.

As an addition, we develop boundary control laws for wave equations. This additional research was conducted to provide an overview of control design using the Lyapunov method that we have used while working with the gas coning control problems.

6.1 Discussions

Gas coning control

Once the gas enter the production wells, it will dominate the flow inside the well; thus, reducing oil recovery significantly. Therefore, there is an incentive to produce the oil from the production wells in their subcritical phase (before gas breakthrough) for an extended period of time. In gas coning control, we formulate the problem as a boundary control problem of the porous media equation with two boundary conditions; a homogeneous Neumann boundary condition describing no-flow at the outer boundary of the reservoir, and a nonlinear boundary condition describing the well production rate. It should be noted that the model was developed using some simplified assumptions; thus, it needs to be tuned in any application. The model has been tested for several wells in the North Sea and the reliability has been good.

The boundary control problem was solved using the Lyapunov and the backstepping methods for both linear and nonlinear cases. The idea is to design a well rate controllers such that the systems can be exponentially stable in subcritical phase. Stability means that the system states, i.e., the height of oil column, approaches their equilibrium point bounded by exponentially decreasing functions. One may rightly argue that a reservoir will always exhibit stable behavior. The guarantee of exponential stability in this context implies that the

drainage of oil from the reservoir is exponential, thus possibly advantageous from a business point of view.

In a simple definition, the Lyapunov method is a tool to study the stability of a dynamical system without requiring knowledge of its closed form solution or the true physical energy, provided a Lyapunov function can be found to satisfy the above constraints. It is true that some PDEs can be solved in closed form; thus, the stability properties can be analyzed directly from the explicit form. However, for more complex systems, the explicit solution usually can not be found. Further, the method could be used for both linear and nonlinear systems; hence, it is suitable to use in our boundary control designs for different cases of gas coning models.

An alternative to the Lyapunov method is the backstepping method. Originally used for designing boundary control laws of ordinary differential equations, the method has been developed further to solve the PDEs problem. The advantage of using the backstepping method is that we can construct an observer, in case measurements inside the domain are needed, in a similar way to the backstepping control design itself. This particular case happens when we consider outer boundary influx to the reservoir.

To test the control laws, we present an example with a complex reservoir model and show that the proposed method can be used to increase oil recovery significantly during the subcritical phase compared to a conventional method which uses constant production rates.

Water-flooding control

In the water-flooding case, we formulate the problem as an optimal control problem and solve it using the switching time method under bang-bang control. Bang-bang control has a major practical advantage because it can be implemented with simple on-off valves.

In this method, the control inputs, e.g., the flow rates or BHPs, are written as piecewise constant functions. The value of the control settings are limited to zero and one to represent the bang-bang control; hence, the switching time is defined as the time to switch from zero to one and vice versa. The problem is to find the optimal switching times such that the oil revenue (NPV) can be maximized. To this end, the reservoir model is written in a state space representation and was assumed to be free from uncertainty. Since the reservoir states dimension can be hundreds of thousands or even more, an effective gradient-based optimization method is employed. The gradient is obtained using the adjoint method by evaluating the Hamiltonian equation which is basically a linear combination of the objective function and the dynamical system. In order to obtain the Hamiltonian equation, first the dynamical system is simulated forward to get the reservoir states (pressure and saturation). Afterward, the adjoint equation is simulated backward to obtain the Lagrange multipliers. Once the gradient is obtained, the optimal control settings can be found using the halving interval method.

An example of a realistic reservoir model shows that the proposed method can be used to increase oil revenue significantly compared to the reactive control method. A limitation occurs when computing the left and right limit of the Hamiltonian equation since sufficiently small time steps are required. On the other hand, one step of the reservoir simulation will

require a significant amount of computational time; hence, in practice, larger time steps are usually used. To overcome this issue, in each simulation, the quality of the gradient should be checked by the finite difference method. Another limitation is that the proposed method requires a good knowledge of the reservoir model which is often a constraint.

Long-term and short-term optimization

Due to large uncertainties, optimization in an oil production system is usually done in daily basis. The goal is to produce the oil as much as possible under production constraints such as maximum gas and liquid handling capacity. In the other hand, an effort to find a robust long-term optimal strategy to drain the reservoir has been done in recent years. The method is known as closed-loop reservoir management which combines optimal control method to compute the optimal strategy and data assimilation to handle uncertainty.

Optimal production strategies for short-term and long-term objectives may differ quite substantially. In particular, an aggressive short-term strategy may harm long-term effects like recovery. For this reason, in this chapter, we introduce a systematics approach to combine the short-term and long-term optimization. The approach is adopted from a multi-objective optimization method where we define two functions that represent short-term and long-term objectives. Further, we define a new objective function which is a convex combination of the two functions. This method is known as the weighted-sum method. For every convex combination, a new strategy will be obtained; thus, we have a collection of optimal solutions. The solutions are projected onto the actual objective function with different time spans; a short time span represents an evaluation of the short-term strategy, and a long time span represents an evaluation of the long-term strategy. The results are a Pareto-like curve which can be used as a tool to analyze long-term and short-term production optimization.

A limitation of the approach is that since the two functions used in the weighted-sum are not the actual objectives, we can not claim that the solutions are Pareto frontiers. Nevertheless, the curve is still useful since it shows a trade-off between short-term and long-term optimization.

Boundary stabilization of the wave equations

In this chapter, we developed some boundary control laws for wave equations. Two well-known equations are considered; the classical Korteweg-de Vries-Burgers (KdV-Burgers) equation and the more recent Benjamin-Bona-Mahony-Burgers (BBM-Burgers) equations. Those equation have many application, e.g., thermodynamic process, flow in porous media, shear in second order fluids, and option pricing. We were interested in a theoretical side of the solution, in particular, it has been known that for some initial conditions the solution is unbounded.

To this end, we develop stabilizing control laws for both equations. Most of the control laws are written explicitly and only requires measurements at the boundary of the systems. We provide a numerical example to shows the performance of the control laws.

6.2 Recommendations

Some recommendations for future research are as follows:

- Throughout this thesis, we assumed the dynamical systems are free from uncertainties. This is, of course, not true as a result of our limited knowledge of the reservoir. Hence, accounting for uncertainty is crucial. Some stochastic approaches have been developed in recent years and seem promising to handle this problem.

- In chapter 2, the proxy model introduces many assumptions, for instance, the model is simplified into a one-dimensional problem since gas coning was assumed to occur first at the well heel. However, in practice the coning depends also on the reservoir permeability above each well segment. Therefore, a more complex model with less assumptions could be used. Further, since the presented method was developed only for the subcritical phase, a more general method which covers a longer production time might be developed.

- In chapter 3, the gradient computation of the switching times requires sufficiently small time steps. Therefore, a reduced order technique to speed-up the computational time needs to be developed. Further, event though the convergence of the heuristic halving interval method is guaranteed, it is not the best choice for a search method. A better method in term of computation time could be a steepest decent approach.

- In chapter 4, production constraints, e.g., gas and liquid handling capacity, need to be included in the short-term optimization. Further, short-term and long-term objectives should be defined differently in order to generate the correct Pareto frontiers.

- In chapter 5, we have shown that the solution of the generalized KdV-Burgers equation is globally exponentially stable in the L^2-norm. However, the L^2 stability is not sufficient because it does not guarantee boundedness of solutions. Therefore, H^1 stability needs also to be pursued. Further, when deriving the boundary feedback for the BBM-Burgers equation, we assume perfect knowledge of the dissipation coefficient ϵ. Since, in reality, this parameter may be unknown and takes an arbitrary positive value, the objective cannot be achieved by the static feedback; hence, we need to design an adaptive controller which incorporates a parameter estimator as a dynamic component of the control law.

Bibliography

Aanonsen, S. I., Naevdal, G., Oliver, D. S., Reynolds, A. C., Valles, B., 2009. The ensemble kalman filter in reservoir engineering–a review. SPE Journal 14, 393–412.

Aziz, K., Settari, A., 1979. Petroleum reservoir simulation. Kluwer Academic Publishers.

Balogh, A., Krstic, M., 2000a. Boundary control of the korteweg-de vries-burgers equation: Further results on stabilization and well–posedness, with numerical demonstration. IEEE Transaction on Automatic Control 45, 1739–1745.

Balogh, A., Krstic, M., 2000b. Burgers equation with nonlinear boundary feedback: h^1 stability, well-posedness and simulation. Mathematical Problems in Engineering 6, 189–200.

Barenblatt, G., Entov, V., Ryzhik, V., 1990. Theory of fluid flow through natural rocks. Dordrecht: Kluwer.

Bear, J., 1972. Dynamics of Fluids in Porous Media. Elsevier.

Bellman, R., 1956. On the bang-bang control problem. Quarterly of Applied Mathematics 14, 11–18.

Bengea, S. C., DeCarlo, R. A., 2005. Optimal control of switching systems. Automatica 41, 11–27.

Benjamin, T. B., Bona, J. L., Mahony, J. J., 1972. Model equations for long waves in nonlinear dispersive systems. Philosophical Transactions of the Royal Society of London 272 (1220), 47–78.

Bona, J. L., Dougalis, V. A., 1980. An initial and boundary value problem for a model equation for propagation of long waves. Journal of Mathematical Analysis and Applications 75 (2), 503–522.

Bona, J. L., Dougalis, V. A., Karakashian, O. A., McKinney, W. R., 1995. High-order numerical schemes for the generalized korteweg-de vries equation. Philosophical Transactions: Physical Sciences and Engineering 351, 107–164.

Bona, J. L., Dougalis, V. A., Karakashian, O. A., McKinney, W. R., 1996. The effect of dissipation on solution of the generalized korteweg de vries equation. Journal of Computational and Applied Mathematics 74, 127–154.

Bona, J. L., Luo, L., 1993. Decay of solutions to nonlinear dispersive wave equations. Differential and Integral Equations 6, 961–980.

Bona, J. L., Luo, L., 1995. Initial-boundary value problems for model equations for the propagation of long waves, in: Evolution Equations. Marcel Dekker.

Bona, J. L., McKinney, W. R., Restrepo, J. M., 2000. Stable and unstable solitary-wave solutions of the generalized regularized long-wave equation. Journal of Nonlinear Science 10 (6), 603–638.

Bona, J. L., Pritchard, W. G., Scott, L. R., 1980a. A comparison of laboratory experiments with a model equation for long waves. In: Report No. 100, Fluid Mechanics Research Institute, University of Essex. Essex, UK.

Bona, J. L., Pritchard, W. G., Scott, L. R., 1980b. An evaluation of a model equation for water waves. Philosophical Transactions of the Royal Society of London 302 (1471), 457–510.

Bona, J. L., Sun, S., Zhang, B. Y., 2008. Non-homogeneous boundary value problems of he korteweg-de vries and the korteweg-de vries-burgers equations in a quarter plane. Ann. Inst. H. Poincare Anal. Non-Lineaire 25, 1145–1185.

Bona, J. L., Sun, S. M., Zhang, B. Y., 2009. A non-homogeneous boundary-value problem for the korteweg-de vries equation posed on a finite domain ii. Journal of Differential Equations 247, 2558–2596.

Brouwer, D. R., Jansen, J. D., 2004. Dynamic optimization of waterflooding with smart wells using optimal control theory. SPE Journal 9 (4), 391–402.

Chen, C., Li, G., Reynolds, A. C., 2012. Robust constrained optimization of short-term and long-term net present value for closed-loop reservoir management. SPE Journal 17 (3), 849–864.

Chen, P. J., Gurtin, M. E., 1968. On a theory of heat conduction involving two temperatures. Zeitschrift fur Angewandte Mathematik und Physik 19 (4), 614–627.

Chu, H. P., Chang, T., 2012. Nuclear energy consumption, oil consumption and economic growth in g-6 countries: Bootstrap panel causality test. Vol. 48. pp. 762–769.

Coleman, B. D., Noll, W., 1960. An approximation theorem for functionals with applications to continuum mechanics. Archive for Rational Mechanics and Analysis 6 (1), 355–370.

Colin, T., Ghidaglia, J. M., 2001. An initial-boundary-value problem for the korteweg-de vries equation posed on a finite interval. Advances in Differential Equations 6, 1463–1492.

Cuesta, C. M., Hulshof, J., 2003. A model problem for groundwater flow with dynamic capillary pressure: stability of travelling waves. Nonlinear Analysis 52 (4), 1199–1218.

Dake, L. P., 1983. Fundamentals of reservoir engineering. Elsevier Science.

Dutykh, D., 2007. Modelisation mathematique des tsunamis. PhD Thesis, Ecole Normale Superieure De Cachan.

Eck-Olsen, J., Vollen, E., Tonnessen, T., 2004. Challenges in implementing ubo technology. In: Proceedings of the SPE/IADC Underbalanced Technology Conference and Exhibition. Houston, USA.

Egerstedt, M., Wardi, Y., Delmotte, F., 2003. Optimal control of switching times in switched dynamical systems. In: Proceedings of the conference on decision and control. Atlanta, USA.

Ertekin, T., Abou-Kassem, J. H., King, G. R., 2001. Basic applied reservoir simulation. Society Of Petroleum Engineer.

Fernandes, P., Li, Z., Zhu, D., 2009. Understanding the roles of inflow-control devices in optimizing horizontal-well performance. In: Proceedings of the SPE Annual Technical Conference and Exhibition. New Orleans, USA.

Foss, B., 2012. Process control in conventional oil and gas fields - challenges and opportunities. Control Engineering Practice 20 (10), 1058–1064.

Foss, B., Jensen, J. P., 2011. Performance analysis for closed-loop reservoir management. SPE Journal 16, 183–190.

Gao, W., Deng, F., 2007. Stability of burgers-korteweg-de vries equation. In: IEEE International Conference on Control and Automation. Guangzhou, China.

Hasan, A., Aamo, O. M., Foss, B., 2013a. Boundary control for a class of pseudoparabolic differential equations. Systems and Control Letters 62, 63–69.

Hasan, A., Foss, B., 2011. Global stabilization of the generalized burgers-korteweg-de vries equation by boundary control. In: 18th IFAC World Congress. Milan, Italy.

Hasan, A., Foss, B., Aamo, O. M., 2011a. Boundary control of long waves in nonlinear dispersive systems. In: Proceedings of the 1st Australian Control Conference. Melbourne, Australia.

Hasan, A., Foss, B., Sagatun, S., 2010a. Boundary control of fluid flow through porous media. In: International Conference on Numerical Analysis and Applied Mathematics. Rhodos, Greece.

Hasan, A., Foss, B. A., Sagatun, S. I., 2012. Flow control of fluids through porous media. Journal of Applied Mathematics and Computation 219 (7), 3323–3335.

Hasan, A., Foss, B. A., Sagatun, S. I., 2013b. Optimization of oil production under gas coning conditions. Journal of Petroleum Science and Engineering (Accepted).

Hasan, A., Foss, B. A., Sagatun, S. I., Tjostheim, B. P., Svandal, A., Hatland, C., 2011b. Modeling, simulation, and optimal control of oil production under gas coning conditions. SPE Journal of Petroleum Technology 63 (7), 79–80.

Hasan, A., Foss, B. A., Sagatun, S. I., Tjostheim, B. P., Svandal, A., Hatland, C., 2011c. Modeling, simulation, and optimal control of oil production under gas coning conditions. In: Proceedings of the SPE EUROPEC. Vienna, Austria.

Hasan, A., Sagatun, S. I., Foss, B. A., 2010b. Well rate control design for gas coning problem. In: Proceedings of the IEEE CDC Conference. Atlanta, USA.

Huang, Y., Lin, D., Bai, B., Ricardez, C., 2009. Pre-salt depth imaging of santos basin, brazil. In: Proceedings of the SEG Annual Meeting. Houston, USA.

Isaacs, E., 2008. Technology innovation and the importance of unconventional gas resources in canada. In: Proceedings of the 19th World Petroleum Congress. Madrid, Spain.

Itkin, A., Carr, P., 2011. Using pseudo-parabolic and fractional equations for option pricing in jump diffusion models. Computational Economics 40 (1), 1–42.

Jansen, J. D., Douma, S. D., Brouwer, D. R., Van Den Hof, P. M. J., Bosgra, O. H., Heemink, A. W., 2009. Closed-loop reservoir management. In: Proceedings of the SPE Reservoir Simulation Symposium. Texas, USA.

Jayawardena, S. S., Zabaras, G. J., Dykhno, L. A., 2007. The use of subsea gas-lift in deep-water applications. In: Offshore Technology Conference. Houston, USA.

Khalil, H., 2001. Nonlinear systems. Prentice Hall.

Kochina, P., 1962. Theory of Ground Water Moovement. Princeton University Press.

Konieczek, J., 1990. The concept of critical rate in gas coning and its use in production forecasting. In: Proceedings of the SPE Annual Technical Conference and Exhibition. Louisiana, USA.

Korteweg, D. J., de Vries, G., 1895. On the change of form of long waves advancing in a rectangular canal and on a new type of long stationary waves. Philosophical Magazine 39, 422–443.

Krogstad, S., Hauge, V. L., Gulbransen, A. F., 2011. Adjoint multiscale mixed finite elements. SPE Journal 16 (1), 162–171.

Krstic, M., 1999. On global stabilization of burgers equation by boundary control. Systems and Control Letters 37, 123–141.

Krstic, M., Kanellakopoulos, I., Kokotovic, P., 1995. Nonlinear and Adaptive Control Design. Wiley.

Krstic, M., Smyshlyaev, A., 2008. Boundary Control of PDEs: A Course on Backstepping Design. SIAM Advances in Design and Control Serries.

Lakatos, I., 2005. Role of chemical ior/eor methods in the 21st century. In: Proceedings of the 18th World Petroleum Congress. Johannesburg, South Africa.

Larsen, E. R., 2005. Are rich countries immune to the resource curse? evidence from norway's management of its oil riches. Resources Policy 30 (2), 75–86.

Leemhuis, A. P., Nennie, E. D., Belfroid, S. P. C., Alberts, G. J. N., Peters, E., Joosten, G. J. P., 2008. Gas coning control for smart wells using a dynamic coupled well-reservoir simulator. In: Proceedings of the Intelligent Energy Conference and Exhibition. Amsterdam, The Netherland.

Li, D., Du, Y., 2004. The history and future of china oil and gas. In: Proceedings of the SPE Annual Technical Conference and Exhibition. Houston, USA.

Lie, K. A., Krogstad, S., Ligaarden, I. S., Natvig, J. R., Nilsen, H. M., Skaflestad, B., 2012. Open source matlab implementation of consistent discretisations on complex grids. Computational Geoscience 16, 297–322.

Liu, W., Ramirez, W. F., Qi, Y. F., 1993. Optimal control of steam flooding. SPE Advanced Technology Series 1 (2), 73–82.

Liu, W. J., Krstic, M., 2002. Global boundary stabilization of the korteweg-de vries-burgers equation. Computational and Applied Mathematics 21, 315–354.

Lorenzatto, R. A., Juiniti, R., Gomes, J. A. T., Martins, J. A., 2004. The marlim field development: Strategies and challenges. In: Proceedings of the Offshore Technology Conference. Houston, USA.

Loxton, R. C., Teo, K. L., Rehbock, V., 2008. Optimal control problems with multiple characteristic time points in the objective and constraints. Automatica 44, 2923–2929.

Loxton, R. C., Teo, K. L., Rehbock, V., Yiu, K. F. C., 2009. Optimal control problems with a continuous inequality constraint on the state and the control. Automatica 45, 2250–2257.

Lucas, S. K., Kaya, C. Y., 2001. Switching-time computation for bang-bang control laws. In: Proceedings of the American control conference. Virginia, USA.

Luenberger, D. G., 1979. Introduction to dynamic systems: Theory, Models and Applications. John wiley and sons Inc.

Marler, R. T., Arora, J. S., 2004. Survey of multi-objective optimization methods for engineering. Structural and Multidisciplinary Optimization 26 (6), 369–395.

Martel, Y., Merle, F., 2001a. Asymptotic stability of solitons for sub-critical generalized kdv equations. Arch. Rational Mech. Anal 157, 219–254.

Martel, Y., Merle, F., 2001b. Instability of solitons for the critical generalized korteweg-de vries equation. Geometric and Functional Analysis 11, 74–123.

Martel, Y., Merle, F., Mizumachi, T., 2010. On description of the inelastic collision of two solitary waves for the bbm equation. Arch. Rational Mech. Anal 196, 517–574.

Matsumoto, K., Voudouris, V., Stasinopoulos, D., Rigby, R., di Maio, C., 2012. Exploring crude oil production and export capacity of the opec middle east countries. Energy Policy 48, 820–828.

Merle, F., 2001. Existence of blow-up solutions in the energy space for the critical generalized kdv equation. Journal of the American Mathematical Society 14, 555–578.

Mjaavatten, A., Aasheim, A., Saelid, S., Gronning, O., 2008. Model for gas coning and rate-dependent gas-oil ratio in an oil-rim reservoir. SPE Reservoir Evaluation and Engineering 11 (5), 842–847.

Muskat, M., 1937. Flow of Homogeneous Fluids. McGraw Hill.

Nennie, E. D., Savenko, S. V., Alberts, G. J. N., Cargnelutti, M. F., Donkelaar, E. V., 2009. Comparing the benefits: Use of various well head gas coning control strategies to optimize production of a thin oil rim. In: Proceedings of the SPE Annual Technical Conference and Exhibition. New Orleans, USA.

Oliver, D. S., Chen, Y., 2011. Recent progress on reservoir history matching: a review. Computational Geosciences 15 (1), 185–221.

Oliver, D. S., Reynolds, A. C., Liu, N., 2008. Inverse theory for petroleum reservoir characterization and history matching. Cambridge University Press.

Pasicznyk, A. M., Hogg, W. C., Williams, D. L., Cordeiro, C. M. P., Sotomayor, G. P. G., Alves, I., De Oliveira, R. L. L., Blauth, M., 1999. Case history of the worlds first level 5 multilateral completed from a semisubmersible rig. In: Proceedings of the SPE Annual Technical Conference and Exhibition. Houston, USA.

Quarteroni, A., 1987. Fourier spectral methods for pseudo-parabolic equations. SIAM Journal on Numerical Analysis 24 (2), 323–335.

Rooks, M. K., Snyder, K., Wilson, L., Fleming, J., Mack, J., Wisnewski, M., 2012. Integral pod intake for electrical submersible pumps. In: SPE Saudi Arabia Section Technical Symposium and Exhibition. Al-Khobar, Saudi Arabia.

Rosier, L., 1997. Exact boundary controllability for the kdv equation on a bounded domain. ESAIM: Control, Optimization, and Calculus of Variation 2, 33–55.

Russell, D. L., Zhang, B. Y., 1996. Exact controllability and stabilizability of the kdv equation. Transaction of the American Mathematical Society 348, 3643–3672.

Sagatun, S. I., 2010. Boundary control of a horizontal oil reservoir. SPE Journal 15 (4), 1020–1027.

Sarma, P., Chen, W. H., 2008. Applications of optimal control theory for efficient production optimization of realistic reservoirs. In: Proceedings of the International Petroleum Technology Conference. Kuala Lumpur, Malaysia.

Showalter, R. E., Ting, T. W., 1970. Pseudo-parabolic partial differential equations. SIAM Journal on Mathematical Analysis 1 (1), 1–26.

Skeel, R., Berzins, M., 1990. A method for the spatial discretisation of parabolic equations. SIAM Journal of Statistic Computation 11 (1), 1–32.

Smaoui, N., Al-Jamal, R. H., 2008. Boundary control of the generalized korteweg-de vries-burgers equation. Nonlinear Dynamics 51, 439–446.

Socha, K., 2002. Modal analysis of long wave equations. PhD Dissertation, U. Texas.

Stenger, B. A., Al-Katheeri, A. B., Hafez, H. H., Al-Kendi, S. A., 2009. Short-term and long-term aspects of a water injection strategy. SPE Reservoir Evaluation and Engineering 12 (6), 841–852.

Sudaryanto, B., Yortsos, Y. C., 2000. Optimization of fluid front dynamics in porous media using rate control. Physics of Fluids 12, 1656–1670.

Sussmann, H. J., 1979. A bang-bang theorem with bounds on the number of switchings. SIAM Journal on Control and Optimization 17, 629–651.

Suwartadi, E., 2012. Gradient-based method for production optimization of oil reservoir. PhD thesis at NTNU.

Talipova, T., Pelinovsky, E., Holloway, P. E., 1997. Dynamics and statistics of intense internal waves over a continental slope. Geoscience and Remote Sensing 3, 1329–1331.

Teo, K. L., Goh, C. J., Wong, K. H., 1991. A unified computational approach to optimal control. Longman scientific and technical.

Ting, T. W., 1963. Certain non-steady flows of second-order fluids. Archive for Rational Mechanics and Analysis 14 (1), 1–26.

Ting, T. W., 1969. Parabolic and pseudo-parabolic partial differential equations. Journal of the Mathematical Society of Japan 21 (3), 440–453.

Ting, T. W., 1974. A cooling process according to two-temperature theory of heat conduction. Journal of Mathematical Analysis and Applications 44 (1), 23–31.

Trujillo, M., Mercado, D., Maya, G., Castro, R., Soto, C., Perez, H., Gomez, V., 2010. Selection methodology for screening evaluation of enhanced-oil-recovery methods. In: SPE Latin American and Caribbean Petroleum Engineering Conference. Lima, Peru.

Tsuji, Y., Yanuma, T., Murata, I., Fujiwara, C., 1991. Tsunami ascending in rivers as an undular bore. Natural Hazards 4 (2), 257–266.

van Essen, G. M., Van den Hof, P. M. J., 2011. Hierarchical long-term and short-term production optimization. SPE Journal 16 (1), 191–199.

Vazquez, J. L., 2007. Porous medium flow in a tube: travelling waves and kpp behaviour. Communications in Contemporary Mathematics 9, 731–751.

Willcox, K., Peraire, J., 2002. Balanced model reduction via the proper orthogonal decomposition. AIAA Journal 40 (11), 2323–2330.

Zadeh, L., 1963. Optimality and non-scalar-valued performance criteria. IEEE Transaction on Automatic Control 8 (1), 59–60.

Zandvliet, M., Bosgra, O. H., Jansen, J. D., Van den Hof, P. M. J., Kraaijevanger, J. F. B. M., 2007. Bang-bang control and singular arcs in reservoir flooding. Journal of Petroleum Science and Engineering 58, 186–200.

Zandvliet, M. J., Handels, M., van Essen, G. M., Brouwer, D. R., Jansen, J. D., 2008. Adjoint-based well-placement optimization under production constraints. SPE Journal 13 (4), 392–399.